Master’s Degree Course in Environmental and Land Engineering

Climate Change

Politecnico di Torino

Assessment of Factors Affecting Urban Air Quality

Supervisor(s)

Prof.ssa. Marina Clerico

Eng. Davide Gallione

Candidate:

Safoura Arab

2025 / 2026

Abstract

Air pollution caused by particulate matter (PM) remains one of the major urban environmental and health concerns. The differences between the size fractions of particulate matter (PM_1, $PM_{2.5}$, PM_4, PM_{10}) reflect the differences in sources and atmospheric processes. Hence, it becomes necessary to apply size-resolved and number-based analysis for the interpretation of aerosol behaviour. The present study aims to examine the characteristics of particulate matter mass concentrations and particle number concentrations (CN) in the urban environment, focusing on pollution episodes, the impact of traffic, and the control of meteorological conditions.

Hourly concentrations of particulate matter (PM_1, $PM_{2.5}$, PM_4, PM_{10}) and particle number concentrations (CN) were measured at Turin, Italy, using a Palas Fidas 200S aerosol spectrometer. The instrument was deployed at an outdoor monitoring station.

Traffic and non-traffic periods were identified using fixed interval definitions based on rush hour periods. Pollution episodes were identified based on a percentile-based threshold method where the 90th percentile (P90) was used as the threshold value based on the hourly average concentration of $PM_{2.5}$. The particle size distribution was identified by comparing the ratio of the particle size fractions such as PM_1/PM_{10}, $PM_{2.5}/PM_{10}$, and PM_4/PM_{10}. Meteorological parameters such as temperature, relative humidity, pressure, and thermal stability (ΔT) were also included in the analysis.

Other than the mass concentration-based parameters, the study has also identified the particle number concentration (CN) and its temporal behavior. The differences in weekday and weekend variations and the diurnal variations related to the activities in the city were also taken into consideration in the analysis. Morning and evening peak indices were calculated to identify the traffic-related variations in the particle number concentration. Moreover, the effective density (ρeff) of the particulate matter was also identified based on the ratio of the mass concentration and the volume concentration.

From the results, it has been identified that all the size fractions of PM show the same pattern in temporal variations. It indicates that the factors influencing the PM concentration are the same for all the size fractions. Moreover, the ratio of the size fraction concentrations is found to be constant over time, indicating minimal changes in the size distribution of the PM. It has been identified that the concentration of PM is more during the nighttime and early morning hours and less in the afternoons. Even though the traffic plays an important role in the variation

in the concentration of PM in the atmosphere in the city, the temporal trends in the PM concentration are not entirely related to the traffic. It has been identified that the meteorological parameters such as the atmospheric stability, ΔT, and the relative humidity are more dominant in the accumulation of the PM in the atmosphere. The concentration of the particle number concentration is found to be having a clear diurnal pattern in the city. It has been identified that there are clear peaks in the concentration during the traffic periods and during the pollution episodes.

However, further analysis reveals that the particle number concentration and effective density vary with different pollution regimes and weather conditions, changing with time as the aerosol composition and atmospheric processing vary. The correlation analysis reveals relationships between PM fractions, CN concentrations, and meteorological conditions. In comparison with background conditions, pollution episodes are characterized by a stronger presence of fine particles and CN.

In conclusion, it can be said that the main factor affecting the site's PM variability is atmospheric stability and accumulation, with traffic and combustion emissions contributing to the enhanced presence of fine particles in pollution episodes. The approach of using a range of methods, including percentile-based episode definition, particle-size fractions, particle number concentrations, and effective densities, is a powerful and accessible approach to understanding urban aerosol dynamics and air pollution in urban environments.

Contents

List of figures

List of Table

This thesis is organized into eight chapters:

- Chapter 0 – History: History of air pollution
- Chapter 1 – Introduction: Introduces the air pollution, types of air pollution and its sources, particular matter and its Characterizations and explains Differences in Density Size Distributions Between Urban and Natural Environments.
- Chapter 2 – Study Area: Introduces The geographical, topographical, climatic, and urban and industrial characteristics of Turin.
- Chapter 3 – Palas Fidas: introduces Palas Fidas device and PDAnalyze Software
- Chapter 4 – Methodology: Describes and pre-processes the data and define traffic and Non traffic hours, types of conditions, and explains the effective density of particulate matter and Particle number concentration (CN)
- Chapter 5 – Results and Analysis: Presents the graphs and relationship between parameters.
- Chapter 6 – Discussion: discusses the study findings and compares with existing research
- Chapter 7 – Conclusion: Summarizes findings

Chapter 0:

History

History of air pollution

In preindustrial societies, the primary source of harmful anthropogenic air pollution was domestic combustion of biomass. Blackened lungs of Ancient Egyptian mummies exhumed as a result [1]. Hippocrates considered how air quality affects human health in Airs, waters and places written around the 4th century BCE, while the health advantages of escaping Rome's "ruinousmess of steamand soot" described by Seneca The Younger in the 1st century AD [2], [3].

In 1273, after Queen Eleanor complained about the "intolerable smoke" emitted from burning bituminous sea coal, English Parliament enacted the Smoke Abatement Law [4]. However, the air quality of London remained poor for hundreds of years and deteriorated further due to a twelvefold increase in coal consumption during the Industrial Revolution [5]. Air pollution not only increased the risk of respiratory diseases but also acted as a natural element of selection pressure for peppered moth pigmentation in Victorian Britain. In this condition, light-winged moths using surfaces blackened by soot for camouflage easily became exposed to predators and over time, darker wings survived more and eventually became the most common phenotype [6].

In 1610, English law recognized harmful effects of polluted air in Aldred's Case as one of the first acknowledgments of air pollution as a societal issue [7].

In 1872, Robert Angus Smith, for the first time, carried out multi-site and multi-pollutant measurements in Britain and investigated the relationship between air pollution level in industrial and rural areas [8].

After World War II, exporting high-quality coal in large scale forced London people to consume low-quality and high-sulphur lignite coal. In December 1952, cold weather led to greater coal consumption while a patch of high air pressure formed a smoke laden with soot and sulfur dioxide over the city. It was the start of the Great London Smog which lasted for five days and resulted in roughly 4,000 deaths that month alone [9]. That disaster led to introduction of the Clean Air Act of 1956. According to the Act, for the first time, local authorities were allowed to announce smoke control zones. It also regulated the emission of dark smoke from industrial sectors and laid the foundation for following pollution policies such as both the Clean Air Act 1968, and the Environment Act 1995 [10].

In the 1950s, the definition of Total Suspended Particles (TSP) covering the total quantity of solid and liquid particulates less than 30 to 50 micrometres in the atmosphere, became one of the first quantitative indicators of air pollution. In the 1970s, it was adopted as an air quality standard under the U.S. Clean Air Act. However, the health risks associated with smaller particles were recognized in the 1980s [11].

Consequently, the U.S. Environmental Protection Agency (EPA) amended its particulate matter regulations to substitute PM_{10}, referring to particulates less than 10 μm in aerodynamic diameter, in place of TSP in the year 1987 as a means of forming the National Ambient Air Quality Standards (NAAQS) [12]. This marked a significant milestone in air quality standards, representing a transition from measuring the total weight of particulate matter in the air to size fraction standards, prepared a better identification of different types of air pollution and what type of them had a greater negative impact on human health. Since this time, both epidemiology and toxicology studies discovered that there is a much stronger association between particulate matter smaller than 2.5 micrometres in size and cardiovascular and respiratory diseases. Consequently, the U.S. EPA introduced new air standards incorporating $PM_{2.5}$ to the PM_{10} standards [13].

Parallel developments occurred in Europe. The European Union Directive 1999/30/EC set a legal limit on PM_{10} and considered a daily concentration threshold and a mean annual of 50 $\mu g/m^3$ and 40 $\mu g/m^3$, respectively which should not be exceeded more than 35 times a year [14]. Based on this, a new target of air quality values was set in Directive 2008/50/EC for $PM_{2.5}$ values, including the new "Average Exposure Indicator" (AEI), which is a method of assessing long-term exposure to air pollutants in cities [15]. Although PM_1, which plays an important role in fine and ultrafine aerosol fraction, have attracted scientific attention since 1990s, it is still not part of regular regulatory frameworks [16].

Current international guidelines, such as those from the World Health Organization (WHO), still focus mainly on PM_{10} and $PM_{2.5}$ due to their established epidemiological evidence and measurement reliability [17]. However, with continuous research, it is stated that PM_1 and even ultrafine particles (< 0.1 μm) could represent the next frontier in health-oriented air quality standards [16].

Chapter 1:

Introduction

1.1. Air pollution

Interactions between humans and the environment have been scrutinized thoroughly because there is no restriction to the human activities that can impact their environment. The environment is defined as the “coupling of the biotic and abiotic [18].

Air pollution can be defined as the Contamination of the ambient atmosphere either indoors or outdoors resulting from the action of any chemical, physical, or biological substance such as gases or particulates with the potential to alter or modify the natural composition of the atmosphere. These contaminating substances have the potential to cause discomfort, diseases, or death to millions of people every year [19], [20].

Air pollution has gradually increased over the past decades. It has increasingly affected public health and has been given growing attention by both government and health sectors [21].

About 90% of the world's population is exposed to air quality levels beyond the air quality standards set by the World Health Organization (WHO) in their regions [22]. Minimizing the effect of air pollution on human health is one of the current hot public health issues. Over the past decades, air pollution effecting human health has been confirmed, particularly because of particulate material (PM) [23]. The burden of disease because of air pollution is still little changed since the 1990s [24].

For air pollution to take place, air pollutants have to be emitted to the atmosphere. Once they reach the atmosphere, they undergo chemical reactions. This results in them going to receptors such as humans, animals, plants, and materials. Air pollution can be categorized depending on the nature of air pollutants according to their size, composition, and emission rates whether indoors or out [25].

1. 1.1. Natural and anthropogenic categories

According to its source, air pollution can be categorized into two broad classes: natural and anthropogenic or stationary and mobile. Natural pollutants are discharged directly from natural sources. Natural pollutants include forest fires, volcanic eruption, dust storm, pollen grain, radon gas produced by the radioactive decay of the Earth’s crust, microorganisms, natural radioactivity, fog, mist, and ozone [26].

However, because of the self-purifying and regenerative capacity of the atmosphere, natural pollutants generally exert only a short-term and limited effect on ecological balance [27].

Most anthropogenic point sources emit pollutants into the atmosphere from tall chimneys, where adequate dilution of emissions occurs before reaching the earth's surface. However, dispersion may be restricted under specific meteorological conditions like low temperature and winds and a highly stable atmosphere that allows the trapping of pollutants close to the source of emission and subsequent settling toward the surface with deterioration of air quality [28].

1.1.2. Primary and secondary sources

Depending on source, air pollutants can be classified into primary and secondary air pollutants. Primary air pollutants are emitted directly from a point source into the air and retain their original composition. Primary air pollutants can be generated naturally as well as through human activities. Primary air pollutants include sulfur oxides, nitrogen oxides, carbon monoxide, hydrocarbons, lead, particulate matter, and VOCs (volatile organic compounds) [20].

Unlike primary air pollutants, secondary air pollutants result from certain chemical reactions that occur in the air and have primary air pollutants and other components of air as their precursors. These air pollutants, resulting from oxidation, photochemical oxidation, and hydrolysis, include sulfuric acid, nitric acid (which is responsible for acid rain), carbonic acid, ozone, ketones, and photochemical smog. Some pollutants, like nitrogen monoxide and parts of particulate matter, can act as both primary and secondary pollutants [29].

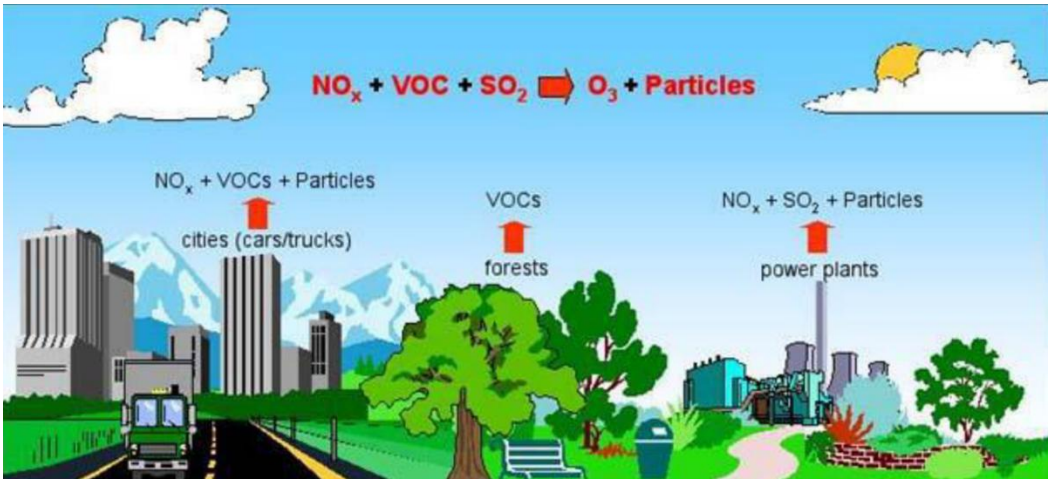

Fig. 1. Primary pollutant combined to form secondary pollutants [20]

Turning to yet another classification, air pollutants can be divided into gaseous and particulate matter on the basis of particle size. Atmospheric particulate matter is a complex mixture of organic and inorganic substances. Particles that are finer are called $PM_{2.5}$ and have sizes below 2.5 µm, while larger particles have sizes above this limit and are coarse particles. Even finer than this are ultrafine particles, having sizes below 0.1 µm [30].

particulate matter that has a diameter of less than 2.5 µm and ozone was listed as having been reported as the most serious air pollutant in Shanghai, especially during winter. this has been attributed by the growth of industrial energy consumption and emission during that time [31].

gaseous and particulate matter as air pollutants, was studied in three of China's major cities on the banks of the Yangtze River, namely Nanjing (downstream), Wuhan (midstream), and Chongqing (upstream). Also, it was acknowledged that PM2.5 was the most prominent pollutant that has caused air pollution [32].

1.2. Particulate matter

As there are complex particles consisting of tiny solids and fluids suspended in the airlifted into human inhalation passages, Airborne particulate matter considers one of the commonest contaminants found in the atmosphere [33].

Based on aerodynamic diameter, particulate matter can generally be categorized into three groups. These are coarse particles with a diameter not to exceed 10 µm (PM_{10}), fine particles up to 2.5 µm ($PM_{2.5}$), and ultrafines smaller than 0.1 µm [34].

According to the World Health Organization (WHO), in 2013, fine particles' harmful health impacts are mostly related to particles with dint sizes less than 10 µm and 2.5 µm. Particles less than 10 µm (PM_{10}) can easily enter the alveoli or bronchi in human lungs. In contrast to PM_{10} particles, particles smaller than 2.5 µm (PM_{2}.5) can potentially enter the walls around the bronchial capillaries and hamper gas transportation between them [35].

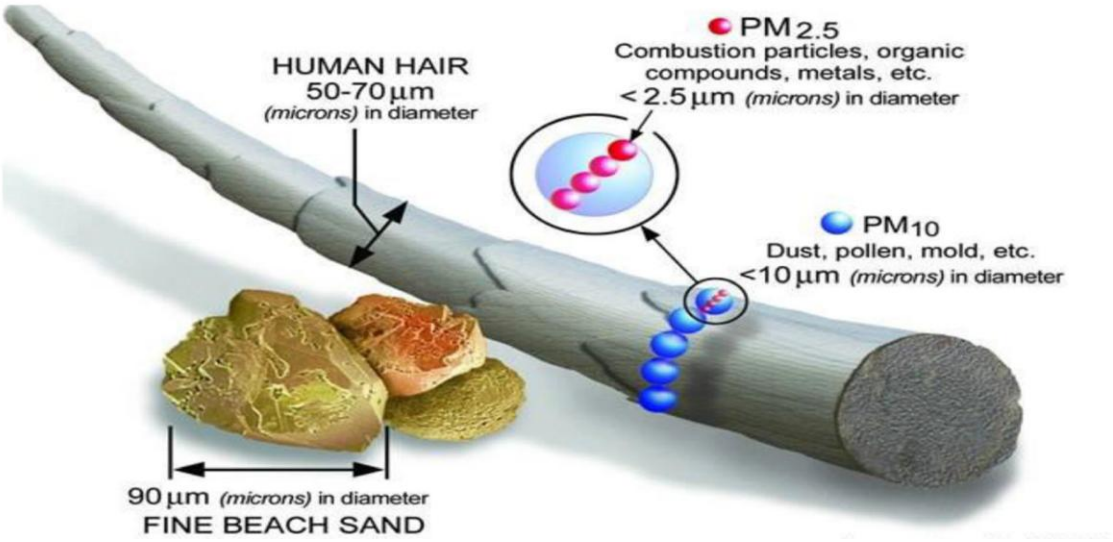

Fig. 2. Different sizes of particulate matter [35]

$PM_{2.5}$ was found to substantially influence haze generation in various areas [36]. most studies showed that particles smaller than or equal to 2.5 µm in aerodynamic diameter are highly toxic compared to coarse particles (particles larger than 2.5 µm), which are more threatening to humans. it was also revealed that $PM_{2.5}$ affects climate change [37], [38].

Onabowale and Owoade [39] observed that in developing nations, PM-related diseases and deaths are estimated to account for almost 28% of the burden. These observations are consistent with those reported by WHO [40], which estimated that exposure to PM in both indoors and outdoors was responsible for more than seven million excess deaths.

Inhaling PM_{10} and $PM_{2.5}$ was found to cause both acute and chronic health effects to breathing and repairing organs [41]. Particulate matter not only reduces ground-level visibility due to its light-scattering properties but also has detrimental effects on both human health and plants [42].

1.2.1. Physical Characterization of Particulate Matter

One of the factors of particulate matter (PM) classification is its aerodynamic diameter (PM_{10}, $PM_{2.5}$,) and even less than one micron which determine deposition in the respiratory system. This classification is limited by particle size only while recent studies have discovered that even at concentrations below current regulatory thresholds, PM exposure can still pose significant health risks [43], [44].

Therefore, current work stresses parameters which play a coupled role in transport, optical effects, and exposure: these include now mainly effective density (ρ_{eff}) and additionally shapes, hygroscopicity [45], [46] with emphasis on effective density, which is mass normalized by total volume: it links physical and chemical effects [47].

The comparison between urban and rural measurement data reveals distinct source-related density values: for organic and soot-containing aerosol particles, ρ_{eff} is 0.5-1.2 g/cm³; for inorganic aerosol particles (sulfate, nitrate, and ammonium), 1.2-2.0 g/cm³, and for mineral or metal aerosols above 2.0 g/cm³ [48], [49].

Density determination by means of combined DMA-APM and AMS analysing instruments has confirmed that aerosol density differs systematically with respect to composition and processing, which makes it possible to distinguish between natural dust aerosols, industrial emissions, and combustion aerosols through their characteristic density–size signatures [50]. Hence, functional density is a critical parameter for source identification and atmospheric processing mechanisms related to aerosol origin [51].

Two supporting parameters frame the interpretation for ρ_{e}ff. The dynamic shape factor (χ) is used to correct for non-sphericity in measurements made on the basis of mobility or aerodynamic diameters, which is beneficial for density estimation and interpretation related to mineral and soot morphologies [52]. On the other hand, the hygroscopicity parameter (κ) is used to express a measure of a particle's capacity to absorb water vapor with increasing humidity, thus affecting overall particle size and scattering efficiency [53].

Recent model compilations have demonstrated that hygroscopicity parameter values increase for ammonium salts and decrease for organics, suggesting a humidity-related variation of optical and physical effects even when mass concentration is held constant [54]. Although other features such as mixing state or phase (solid, semi-solid, or liquid) influencing aerosol properties, effective density is considered as the parameter with physical characteristics coupled with chemical composition. Hence, this study focuses on density-related classification and distribution analyses for PM to illustrate source-related particle performance in both urban and natural environments [44], [46].

1.2. 2. Density–Distribution Relationship

After classifying particles on the basis of effective density, a mass-density distribution function can be obtained to present the allocation of masses to defined density ranges. The mass-density distribution function can be presented as the plot of the mass fraction vs. density; such functions present an alternative to the usual size distributions in aerosol classifications [44], [46].

The function combines the physics and chemistry to present the composing elements that predominantly exist in ambient air; though deposition and transport are governed by the restrictions imposed by the aerodynamic diameter, composition and heavy particles' proportion in the air masses are obtained from the mass-density function [48].

In reality, the form that this distribution takes enables researchers to distinguish between aerosols with different origins.Particulates with low effective densities (≤1.2 g/cm³) are generally linked to combustion-related particles such as soot, secondary organics, volatile hydrocarbon residues, and so forth [47]. These fall within the range of intermediate density (1.2-2.0 g/cm³), and these are secondary inorganic aerosols such as sulfate, nitrate, and ammonium salts, formed by atmospheric oxidation reactions [51]

Lastly, values above 2.0 g/cm³ correspond to mineral dust, crustal composition particles, and particles that contain metals and are generally associated with either natural resuspension [50]. Therefore, the mass density profile constitutes an empirical basis to identify the most influential sources of the atmospheric particulate matter and to assess the level of atmospheric processing affecting the composition [45]. Furthermore, the shape represented by the density distribution is related to the prevailing environment. Urban environments, which are strongly affected by traffic and combustion-related gases, tend to be unimodally distributed with values concentrated on the lower side due to higher organic matter content [47]. In contrast, natural or rural environments tend to have broader or even bimodal profiles of effective density, as a consequence of both low-density organic/biogenic secondary aerosol and the mineral components, as seen at rural background locations and rural long-term networks [55], [56].

These variations in distribution shape enable the analysis of source contribution and transformation dynamics in urban areas and natural environments that is targeted in this study. The specifics of density-resolved analysis of mass fraction and corresponding instrumental techniques (DMA-APM and AMS) are shown in the Materials and Methods section [44].

1.2.3. Measurement Techniques for Particle Density

Precise ρ_{eff} measurement is contingent upon the availability of experimental apparatus capable of making concurrent measurements related to particle size and mass. The Aerosol Particle Mass Analyzer (APM) is, and continues to be, the principal device used for this purpose. It discriminates between aerosol particles, basing the discrimination solely on the interaction between the centrifugal and electrostatic forces acting on charged particles, thus allowing direct particle mass measurement [46], [47].

When coupled with a Differential Mobility Analyzer (DMA), commonly known as a DMA-APM system, paired measurements of both mobility diameter and particle mass are achieved, hence facilitating the determination of particle densities over a broad size distributive range [48]. Such a system has established a standard procedure to determine densities related to atmospheric aerosol characteristics [44].

Recent technological developments, including the Centrifugal Particle Mass Analyzer (CPMA) and other Couette-type classifiers, now offer better mass resolution and long-term accuracy, enabling measurements over ultrafine sizes (<100 nm) with greater accuracy [57]. Other ancillary tools, like the Aerosol Time-of-Flight Mass Spectrometer (ATOFMS), offer detailed, single-particle chemical speciation, as well as size and relative mass, to facilitate real-time speciation apportionments of combustion, mineral, or secondary aerosol components [58].

Taken together, the resulting mass-density phase space facilitates the attribution of point sources as well as the distinction between urban and natural environments, a primary aim of this study [51].

1.3. Density and Chemical Composition

The actual density of particulate matter, ρ_{eff}, is determined by the internal matter composition and the phase, as ρ_{eff} represents the weighted sum of the contributions by the organic, inorganic, or mineral matter components to particle density. An increase in the organic matter concentration, representing fresh soot or secondary organic aerosol, reduces ρ_{eff} due to the lower inherent densities and porous structure of the organic components, as opposed to the other two matter constituents [44], [48].

Observations validate an elevated matter concentration and particle

deviations from a spherical geometry, as indicated by a lower ρ_{eff} [59]. On the other hand, a greater proportion of inorganic salts, such as sulfate, nitrate, or ammonium salts, or minerals/metallic substances results in a greater effective density, which expresses the impacts exerted by the high-density substances [49]. Additional processes, including atmospheric aging and internal mixing, render this relation even more complex: as volatile organic compounds oxidize and accumulate onto pre-existing particles, their density and hygroscopicity increase, signalling the transformation and transition from externally mixed to internally mixed particles [52].

Accordingly, ρ_{eff} performs a role that is even beyond a physical attribute, acting as a proxy regarding the characterization of a source as well as transformation processes in the atmosphere. Recent observational studies involving the integration of mobility/mass, or DMA/APM or CPMA, measurements with the analysis of chemical composition, or AMS or ATOFMS, have confirmed that the distribution of an effective density is consistent with the distribution of the modes of composition, thus making a diagnostic distinction between combustion, organic-rich, or mineral/secondary inorganic particles possible [44], [49], [58].

1.4. Differences in Density Size Distributions Between Urban and Natural Environments

The contrasting size and density distributions of particles within urban and natural environments offer a crucial basis for distinguishing aerosol sources, atmospheric processes, and transport patterns. In contrast to the classifications based on aerodynamic diameters, size distributions resolved by particle densities provide clearer indicators concerning the role of either anthropogenic or natural aerosols, mainly because particle density is sensitive to chemical, morphological, and hygroscopic properties [44], [60].

1.4.1. Source-Driven Density Characteristics

Over various global metropolitan areas, the particle concentration usually follows multimodal size distribution patterns, which correspond to various anthropogenic sources. The low-density region (about 1.0 - 1.3 g/cm³) is mainly composed of traffic-related and other burning activities, domestic heating, cooking, and fresh organic material, while secondary inorganic aerosols, sulfates, nitrates, and ammonium salts are the intermediate-density mode (1.3 - 1.7 g/cm³). The

high-density mode consists of mechanically produced particles, for example, road dust, construction material, and industrial minerals ($\rho_{eff} \geq 2.0$ g/cm³) [44], [61].

In contrast, natural environments are generally dominated by mineral dust, crustal components, sea salt, and the resuspension of soil, all of which are distinguished by elevated material densities in excess of 2.2 g/cm³. Biogenic organic aerosol, in the form of pollen, spores, and plant material, is the lower-density mode, although this is seasonal and sporadic [62]. In this case, urban aerosol populations are more variable and have greater range in their recorded material densities, whereas natural locations have more uniform mineral-related material-density distributions [44].

1.4.2. Differences in Particle Size Distributions

There also appear contrasting sources through distinctive patterns of particle size distribution (PSD). PSDs in urban environments are often dominated by nucleation (10-30 nm), Aitken (30-100 nm), and accumulation modes (100-300 nm), linked to emissions and secondary aerosol formation [63].

Mass PSDs (dM/dlogDp) in urban environments are known to be typically peaked within the size range of $PM_{2.5}$, showing significant anthrop Natural systems, on the other hand, are dominated by coarse mode particles (>1 μm), produced by wind-blown dust, sea salt, and biological particles. Hence, it is evident that fine modes dominate the concentration in urban areas, whereas coarse mineral particles dominate mass concentration in natural systems [64].

1.4.3. Effective Density Variability and Chemical Implications

The Effective Density (ρ_{eff}) provides more contrasts. The urban site usually indicates high diurnal variations:

• Reduced ρ_{eff} in the morning and/or evening traffic peaks (new, fresh, and organic-rich particles

• Higher ρ_{eff} during daytime because of secondary inorganic aerosol formation.

Laboratory and field studies have shown the negative correlation of ρ_{eff} with organic matter and positive correlation with inorganic sulfate, nitrate, and ammonium compounds [44], [60], [61].

In natural environments, there is more stable ρ_{eff} behaviour, predominantly due to mineral dust, and only occasional episodes related to high biogenic emissions [62].

1.4.4. Seasonal and Meteorological Influences

The seasonal and meteorological conditions tend to accentuate the differences between the urban atmosphere in terms of aerosol content, as opposed to natural conditions. In the urban area, the winter season is distinguished by reduced boundary layer heights, increased residential heating, as well as temperature inversion conditions, which accentuate the mass accumulation of the fine mode fractions (PM1-PM2.5). The conditions prevailing in the summer season in the urban area tend to enhance the level of photochemical transformation, thereby accentuating the secondary mass concentrations, as well as the effective density(ρ_{eff}) values in the atmosphere [65].

Natural environments also show a seasonal variability, having a greater load of coarse mode in dry, windy conditions as a result of the resuspension of mineral dust. Observational evidence in Mediterranean to semi-arid regions indicates that coarse mode (>1 μm) becomes significantly greater in warm, dry, and wet conditions, while the emission of biogenic organic compounds (spores, pollen, leaf litter) becomes substantially greater in spring and summer [64]. In addition, the trans-Saharan transport of dust can periodically reach European sites, both rural and urban, favouring the presence of coarse mineral dust over other particle sizes, along with an elevated effective density of the remaining aerosol population [66].

1.4.5. Integration into Urban–Natural Comparative Frameworks

Combined examination of density-size distributions in both urban and natural environments is a strong approach to quantitatively assess the contributions of human and natural sources to aerosol emissions. It has been demonstrated that including information on particle density, mass fractions, and state of mixing provides more accurate source apportionment than aerodynamic diameter alone [63], [67]. Joint characterization of density-resolved PSDs, incorporating temporal features like traffic patterns, weekend differences, and meteorological factors including dust intrusion episodes, stagnation periods, and precipitation-driven removal, can lead to better reproduction of source dynamics and processing [64], [66], [68].

These approaches have already shown their capability to distinguish combustion-sourced, mineral dust, sulphate, and biogenic sources on varying metropolitan-natural domains [63], [69].

Chapter 2:

Study Area

2.1. The City of Turin (Italy)

Turin (Torino) is located in the northwest of Italy at approximately 45.0706° N and 7.68662° E, with a municipal area of about 130.17 km² and an average elevation of ~239 m above sea level, one of the most industrialized and densely populated regions in Europe. The city proper has an estimated population of around 886,837 inhabitants, resulting in an average population density of about 6,700 inhabitants km^{-2}, while the broader urban and metropolitan areas host roughly 1.7–2.2 million people. Turin lies on the western bank of the Po River near several tributaries and is surrounded by the Alpine district to the north and west, with hilly terrain to the east such as Superga hill [70].

Fig. 3. Geographical location of the city of Turin

2.2. Geographic and Topographic Setting

Turin started developing around the junction of the Po River and its affluents, especially the Dora Riparia River, and is limited on the western and northwestern side by the Alpine mountain ranges, while the eastern side is occupied by low hills, including the Superga hill. Such a semi-closed topographic situation limits the flow of atmospheric ventilation during stable meteorological situations, hence favoring the accumulation of air pollution, particularly during winter anticyclonic periods [71].

2.3. Climatic and Meteorological Characteristics

According to the Köppen–Geiger classification, Turin experiences a humid subtropical climate (Cfa), characterized by hot summers, cool winters, and the absence of a pronounced dry season [6]. Mean monthly air temperatures range from approximately 2 °C in January to 22–23 °C in July, with an annual mean temperature close to 13 °C [72].

Annual precipitation averages around 950–1,000 mm, distributed over roughly 80 rainy days per year, while the mean relative humidity is about 70–75% [4]. Winter months are frequently affected by thermal inversions, low wind speeds, and fog events, all of which substantially reduce boundary-layer mixing and enhance the persistence of airborne particulate matter [73].

2.4. Urban Structure, Industry, and Emission Sources

Turin is historically recognized as one of Italy's major industrial hubs, particularly due to its long-standing automotive and manufacturing sectors, including vehicle production, metalworking, and mechanical engineering. Although heavy industrial emissions have declined over recent decades, road traffic, residential and commercial heating, and secondary aerosol formation remain dominant contributors to urban air pollution. In addition, the city's high traffic density and frequent congestion lead to elevated emissions of PM_{10}, $PM_{2.5}$, NO_2, and precursor gases, especially at traffic-oriented monitoring stations [74].

2.5. Air Pollution Context

Turin is part of the "Agglomerato di Torino," an area officially designated by Italian and European air-quality legislation due to its recurrent exceedances of regulatory thresholds. Numerous studies and reports highlight that, despite long-term improvements, PM_{10} and $PM_{2.5}$ concentrations still frequently exceed WHO guideline levels, particularly during winter episodes characterized by stagnant atmospheric conditions. The combination of intense anthropogenic emissions, secondary aerosol production, and unfavorable meteorology makes Turin a representative and highly relevant case study for investigating particulate matter dynamics in urban environments [75].

Chapter 3:

Palas Fidas

3.1. Palas Fidas device

The required information for the study was obtained from the CC-Green-Roof-Lab, an outdoor testbed, and was measured by a Palas Fidas 200S aerosol spectrometer. The device is capable of analyzing the concentration of solid particles with sizes ranging from 0.18 µm to 18 µm and is programmed to analyze particulate matter concentrations for PM_1, $PM_{2.5}$, PM_4, PM_{10}, and total suspended particulate matter (TSP). It also has an optical sensor and spectrometer that measures the particle number concentrations and sizes based on the light-scattering technique. According to the technical specifications provided by the manufacturer, the device's functionality of determining particles involves a single particle counting method whereby individual aerosol particles are optically detected and sized one by one in a defined volume. This approach to determination differs from the conventional technique based on the total light extinction in the measured volume and allows a consistent reconstruction of the particle size distribution before the determination of mass, as used in the FIDAS method of measurements [76].

Fig. 4. Palas Fidas® 200S aerosol spectrometer [77]

The air sampling data has a flow rate of 0.3 $m^3 h^{-1}$ using the Sigma-2 air intake unit meeting the VDI 2119-4 specifications. Finally, the size calibration of the Fidas 200S is defined in a way thatis traceable back to monodisperse calibration aerosols and is not intended for the user to modify during the actual use. The size calibration defined in this manner has less variability in the data when compared using the same device in different sites [76].

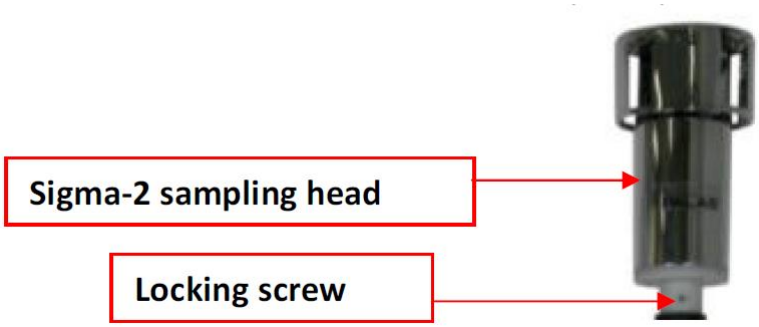

Fig. 5. Sigma-2 sampling head [77]

The analyzer is also equipped with an Intelligent Aerosol Drying System (IADS) produced by Palas GmbH, a German company, as well as sensors for ambient temperature, atmospheric pressure, and relative humidity. IADS reduces haze measurement artifacts when condensation occurs at high levels of relative humidity by ensuring that the sample temperature is kept above the dew point, with a system that responds to ambient climatic conditions [78].

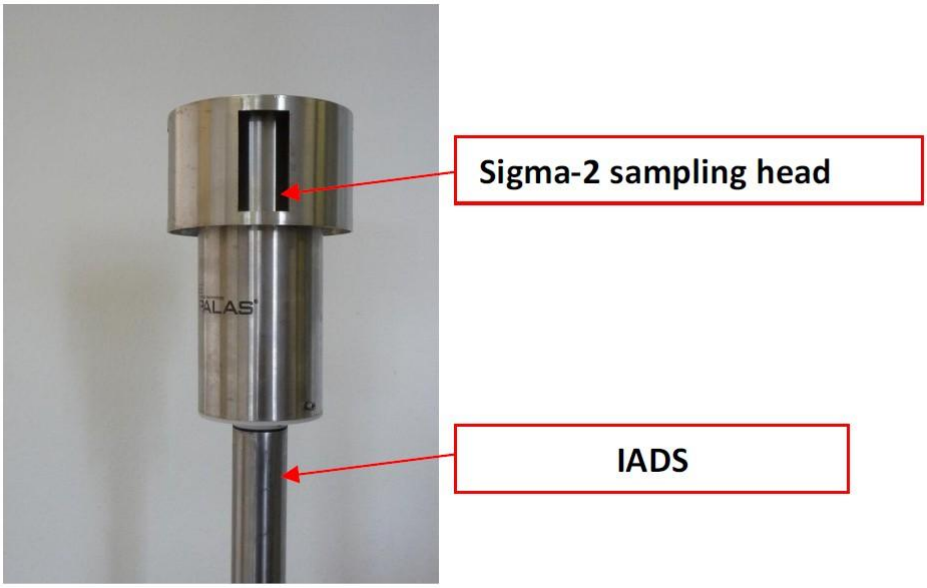

Fig. 6. Sigma-2 sampling head with IADS [77]

The Palas Fidas 200S is a genuine optical aerosol spectrometer meeting the standard of the EN 16450 series for joint measurement of $PM_{2.5}$ and PM_{10} in the environment. The device is regularly verified and calibrated every three months and designed for unattended operation at permanent environmental monitoring stations. Built-in diagnostic capabilities are used for ensuring the long-term stability of the optical part of the system and the data processing chains during the extended operation in outdoor environment [76].

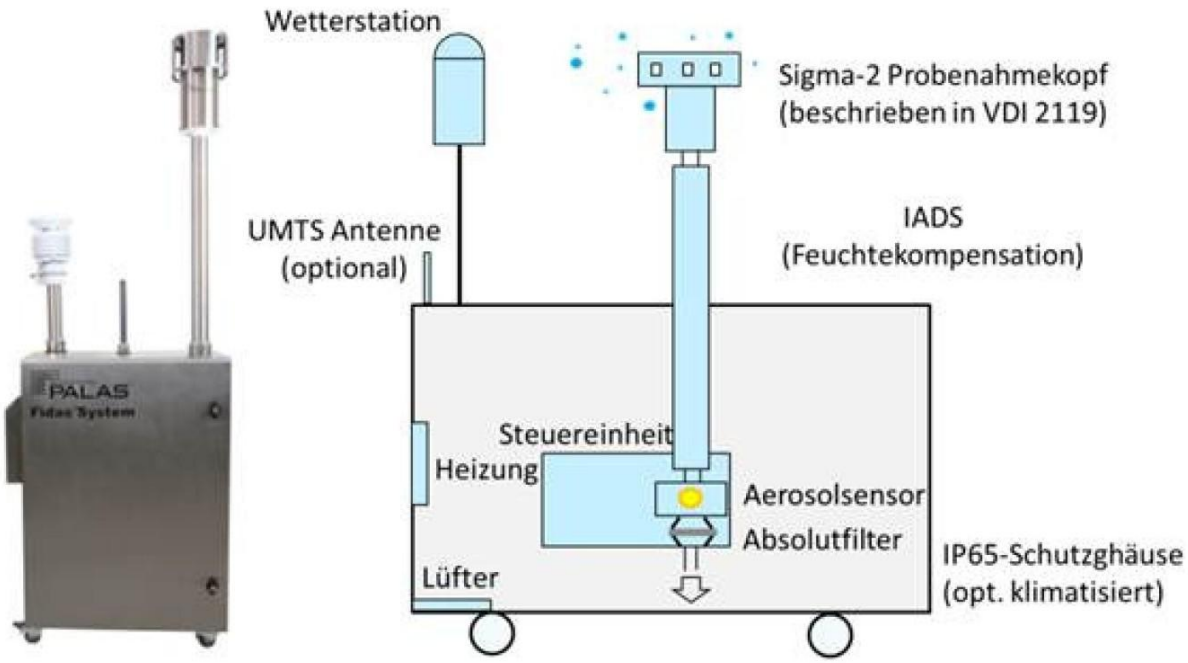

Fig. 7. Design of the Fidas® 200 S fine dust measurement system [79]

It must be noted that there are various interruptions in the collected data, which could be ascribed to the maintenance of the power grid as well as unplanned shutdowns of the grid. There were periods in which the measurements were halted to avoid any damage to the equipment.

3.2. PDAnalyze Software

The PDAnalyze Software is a proprietary data acquisition, data processing, and device control software. It was developed by Palas GmbH specifically for the use of FIDAS aerosol spectrometers. PDAnalyze supports a wide range of particle measurement instruments, such as Fidas aerosol spectrometers, Promo aerosol spectrometers, UF-CPC instruments, U-SMPS instruments, U-RANGE wide-range counters, among other instruments, allowing for the analysis of particle size and concentration data [80].

The software allows for the continuous, online determination of aerosol parameters as well as supporting parameters measured by the Palas Fidas 200S. This provides a complete description of particulate matter and ambient conditions. It also determines particulate matter concentration on a mass basis, as well as other particle number concentration data, including size-fractionated number distributions determined by optical light scattering [77].

Based on the measured size distributions, the software provides various parameters derived from aerosol size characteristics, such as moment parameters (e.g., total number, surface-related, and volume-related parameters), percentiles as functions of the number concentration size distribution, and parameters related to surface and concentration. The mass concentration parameters for regulatory particulate matter fractions like PM1, PM2.5, PM4, PM10, and the total suspended particulate matter (TSP) are automatically determined based on algorithms set by the factory and size definitions that follow defined assumptions about optical properties [79].

At the same time, the software integrates continuous monitoring and recording of auxiliary environmental parameters and operation data, such as air temperature, humidity, atmospheric pressure, vapor pressure, and dew point temperature, along with the measurements obtained from within the instruments themselves, such as sample flow rates and status indicators. These data enable data quality checks and combined analysis of aerosol concentration data correlated with meteorological data. The software allows time-series averaging data with user-definable time intervals and basic data quality checks to detect false data from unstable sampling or instrument malfunction. All measured and calculated data parameters can be exported to standard formats to easily integrate with other data, such as independent weather data [81].

Chapter 4:

Methodology

4.1. Description and Pre-Processing of Data

In this study, the data considered is the hourly average mass concentration of particulate matter, including PM1, PM2.5, PM4, and PM10. For each data value, temporal information including the day number, the clock hour from 0 to 23, and the distinction between weekdays and weekend days has been provided. Initially, before the data can be analyzed, a preliminary quality control check has been conducted to ensure consistency and includes the following steps:

(i) checking for temporal consistency,

(ii) detecting and isolating missing and non-numeric data, and

(iii) ensuring that the concentration of particulate matter and the ratios considered for analysis are stored as numbers.

4.2. Classifying Traffic and Non-Traffic Hours Based on Time

To evaluate the effect of urban vehicle traffic on particulate matter attributes, two classifications have been considered for each hour of the day, traffic hours and non-traffic hours. Traffic hours were defined as fixed time windows corresponding to typical urban rush-hour periods, namely 07:00–09:00 in the morning and 18:00–21:00 in the evening. All remaining hours of the day were classified as non-traffic hours. This temporal classification prepares the assessment of potential traffic-related signatures in PM concentrations and size-related indicators.

4-3. Definition of Pollution Episodes and Background Conditions

In research on air pollution, a "pollution episode" is a genuine physical state of the atmospheric system with abnormal and substantially elevated concentrations of pollutants. This increase is typically the result of a combination of factors, including enhanced emission intensity, stable meteorological conditions (such as temperature inversions or reduced boundary-layer height), and, in some cases, the transport of pollutants from surrounding regions [82].

From this point of view, a pollution episode is a phenomenon representing a change in a pollution regime from standard background conditions to abnormal or critical conditions.

However, because pollution episodes cannot be directly observed or qualitatively defined, their identification in practice requires the application of quantitative and statistical criteria. Accordingly, episodes are operationally defined by applying thresholds to pollutant concentration time series. These thresholds may be based on absolute values (e.g., health-based guideline limits) or on the statistical distribution of the data (e.g., upper percentiles) [83].

Within this framework, an episode is not merely a numerical label but rather a statistical representation of an underlying physical state of the atmosphere characterised by anomalously high pollution levels [84]. In other words, the concept of an episode has a dual nature: on the one hand, it denotes a physical phenomenon in the urban–atmospheric system associated with pollutant accumulation or intensified emissions; on the other hand, for analytical and comparative purposes, it is identified and extracted using statistical methods [83]. Consequently, the definition of an episode is inherently dependent on the objectives of the study and on the type and temporal resolution of the available data [84]. episodes can be considered as extended periods of continuously high concentrations in studies focusing on large-scale atmospheric processes. In contrast, in studies based on hourly data and aimed at characterising urban behaviour, episodes may be defined as individual hours exhibiting unusually high pollutant levels [83], [84].

This approach demonstrates that an episode is not purely a statistical construct, but rather a physical atmospheric phenomenon that is detected through statistical tools. Therefore, the use of statistical criteria to define episodes does not imply a simplification of the underlying physical reality; instead, it provides a practical means of extracting and comparing abnormal pollution states from observational datasets. On this basis, the distinction between episodic and background conditions enables the investigation of differences in particle characteristics, emission sources, and the role of meteorological factors [85].

To distinguish high-pollution conditions (episodes) from typical background levels, a percentile-based threshold was adopted. This choice was motivated by the fact that unusually high particulate matter concentrations are mainly represented by the upper tail of the distribution, while most observations describe ordinary urban aerosol conditions. In contrast to fixed concentration limits based on regulatory standards, percentile thresholds are derived directly from the dataset itself. This approach makes it possible to adapt the distinction between episode and background conditions to the features of the monitoring site, rather than to predefined external limits [86].

In practical terms, the 90th percentile (P90) represents the value below which most observations are found, while only a small fraction of the data lies above it. To determine this threshold, after hourly PM concentrations for all days of January have been ordered from the lowest to the highest values, the concentration corresponding to P90 was then extracted. Because this value is expressed in the same unit as the original measurements (μg/m³), it maintains the physical meaning of the data and simply indicates its position within the overall distribution.

All hours exceeding this threshold were classified as episode conditions, whereas the remaining observations were assigned to background conditions. In this framework, episode periods correspond to the upper tail of the concentration distribution and are commonly linked to specific emission sources or atmospheric accumulation processes.

The 90th percentile was chosen as the threshold for defining pollution episodes to balance the severity of the selected conditions with the number of available observations. A lower threshold, such as the 85th percentile, would include many moderately polluted hours and therefore reduce the distinction between background levels and clearly elevated concentrations while very high thresholds (e.g., the 95th or 99th percentile) would isolate only a small number of extreme cases, causing the analysis to rely heavily on a limited set of values and reducing its statistical robustness. The 90th percentile allows the analysis to focus on the upper part of the concentration distribution, where unusually high values occur, and there are still enough data points for statistical comparisons reliably [83].

On this basis, the 90th percentile was adopted in the present study to distinguish episode hours from background conditions. This choice makes it possible to identify periods marked by unusually high particulate matter concentrations without relying on fixed regulatory limits. The resulting classification provides a coherent framework for comparing particle behaviour under episode and background regimes and for interpreting differences in urban aerosol characteristics under contrasting pollution conditions.

Like the existing literature on air quality analysis, in this study, the 90th percentile criterion is applied for distinguishing episode hours from background conditions. This criterion enables the identification of hours during which anomalously high concentrations of particulate matter are present. Additionally, it ensures independence from regulatory criteria. The application of

such a criterion enables a holistic framework for comparing the behaviour of particles during episode and background conditions. Moreover, it enables an informed assessment of differences in the characteristics of urban aerosol during contrasting conditions.

4. 4. Size-Related Interpretation Using the Ratio PMs

4. 4. 1. PM1/PM10 ratio

After identifying the pollution episodes, the PM1/PM10 ratio per hour was computed as follows:

$$R = \frac{PM_1}{PM_{10}} \quad (1)$$

PM1 represents the mass sum of particles with an aerodynamic diameter ≤ 1 μm. The PM1 component represents the submicron fraction of particulate matter. The PM1 component is dominated by particles generated by combustion processes and those generated by secondary aerosol formation. The ratio (R) represents the proportion of submicron particulates in the total PM10 mass in the environment. Higher values of the PM1/PM10 ratio indicate that ultrafine and very fine particles dominate PM10. On the other hand, lower values of the PM1/PM10 ratio indicate the opposite. Thus, the PM1/PM10 ratio helps in identifying pollution regimes dominated by ultrafine and very fine particles compared to those dominated by coarse particles.

4. 4. 2. PM2.5/PM10 ratio

the $PM_{2.5}/PM_{10}$ ratio value for each hourly observation was calculated as:

$$R = \frac{PM_{2.5}}{PM_{10}} \quad (2)$$

As $PM_{2.5}$ represents the sum of the mass of particles with an aerodynamic diameter ≤ 2.5 μm, it shows a subset of PM_{10}. This ratio(R) shows the contribution of fine particulates to the total mass in the environment. The greater the ratio value, the greater the dominance by fine particulates, and vice versa. This ratio helps to recognize changes in size regimes.

4. 4. 3. PM4/PM10 ratio

The PM4/PM10 ratio was also computed as follows:

$$R = \frac{PM_4}{PM_{10}} \quad (3)$$

PM4 represents the mass sum of particles with an aerodynamic diameter ≤ 4 μm. The PM4 component represents an intermediate range of particulate matter. The PM4 component represents an intermediate range of particulate matter. The PM4/PM10 ratio helps in identifying the proportion of respirable particles in the total PM10 mass. Higher PM4/PM10 ratio values indicate that a large proportion of PM10 mass falls in the respirable range. On the other hand, lower PM4/PM10 ratio values indicate that a large proportion of PM10 mass falls in the coarse particle range.

4. 5. Effective Density of Particulate Matter (ρ_{eff})

The effective density of the particles, represented by ρ_{eff}, measures the ratio of particle mass concentration to particle volume concentration over a certain range of particle size. While particle number-based parameters, such as CN, represent particle concentration, and mass-based parameters, such as PM2.5 and PM10, represent mass per unit volume of the atmosphere, ρ_{eff} provides information on the physicochemical structure and compactness of aerosol particles [87].

ρ_{eff} may be represented mathematically as

$$\rho_{eff} = \frac{Cm}{V} \quad (4)$$

In this study, Cm was derived using an optical spectrometer, whereas V was derived by summing dV over the range of valid size measurements of the spectrometer (0.18-18 μm). While ρ_{eff} represents information on the chemical composition of aerosol particles, it also provides information on the morphology of the particles. In the atmosphere, aerosol particles are rarely compact and may exist in other forms, for example, fractal structures, internally mixed particles, and hygroscopic particles. Therefore, ρ_{eff} is always less than the actual density of the chemical components of the aerosol particles [88].

From a source perspective, the value of ρ_{eff} varies significantly depending on the dominating source of emissions. For example, the density of soot and traffic aerosol, which are associated with combustion emissions, tends to be lower compared to other types of aerosols, such as dust and sea salt, which have a more compact structure and a crystalline composition [89]. Therefore, the variation of ρ_{eff} over time can be attributed to changes in the dominating source of emissions.

Atmospheric aging and secondary aerosol formation also affect the value of ρ_{eff}. For example, secondary inorganic aerosol species, such as ammonium sulfate and ammonium nitrate, and secondary organic aerosol formed through photochemical reactions, increase the compactness of the aerosol and, consequently, the value of ρ_{eff} compared to freshly emitted soot aerosol. In addition, hygroscopic growth of aerosol under high relative humidity can also affect the volume of the aerosol, leading to a change in the value of ρ_{eff} [90].

The relationship between effective density and meteorological parameters is complex and nonlinear. Temperature and solar radiation influence the photochemical activity and the formation of secondary aerosol particles. Relative humidity affects the hygroscopic growth and phase change of particles. Similarly, wind speed affects the boundary layer. Thus, the variation in effective density is influenced by a variety of atmospheric processes. It is not influenced by a single factor [91]. While the regulatory guidelines traditionally focus on mass-based metrics like PM2.5 and PM10, the importance of particle physicochemical properties, which include density, morphology, and mixing state, is increasingly realized for the assessment of human health-relevant exposure. Effective density is significant for the interpretation of the behaviour of particles during the deposition in the respiratory tract and the progress of aerosol modelling and source apportionment studies [92].

Effective density was calculated over the entire size range using the formula above. Consistency was checked between the mass and volume measurements. Unit conversions were carried out for ensuring dimension consistency. Similarly, quality controls were performed on the data for the removal of zero values and other invalid values. Thus, the effective density values were not considered material density values.

4. 6. Particle number concentration (CN)

The particle number concentration, denoted as CN, represents the number of particles present per unit volume of air, typically expressed as particles per cubic centimetre or particles per cubic metre. In contrast to mass-based parameters like $PM_{2.5}$ and PM_{10}, which represent the mass concentrations of particulate matter, CN represents a number-based measurement of particle concentration [93]. As CN represents a count-based measurement rather than a mass-based measurement, CN is heavily influenced by ultrafine particles. Ultrafine particles are particles that have a diameter of less than 100 nm and contain a negligible amount of mass. As a result, CN and $PM_{2.5}$ are not typically representative and may be controlled by different mechanisms and sources [94].

From a source perspective, CN in urban areas is heavily controlled by combustion-related emissions, particularly from road traffic. In addition, nucleation processes also play an important role. From a series of reviews and measurement-based studies, nucleation and traffic emissions are key factors that influence urban ultrafine particles/PNC. In urban areas, particle number is composed primarily of ultrafine particles [95].

The relationship between CN and meteorological parameters is complex and nonlinear. Temperature and solar radiation influence photochemistry and nucleation processes. In addition, relative humidity may influence aerosol processes and particle evolution. In terms of meteorology, multi-site studies of nucleation and urban particles indicate that meteorology controls particle number through a variety of mechanisms rather than a simple linear effect [96]. While there has historically been a major emphasis on mass-based parameters like PM, there is growing evidence that exposure to ultrafine particles, which are related to CN and PNC, is linked to adverse health effects. In addition, major health advisory bodies have emphasized the importance of UFPs and have encouraged further evidence development [97].

4. 6. 1. Dataset and temporal structure

Particle number concentration (CN) data which were recorded hourly for January 2025 analysed to investigate temporal patterns and their relationship with pollution episodes. The values of CN are expressed as particles per cubic centimetre (P/cm^3) to demonstrate the number of particles present in the atmosphere.

4. 6. 2. Classification of weekdays and weekends

The data was classified into weekdays and weekend days to analyze the behavior of the activities in the urban area, particularly those associated with traffic emissions. Based on the standard European convention, Mondays to Fridays are regarded weekdays, and Saturdays and Sundays as weekends and the 1st of January was considered as a weekday by using calendar of 2025.

4. 6. 3. Derivation of the diurnal CN profile

A diurnal curve was selected as a proper tool to illustrate typical daily behaviour of CN. The average CN concentration was calculated for each hour of a day during the January month and apart from this general diurnal pattern, separate diurnal profiles for weekdays and weekends were also calculated to highlight differences related to human activity patterns.

4. 6. 4. Definition of urban peak indices

To quantify the intensity of urban temporal patterns, morning and evening peak indices were defined corresponding to urban traffic hours.

- Morning peak: mean CN concentration during 07:00–09:00
- Evening peak: mean CN concentration during 18:00–21:00

To provide a strong reference level, the daily trough was defined as the minimum of the mean diurnal curve of CN concentration rather than the overall minimum of the data, as the latter might affect the trends with outliers or small-scale variations. Then the ratio of peak both morning and evening -to-trough was separately calculated.

calculation of these indices is involved entire data and even were calculated for weekdays and weekends, preparing the quantitative estimation of the strength of the urban activity signals within CN.

4. 7. Pollution Episode vs Background Analysis

The pollution events were identified without consideration to CN, using $PM_{2.5}$ concentrations to study the CN concentrations in the context of a mass-related pollution event. Given that both

datasets shared the same temporal resolution (hourly), identical time coverage, and identical ordering of records, the Episode/Background classification was transferred directly from the $PM_{2.5}$ dataset to the CN dataset. A consistency check was performed to ensure correct temporal alignment, including verification of the number of episode hours and a logical comparison of CN levels between episode and background conditions. After this integration, the concentrations of CN in episodes and background data were compared statistically. The descriptive statistics done include:

- Average CN concentration in episodes and in background conditions

- Median CN concentration (if required)

- Number and fraction of hours classified as episodes

- Ratio of episode to background mean CN concentrations

To explain the distributional discrepancies, values for episode and background conditions in the CN measure were passed through separate subsets and evaluated by distribution plots such as box-and-whisker plots.

Chapter 5:

Results and Analyses

5.1. Particulate Matter mass concentration behaviour and Size Fractions

This section presents the temporal behavior of PM mass concentrations across different size fractions. Daily and diurnal variations are examined together with size-segregated ratios.

The daily mean time series for PM1, PM2.5, PM4, and PM10 shows high variability over the monthly time period. It starts with a high concentration at the beginning of the month, followed by a sharp fall in concentration over the initial few days. Thereafter, it shows a series of maxima and minima, indicating multiple episodes of high and low concentrations, rather than a monotonic trend.

A secondary peak is seen in the middle of the month, followed by a fall in concentrations to the minimum, which is seen on days 19-22. Finally, in the later part of the month, PM concentrations are relatively low and constant, with only moderate fluctuations.

The concentrations of PM1, PM2.5, PM4, and PM10 vary in parallel over the month, and their relative order remains the same, with PM10 > PM4 > PM2.5 > PM1. This supports the idea of cumulative size distribution and suggests that changes in concentrations over time are driven primarily by changes in the overall amount of particles, rather than changes in size distribution. The presence of distinct daily maxima supports the idea of episodic pollution events with a background concentration.

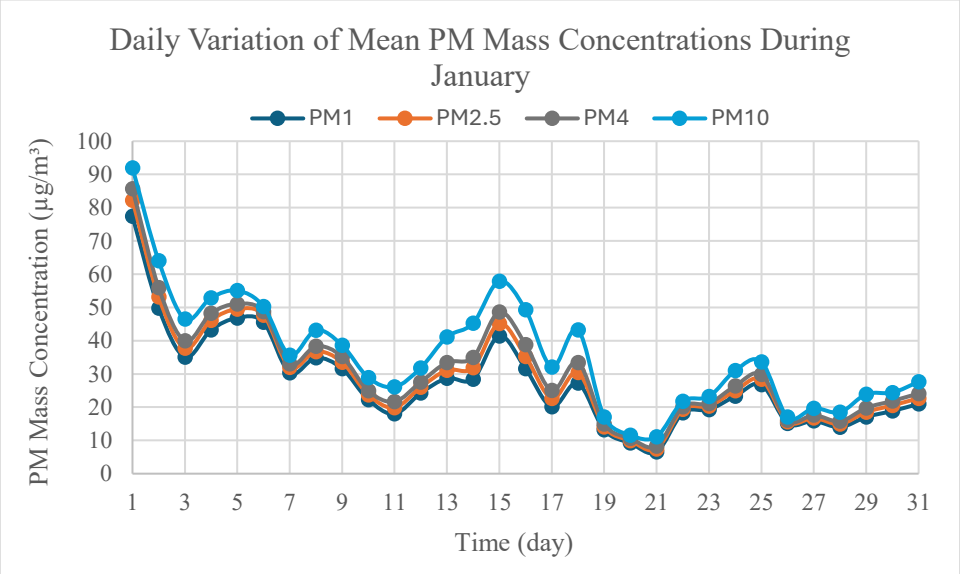

Fig8 .. Daily mean concentration of PMs over the study period

The daily mean mass ratios PM_1/PM_{10}, $PM_{2.5}/PM_{10}$, and PM_4/PM_{10} vary moderately from day to day throughout the month but remain within a relatively narrow range, suggesting a relatively stable particle size distribution. The three particle size ratio time series move in parallel and maintain the same ranking throughout the month, with PM_4/PM_{10} always the highest, $PM_{2.5}/PM_{10}$ in the middle, and PM_1/PM_{10} the lowest. This pattern is consistent with the cumulative nature of the size fractions and the lack of sudden changes in particle size distribution. A clear minimum in the particle size ratios occurs around day 21, where all three particle size ratios simultaneously drop, indicating a temporary increase in the proportion of coarse particles. However, several days throughout the month, particularly in the early and late days, experience a maximum in the particle size ratios, indicating a larger proportion of fine particles in the PM_{10} mass. The particle size ratios vary relatively smoothly from day to day in comparison to the daily PM mass data, with a relatively low amplitude. This pattern suggests that the vast majority of days with large PM mass are driven by a general increase in PM mass rather than a dramatic change in particle size composition.

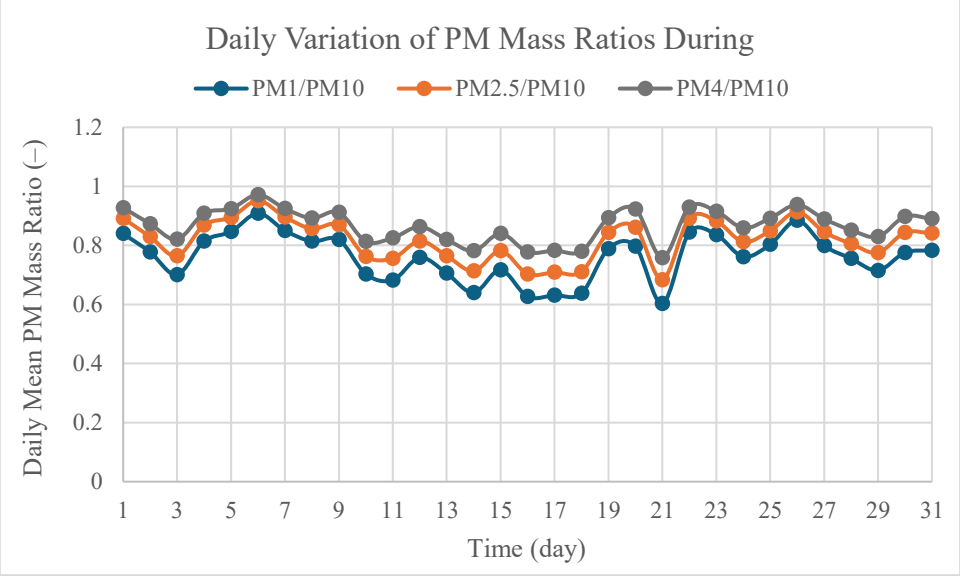

Fig. 9. Daily mean ratios of PM_1/PM_{10}, $PM_{2.5}/PM_{10}$, and PM_4/PM_{10}

The diurnal pattern of cumulative mass concentration of particulate matter of size fractions PM1, PM2.5, PM4, and PM10 shows a coherent and synchronized temporal sequence for all size fractions. In other words, all PM size fractions show an equivalent hourly pattern, suggesting that the major drivers are affecting the entire mass concentration and not any

individual fraction of PM. Elevated mass concentration levels are evident in the late night and early morning hours, which are then followed by a gradual fall in concentration in the early morning hours. After this, there is a moderate peak in the late morning hours, which then shows a gradual fall to a minimum in the mid to late afternoon period, i.e., between 15:00 and 18:00 hours. After this period, the PM concentration levels show an increase again in the evening and nighttime hours.

Throughout the day, the expected order of cumulative size fraction concentration is maintained, i.e., PM10 > PM4 > PM2.5 > PM1, which further reinforces the physical validity of the results and the proper handling of the cumulative mass concentration fractions. The minimum concentration levels in the afternoon period are expected to result from enhanced mixing and development of the boundary layer, which are known to facilitate the dispersion of pollutants. Conversely, the higher concentration levels in the nighttime and early morning hours could result from unfavorable mixing conditions in the atmosphere. In addition, the mass concentration diurnal pattern does not show any major double peak, which is expected in purely traffic-influenced PM concentration patterns. This further reinforces the assumption that mixing conditions in the atmosphere are most probably responsible for the PM concentration pattern.

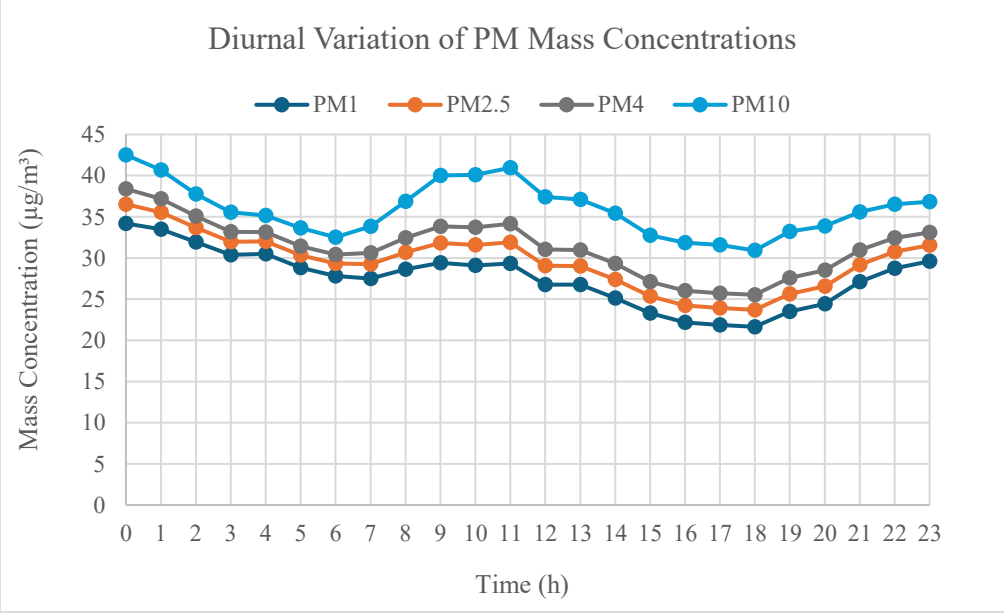

Fig. 10. Diurnal profiles of hourly mean PM mass concentrations

The diurnal profile of the PM mass ratios shows an identical pattern in the three fractions: PM1/PM10, PM2.5/PM10, and PM4/PM10. The three fractions decline slightly until the afternoon and then increase in the evening hours.

The high values in the early morning and evening hours and the low values in the midday hours are evident from the diurnal profile. This shows that the contribution of fine particles is significant when the atmosphere is not mixed as strongly, and midday hours indicate higher concentrations of coarse particles. The diurnal profile shows that the three fractions maintain their relative order throughout the day. The highest curve is that of PM4/PM10, followed by PM2.5/PM10 and then PM1/PM10. This shows that these fractions are cumulative in nature.

From the graph, the fine particles make up a significant fraction of the composition of PM10, and the weather conditions affect the fraction composition.However, the diurnal pattern does not exhibit a clear double-peak structure corresponding to typical traffic rush hours; instead, the variations are smoother and more consistent with boundary layer development and atmospheric mixing than with a purely traffic-driven signal.

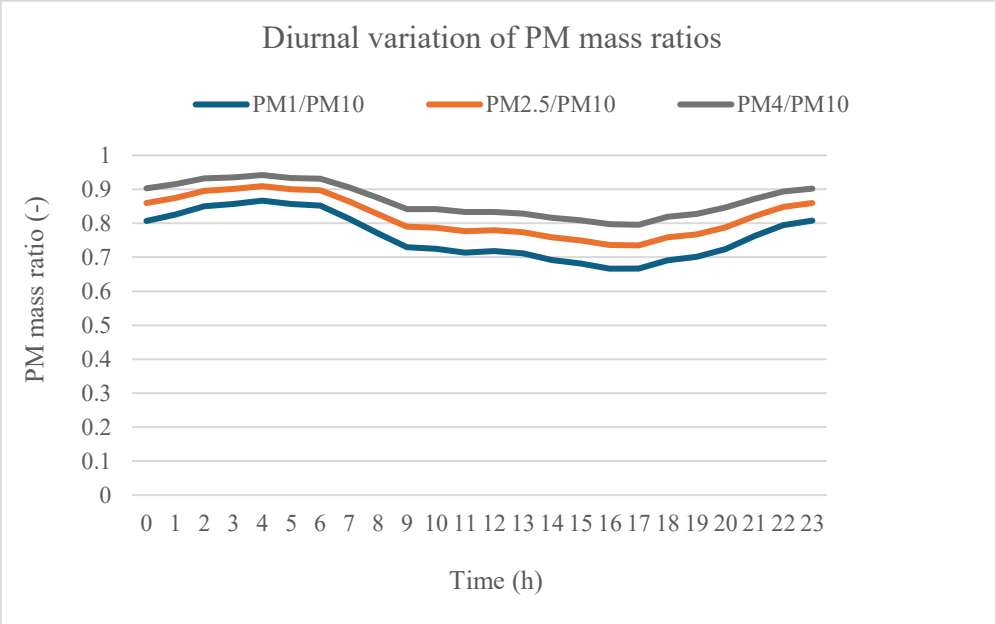

Fig. 11. Diurnal variation of PM mass ratios relative to PM_{10}

Figure.12 below illustrates the hourly variation of PM1/PM10, PM2.5/PM10, and PM4/PM10 mass ratios. From an analysis of these hourly average values, it is apparent that there is a regular diurnal pattern. The values of these mass ratios increase during late night and early hours of

the morning, from 02:00 to 06:00. After that, they decrease steadily, with a minimum occurring in the middle of the day, around 15:00-17:00. In the evening, these values begin to increase again. It is noticeable that PM4/PM10 is always higher than PM2.5/PM10, and PM1/PM10. There are no intersections between these curves. This means that there were no sudden changes in the relative importance of these size fractions during the day. Although these variations are small, PM1/PM10 variations seem a bit more evident compared with those of PM2.5/PM10 and PM4/PM10. The timing of maximum and minimum values is consistent with the regular daily development of the boundary layer, with lower heights during night hours and higher heights in the afternoon. It can be concluded that there were no sudden changes in size distribution during the day. Instead, there were gradual changes, consistent with regular diurnal development.

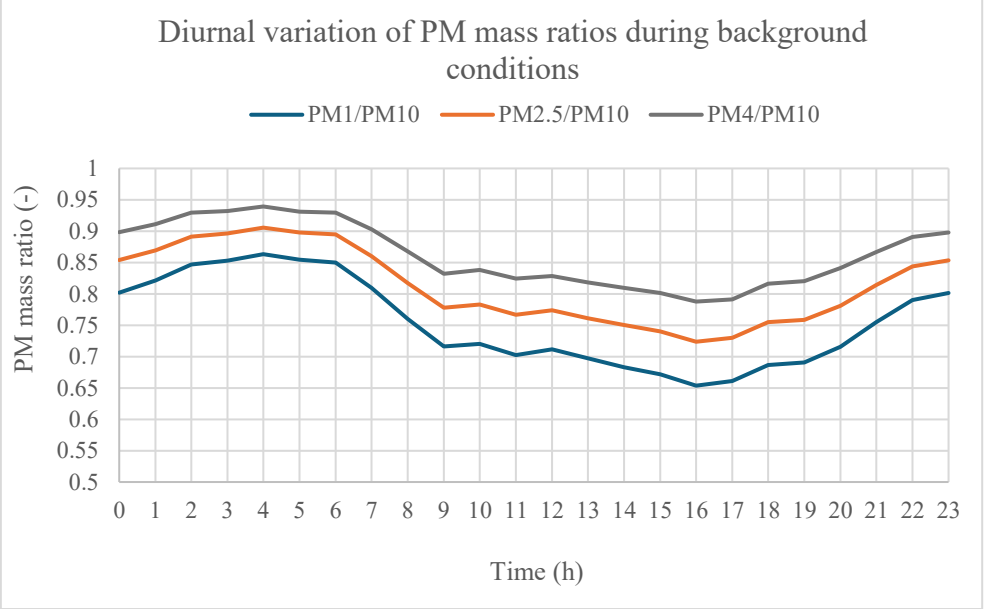

Fig. 12. Hourly variation of PM size-fraction ratios to PM_{10}

Figure 13 shows the temporal evolution of the mass ratios of PM1/PM10, PM2.5/PM10, and PM4/PM10 during the entire period of the pollution episodes. The ratios are elevated compared with the background conditions, and the diurnal variations show specific features. The ratios remain elevated during most of the hours. Specifically, the mass ratio of PM1/PM10 tends to remain above 0.85, whereas the ratios of PM2.5/PM10 and PM4/PM10 remain close to or above 0.90. This means that during the episode days, a large fraction of the mass of the PM10 is associated with fine particles.

During the night and the early hours of the day, the ratios remain relatively stable and are already elevated. A small increase is observed around midday (11:00-13:00), more pronounced for the ratios of PM2.5/PM10 and PM4/PM10. During the hours of the day (14:00-17:00), the values of the ratios decrease somewhat, and then they increase during the hours of the night. The ranking of the three ratios remains the same throughout the day. The highest values of the ratios are for the mass ratio of PM4/PM10, followed by the mass ratio of PM2.5/PM10, and then the mass ratio of PM1/PM10. The three curves do not intersect, meaning that the size structure of the aerosols is preserved during the entire period of the episode, and the only change is the shift of the entire curve to a higher level compared with the background conditions.

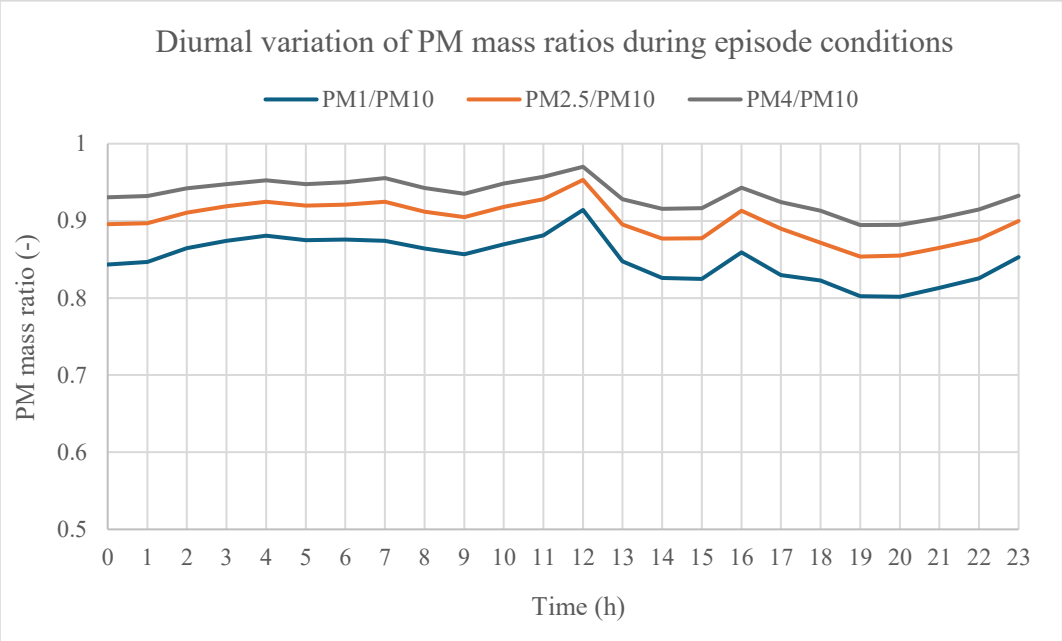

Fig. 13. Diurnal evolution of PM mass ratios during pollution episodes

The daily pattern of concentration shows a clear peak for each PM mass category: PM1, PM2.5, PM4, and PM10. For each of the PM mass categories, the minimum concentrations are observed in the evening, along with the observation of increased concentrations during the night and the morning, with midday concentrations peaking in between.

As is expected from their accumulation characteristics, their concentrations also peak most strongly for each time interval with PM_{10}, followed by PM_4, $PM_{2.5}$, and PM_1. Although their magnitudes vary, their patterns track one another over the course of a day, which suggests that

there is similar controlling influence over the entire size range, rather than one size range being affected differently from all the others.

The concentrations in the evenings decrease, and this trend aligns well with the stronger mixing and dispersion that often occurs in the atmosphere from the afternoon to the evening. The converse is also true, where the high concentrations at night and during the morning reflect well the stable conditions, weaker dilution, and boundary layer.

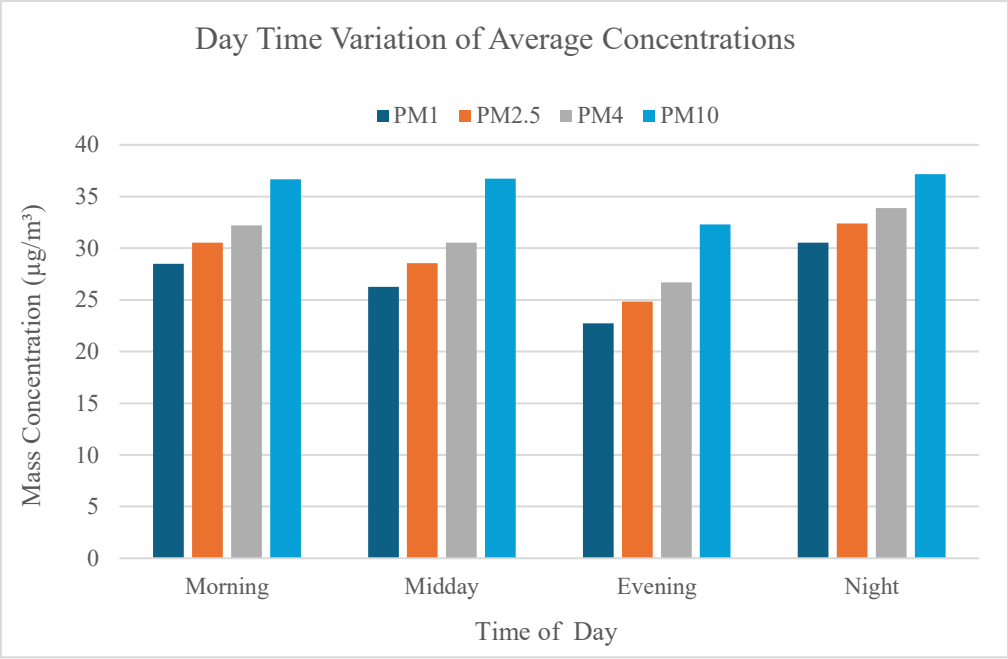

Fig. 14. Average diurnal pattern of PM mass concentrations by size fraction

The diurnal variation in PM mass ratio follows a definite and consistent pattern over all time categories. The three PM mass ratios PM1/PM10, PM2.5/PM10, and PM4/PM10, follow a similar temporal trend. The minimum ratio is observed around midday and evening hours, while the highest ratio is observed during nighttime and morning hours.

It is also observed that nighttime experiences the highest ratio value, which means that a larger proportion of PM10 is made up of fine particles. This is because atmospheric mixing is weaker and boundary layer height is lower, which favors the accumulation of fine particles. On the other hand, lower ratio values observed around midday and evening hours suggest that coarse particles make up a larger proportion of PM10, which is because vertical mixing is stronger and atmospheric dilution is effective during these times.

It is observed that over all time categories, PM2.5/PM10 is always higher than PM1/PM10, while PM4/PM10 is always the highest ratio, as expected from their cumulative size range. The relative positions of the three PM mass ratios remain constant over time, with parallel curves. This suggests that the diurnal evolution is smooth and continuous, with no sharp peaks observed over any specific time period. The smooth and continuous temporal evolution suggests that there is no specific rush hour phenomenon. The observed temporal evolution follows a regular diurnal cycle.

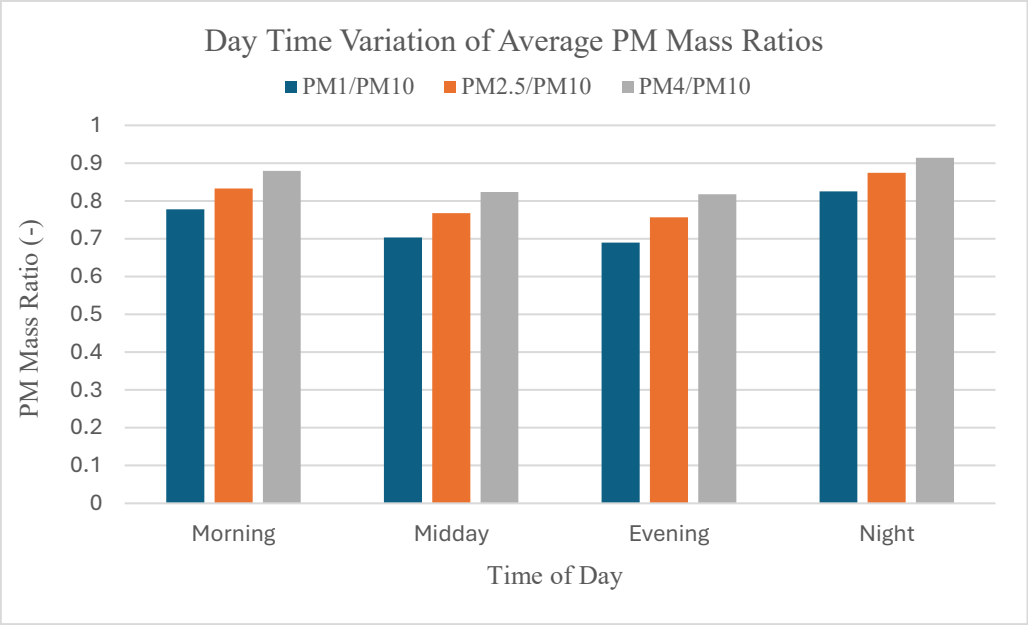

Fig. 15. Diurnal variation of PM mass ratios across time categories

Overall, it is quite evident from the above analysis that the concentrations of PM across different size fractions have been exhibiting similar trends over time, both on a daily and diurnal basis. Despite significant changes in absolute concentrations over time, their relative contribution has remained nearly constant. This suggests that changes in particle mass, not changes in particle size, have primarily caused changes in PM concentrations.

5.2. Weekly Variability of PM Concentrations and Ratios

With the aim of identifying systematic days of week patterns, PM concentrations and size ratios have been analyzed on a weekly basis.

Day of week results for average PM mass concentration show a coherent pattern for all four size fractions: PM1, PM2.5, PM4, and PM10. In all cases, PM10 has the highest concentration and PM1 the lowest on each day of the week, thereby demonstrating the internal measurement consistency.

All four size fractions of PM show similar trends on any given day of the week, with concentration increasing throughout the week to peak on Wednesday. From Thursday to Friday, the concentration decreases before rising again on Saturday and falling slightly on Sunday. Such similar trends for all size fractions of PM demonstrate that the driving forces are those that act on all PM mass concentrations rather than any particular size fraction of PM. The peak on Wednesday and the general trends throughout the week demonstrate a weekly cycle, possibly driven by the buildup of emissions and prevailing conditions, which are conducive to the nondispersal of PM. The lower concentrations of PM at the beginning and end of the week reflect less conducive conditions for the build-up of PM. Smooth trends are evident for all four size fractions of PM, demonstrating that its size composition remains stable throughout the week.

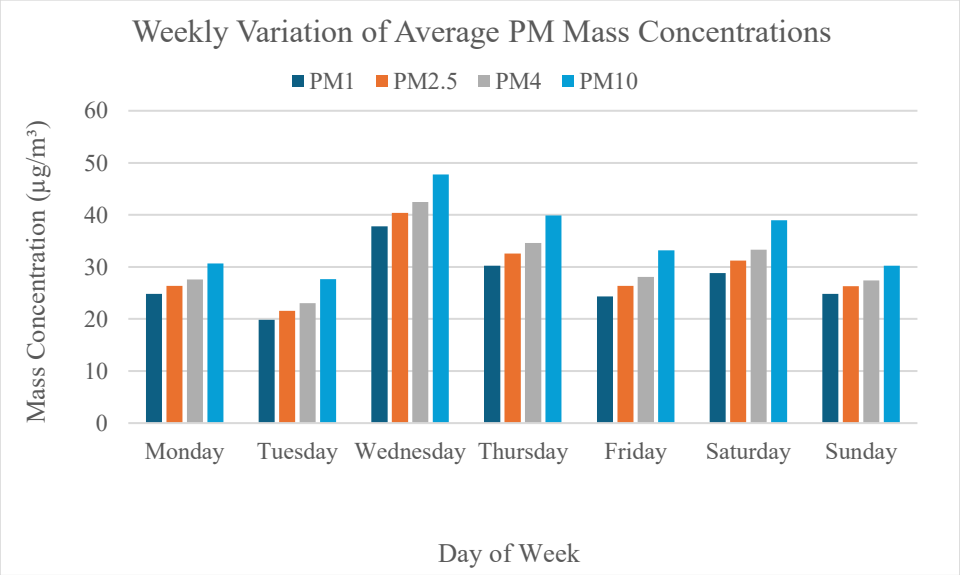

Fig. 16. Average PM mass concentrations by day of the week

The weekly variation of the ratios of PM mass has a stable and regular weekly pattern in all three fractions: PM_1/PM_{10}, $PM_{2.5}/PM_{10}$, and PM_4/PM_{10}. The three ratios are following the same pattern, with relatively higher values at the beginning and end of the week and relatively lower values on Tuesday and Friday.

Overall, the ratio of PM_4/PM_{10} is the largest on all days of the week, followed by the ratio of $PM_{2.5}/PM_{10}$ and the ratio of PM_1/PM_{10}, as expected from the definition of the particle size fractions as the cumulative size fractions. The ranking of the three ratios is maintained during the entire week, and the three curves vary in parallel, indicating that the weekly variation is not related to sudden changes in the dominant particle sources.

The decrease in the three ratios during the middle and end of the week indicates that there are relatively more mixed or coarse particle contributions during this period, while the relatively higher ratios on Monday and Sunday suggest relatively more fine particle contributions to the mass of the PM_{10} fraction. The smooth variation of the three ratios during the week, without sharp peaks, indicates that the weekly variation is not related to sudden changes in the sources of the three fractions of the PM mass but rather to regular patterns of human activity and the atmosphere.

The fact that the three ratios of the fractions of the mass of the PM exhibit the same weekly variation supports the suggestion that the weekly variation is related to regular patterns of human activity and the atmosphere rather than to sudden changes in the sources of the three fractions of the mass of the PM.

While the weekly averages show a stable and regular pattern in PM mass ratios, examining individual weekdays across different weeks reveals substantial variability in absolute PM concentrations.

When individual Mondays are compared, a wide range of variability is seen in PM mass concentrations from week to week. The range for PM10 concentrations is from approximately 12 to 50 $\mu g/m^3$. This range shows that Monday concentrations vary significantly with episodic conditions and do not follow a set pattern. Similar variability is also seen with PM2.5 and other fractions. In contrast, PM mass ratios vary by a smaller range and continue to follow their expected ranking from week to week. This may suggest that while the total mass concentration may vary significantly from week to week, the size composition remains steady. The analysis above suggests that when examining weekly averages, episodic conditions should always be considered as a factor. Based on representative checks across multiple weekdays (Monday, Wednesday, and Saturday), PM mass concentrations show substantial week-to-week variability, while PM mass ratios remain comparatively stable. This indicates that the monthly and weekly patterns reflect averaged tendencies influenced by short-term events rather than strictly repeatable day-specific behavior.

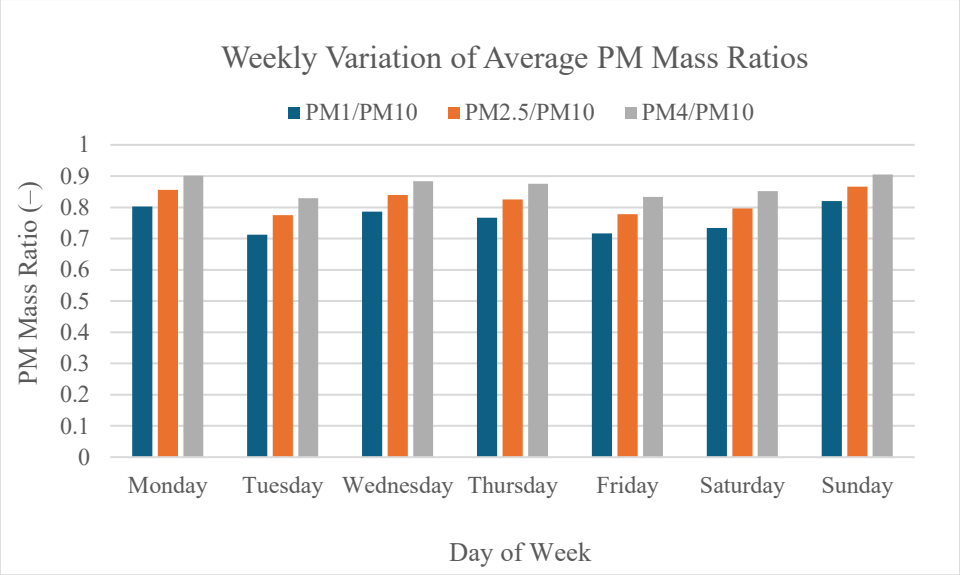

Fig. 17. Weekly variation of PM mass ratios

The above analysis over weekly periods shows moderate variability in PM concentrations during the week, while the size composition remains almost unchanged. Although the overall concentrations vary over time, the relationships among the size fractions remain relatively stable throughout the week, indicating that PM variability is mainly associated with changes in particle mass rather than particle size.

5.3. Site Location and Traffic Context Analysis

The location of the measurement site is at the Politecnico di Torino (DIATI department), which is in close proximity to Corso Castelfidardo. This is a major traffic route and is likely to experience a constant flow of commuting traffic during the day. Thus, the location of the measurement site provides a good condition to study the potential effect of traffic-related emissions on the concentrations of particulate matter.

The traffic conditions around the measurement location were evaluated using the Google Maps traffic tool, which provided information about the traffic conditions around the location over a week. The color scheme provided in the Google Maps traffic tool is a good indicator of the traffic conditions around the location. The colors change from green to yellow to red, depending upon the speed of the vehicles in relation to the typical conditions of the road. The traffic conditions around the location were found to be constant throughout the day, with a higher occurrence of congested conditions in the morning and the late afternoon/early evening

periods. The midday conditions were found to be moderate, whereas the nighttime conditions were found to be low to moderate. Severe conditions were found to be very few, indicating that such conditions are not constant around the location. The diurnal pattern of PM concentrations also showed some similarity in the periods of the day when the concentrations were higher. The PM concentrations were found to be higher in the morning, which could be attributed to the higher traffic conditions during the day. However, the higher ratio of fine particles was also observed during the nighttime, which could be attributed to the effect of meteorology. Note that the Google Maps traffic is a qualitative tool and does not provide information about the quantity of the traffic.

The analysis of the site location and surrounding traffic conditions suggests that local emissions may contribute to the observed PM variability. However, the time evolution of PM should also be related to the effects of the atmospheric mixing conditions. This implies that the observed variability of PM is associated with the combined effects of emissions and meteorology.

5.4. Meteorological parameters

The main meteorological variables observed during the study period are summarized here. Their temporal behavior is shown before evaluating their influence on PM.

The figure shows the hourly average air temperature in Turin calculated from all measurements recorded during the month of January.

Each point represents the mean value for that specific hour aggregated over the full monthly dataset. Temperature decreases gradually from midnight toward the early morning hours, dropping from about 5°C to a minimum near 4°C around 05:00–06:00. After this time, a steady increase begins, becoming more noticeable after approximately 09:00. Between late morning and mid-afternoon, the curve rises continuously, reaching its highest hourly averages around 14:00–16:00, with values slightly above 8°C. After the afternoon maximum, temperatures decline progressively through the evening and nighttime hours, with a smooth downward slope toward late-night values near 5°C.

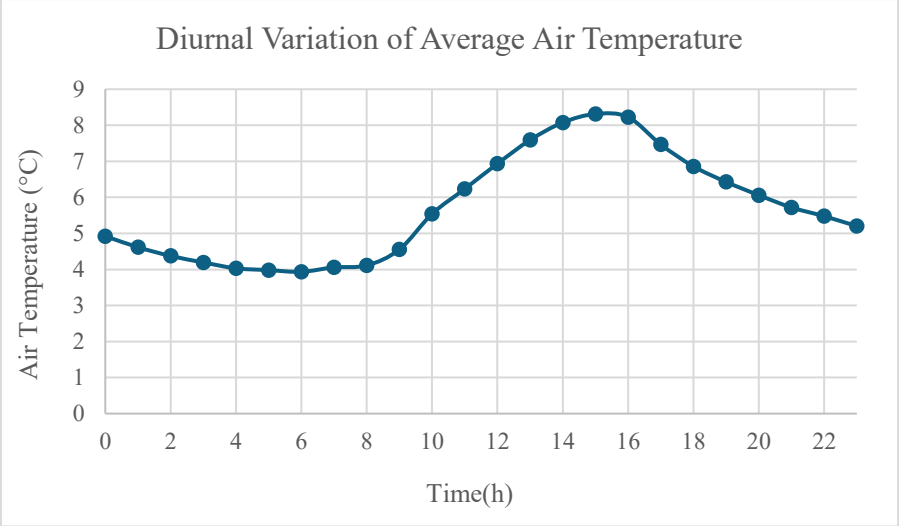

Fig. 18. Hourly mean air temperature profile for the study month

The graph below represents the hourly averages of the dew point temperature, which have been aggregated over the entire month. During the night and early morning, the dew point temperature is relatively low and steady, increasing from about 1.35°C at midnight and continuing down towards a minimum at about 1.05–1.10°C at 05:00–06:00. The dew point temperature increases continuously from early morning, with a sharp increase between 09:00 and 11:00, during which time the temperature increases from about 1.35°C to a range of 1.8–1.9°C.

The late morning and early afternoon period represents a broad plateau with minor fluctuations at a temperature range of 1.9–2.0°C. The maximum hourly averages occur during the early evening period, between 17:00 and 19:00, during which time the dew point temperature slightly exceeds 2.1°C. From this maximum, a gradual decrease is seen through the late evening, with a decrease towards a temperature of about 1.7°C at 23:00.

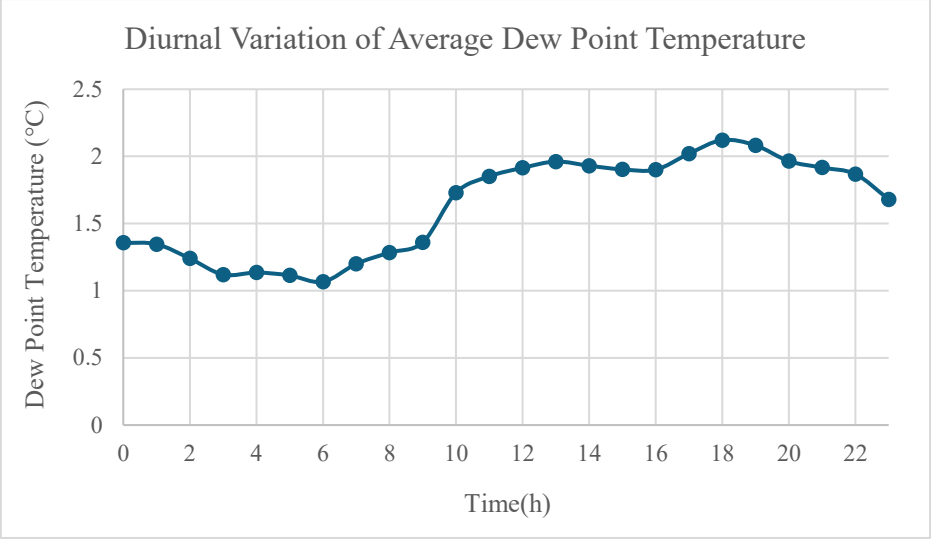

Fig. 19. Hourly mean dew point temperature profile

The graph represents the hourly average relative humidity in the study area, obtained by considering the complete set of observations available for January. The maximum levels of relative humidity occur during nocturnal and early morning hours, with levels between 78% and 82% prevailing between midnight and roughly 08:00 local time. There is a gradual decrease after the morning period, with a steady decrease starting at 09:00. The minimum levels of hourly averages are found between 14:00 and 16:00, with levels dropping down to between 65% and 67%. Then, there is a steady increase during the late afternoon and early evening, with levels rising towards the upper end of the range by late evening.

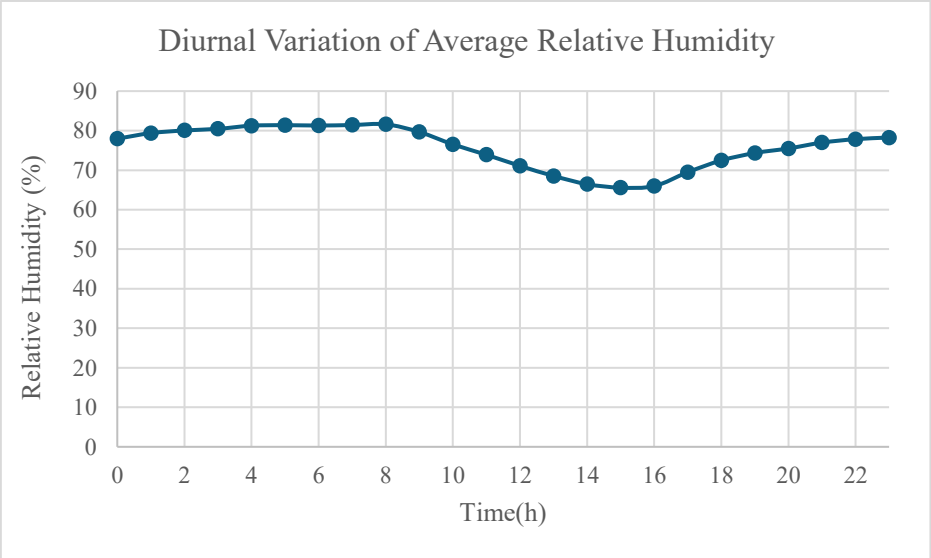

Fig. 20. Hourly average relative humidity profile

Figure.21 shows the hourly average air pressure, calculated by aggregating the measurements on an hourly basis in January in Turin. Air pressure shows an overall trend of gradual decline from midnight into the early morning, with pressure levels ranging from 988.1 hPa to a minimum value close to 05:00, where levels are close to 987.0 hPa.

Following the minimum pressure in the early morning, pressure levels gradually increase during the morning, reaching a maximum value between 10:00 and 11:00, with levels slightly higher than 988 hPa. After that, air pressure shows a significant decline between 12:00 and 15:00, during which the hourly average air pressure levels reach their minimum value, close to 986.6 hPa. Following that, air pressure levels show an increasing trend during the evening and night hours, with levels continuously increasing from 16:00 to 23:00, close to 988 hPa.

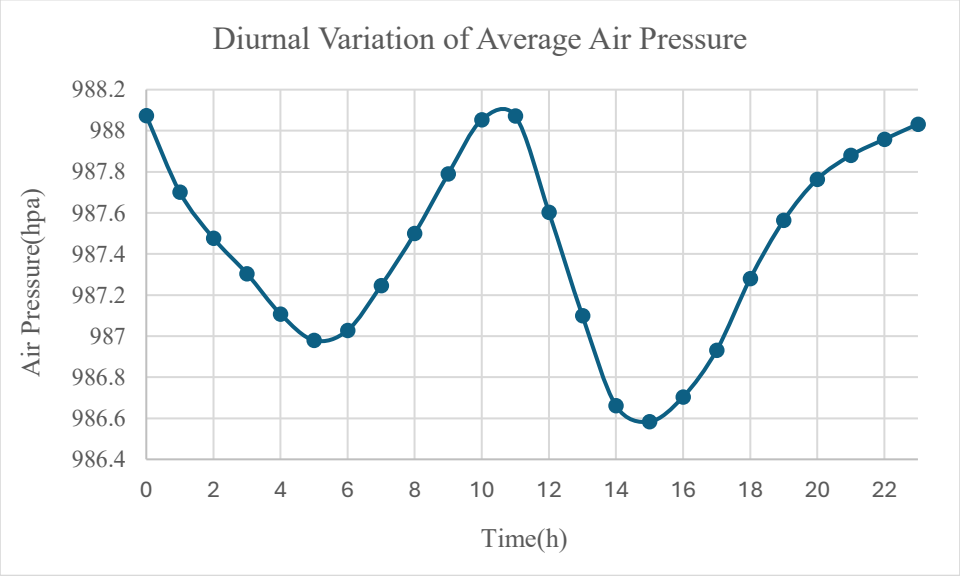

Fig. 21. Hourly average air pressure profile

5.5. Impact of Meteorological Conditions on PM Mass

This section examines how PM concentrations vary across meteorological classes. Results are grouped by humidity, temperature difference, and pressure conditions.

5.5.1. Relative humidity

The figure shows the variation in the mean PM mass concentrations as a function of the different relative humidity (RH) classes. It can be seen that there is a consistent variation with

humidity levels for all particle size fractions. The maximum concentrations are measured at intermediate humidity levels (RH between 60% and 80%), while they are minimized at low humidity levels (RH < 60%). The concentrations are minimized at very humid conditions (RH > 80%).

The above trend is seen for PM_1, $PM_{2.5}$, PM_4, and PM_{10}. The sum of the size fractions increases in every humidity class: $PM_{10} > PM_4 > PM_{2.5} > PM_1$. The parallel trend in all size fractions points to the fact that the meteorological conditions related to humidity levels influence the overall particle concentrations rather than a specific size range.

The decreased concentrations at high RH levels are related to increased removal processes such as wet scavenging. The increased concentrations at moderate RH levels are related to more stable meteorological conditions, as well as weaker dispersion processes.

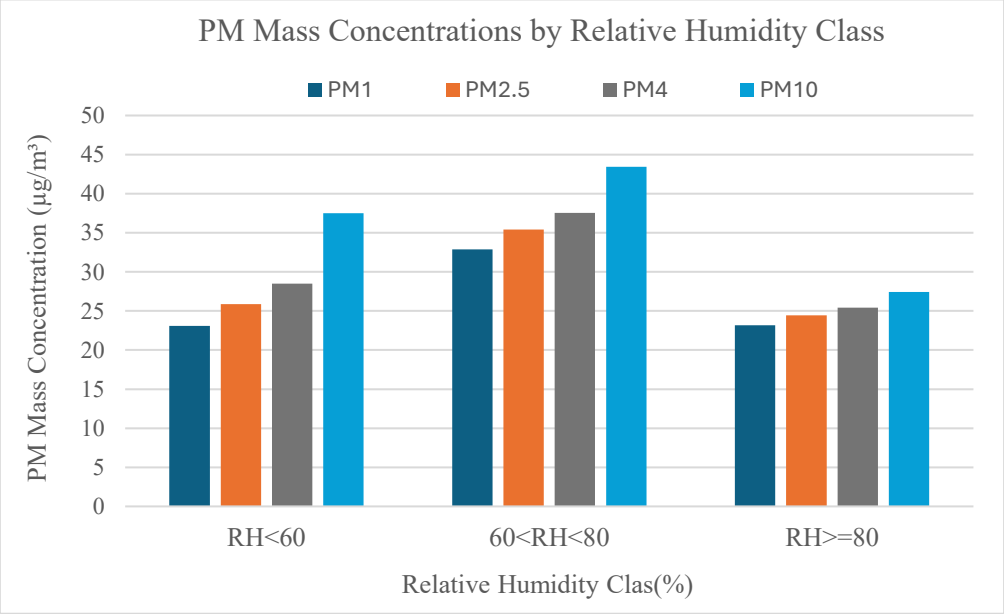

Fig. 22. PM mass concentrations across relative humidity classes

Under background conditions, the PM mass concentrations show a systematic dependence on the relative humidity (RH) class. In all particle size fractions (PM1, PM2.5, PM4, and PM10), the maximum concentrations are observed at intermediate humidity conditions (RH range of 60 to 80%), while the minimum concentrations are found at high humidity conditions (RH ≥ 80%). At low humidity conditions (RH < 60%), intermediate concentrations are found.

This trend holds true for all size fractions, including PM1, PM2.5, PM4, and PM10. The trend also holds the expected cumulative order. The uniform trend in all size fractions suggests that

meteorological conditions related to humidity have a general effect on particle concentrations rather than size-specific effects. The decreased concentrations at very high humidity conditions may be related to increased removal processes such as wet deposition or precipitation scavenging. The increased concentrations at intermediate humidity conditions may be related to more stable meteorological conditions. The findings suggest that meteorological conditions, specifically humidity, have a systematic effect on background PM concentrations.

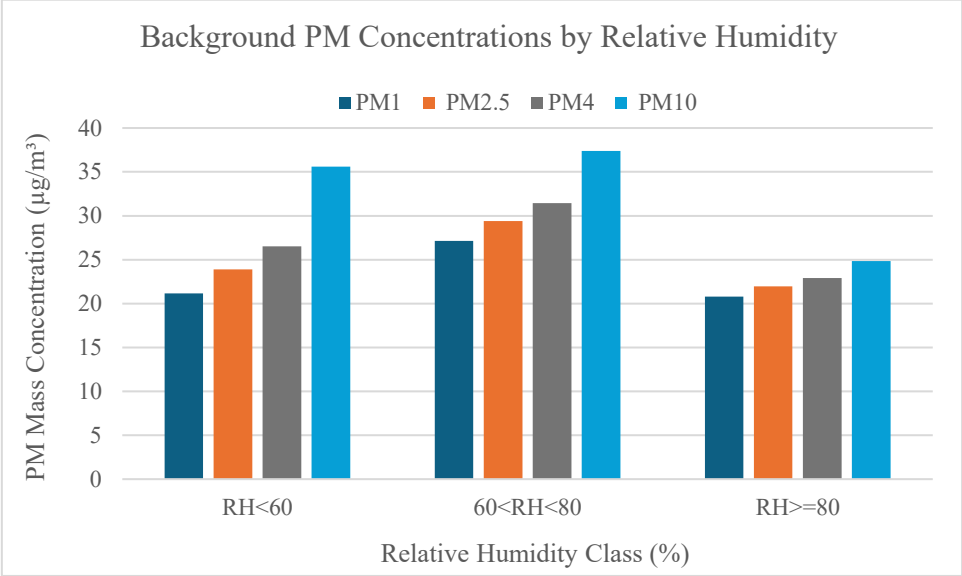

Fig. 23. PM mass concentrations versus relative humidity under background conditions

Under episode conditions, it is found that the ambient PM mass concentrations are higher than those under background conditions for all size fractions. Moreover, a clear relationship is found with respect to the relative humidity (RH) category. For all particle sizes, it is found that the highest concentrations of PM are associated with low humidity (RH < 60%), followed by intermediate RH (60% to 80%), and the lowest concentrations of PM are associated with high humidity (RH ≥ 80%).

This is true for all particle sizes, and retains their cumulative size distribution of them. The similar behavior of all fractions of PM indicates that the meteorological conditions of humidity influence the total particle mass concentration during episodes of pollution.

The influence of humidity is more evident during episodes of pollution when compared to the background scenario. It is inferred that dry and stable atmospheric conditions favor the accumulation of pollutants. On the other hand, high humidity conditions favor the removal of particles.

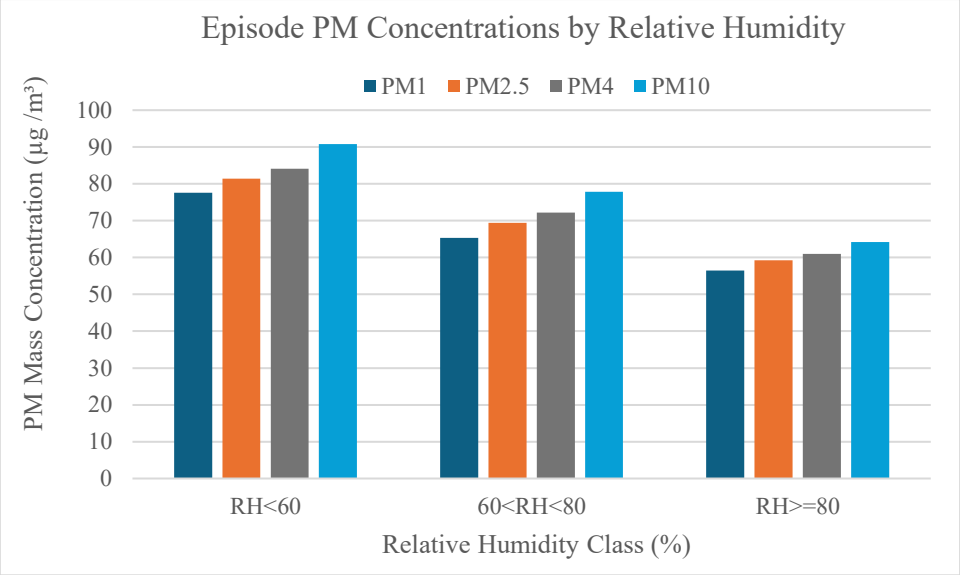

Fig. 24. PM mass concentrations versus relative humidity during pollution episodes

5.5.2. Temperature

Figure.25 shows the variation of mean particulate matter mass concentrations with temperature difference classes, which is used as an indicator of atmospheric thermal stability. There is a strong dependence of particulate matter mass concentrations on temperature difference classes, and the maximum concentrations are observed for high temperature difference classes, i.e., $\Delta T > 5°C$. Similarly, minimum mass concentrations are observed for low temperature difference classes, i.e., $\Delta T < 2°C$. For intermediate temperature difference classes, i.e., $2 < \Delta T < 5°C$, intermediate mass concentrations are observed. A similar pattern is evident across all particulate matter fractions. Moreover, the shape of the size distribution remains the same for all classes. From the above results, it can be observed that high temperature difference classes are responsible for high particulate matter mass concentrations, whereas low temperature difference classes result in low particulate matter mass concentrations. This shows that atmospheric stability, as represented by temperature difference, has a strong effect on particulate matter mass concentrations. High temperature difference classes, i.e., $\Delta T > 5°C$, result in high atmospheric stability, which causes low vertical mixing. This results in high particulate matter mass concentrations. Similarly, low temperature difference classes, i.e., $\Delta T < 2°C$, result in low atmospheric stability, which causes high vertical mixing. This results in low particulate matter mass concentrations.

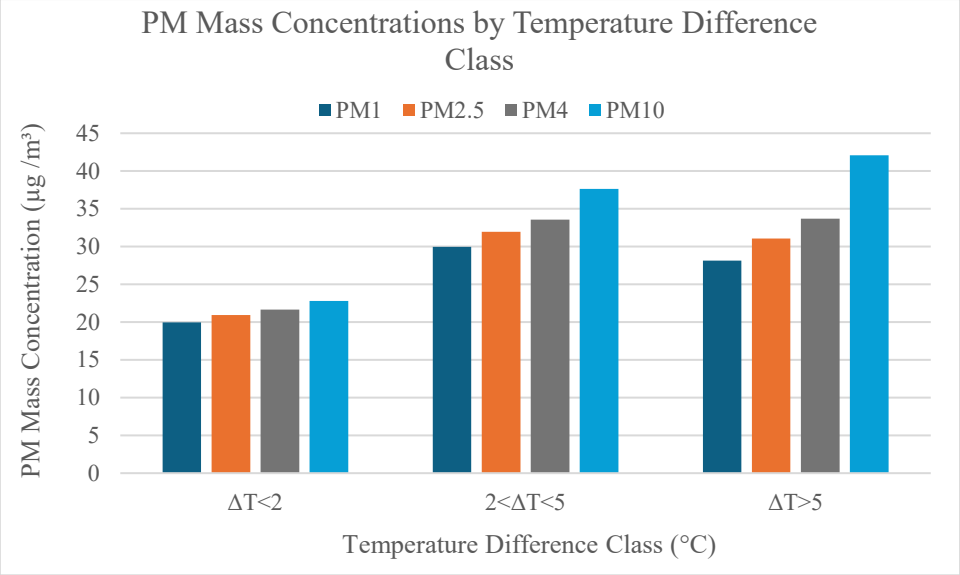

Fig. 25. PM mass concentrations across temperature difference (ΔT) classes

The figure presents the variation of average PM mass concentrations across temperature difference (ΔT) classes during background conditions. A clear trend of increasing concentration is observed with increasing ΔT for all the size fractions of the particles (PM1, PM2.5, PM4, and PM10).

The minimum concentrations of the particles are recorded during low ΔT conditions (i.e., ΔT < 2°C). On the other hand, the maximum concentrations of the particles are recorded when the ΔT value is greater than 5°C.

It has been established that the higher the value of ΔT, the greater the stability of the stratification of the atmosphere and the weaker the mixing of the atmosphere. On the other hand, low ΔT conditions are associated with greater mixing and better dispersion of the particles, resulting in lower concentrations of the particles.

This trend of the concentrations of the particles has been observed for all the size fractions of the particles. This implies that the meteorological stability is a major factor that influences the concentration of the particles.

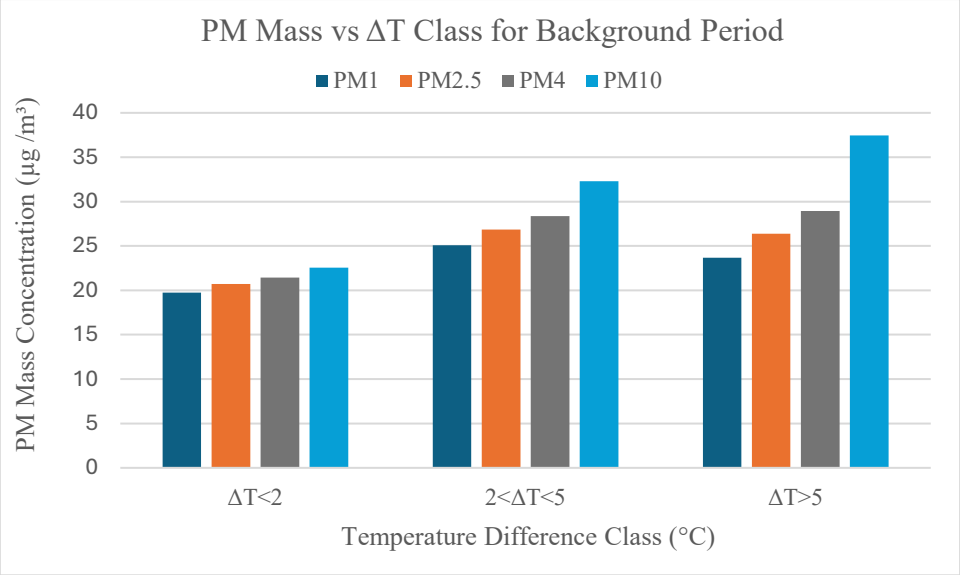

Fig. 26. PM concentrations versus ΔT under background conditions

The figure illustrates the variation in the average mass concentrations of particulate matter (PM) as a function of the temperature difference classes (ΔT) during the pollution episode period. It can be seen that there is a significant and clear trend of increasing PM concentrations with increasing ΔT for all particle size fractions (PM1, PM2.5, PM4, PM10).

At low ΔT classes (ΔT < 2°C), PM concentrations are already high. This implies that during the episode, the background PM concentrations are already high. At intermediate ΔT classes (2 < ΔT < 5°C), there is a moderate increase in PM concentrations for all particle size fractions. At the highest ΔT class (ΔT > 5°C), there is a greater increase in PM concentrations, reaching their maximum values, almost doubling their values at the lowest ΔT classes.

The systematic trend of increasing PM concentrations with increasing ΔT classes implies that during episode periods, increased stability in the atmosphere significantly increases PM accumulation. The trend holds true for all particle size fractions implying that the effect of stability on PM accumulation holds true for total PM mass concentrations rather than size distributions.

The effect of ΔT sensitivity during episode periods is much stronger than during background periods, as illustrated in the previous figure. This implies that stability effects in the atmosphere are more significant during episode periods.

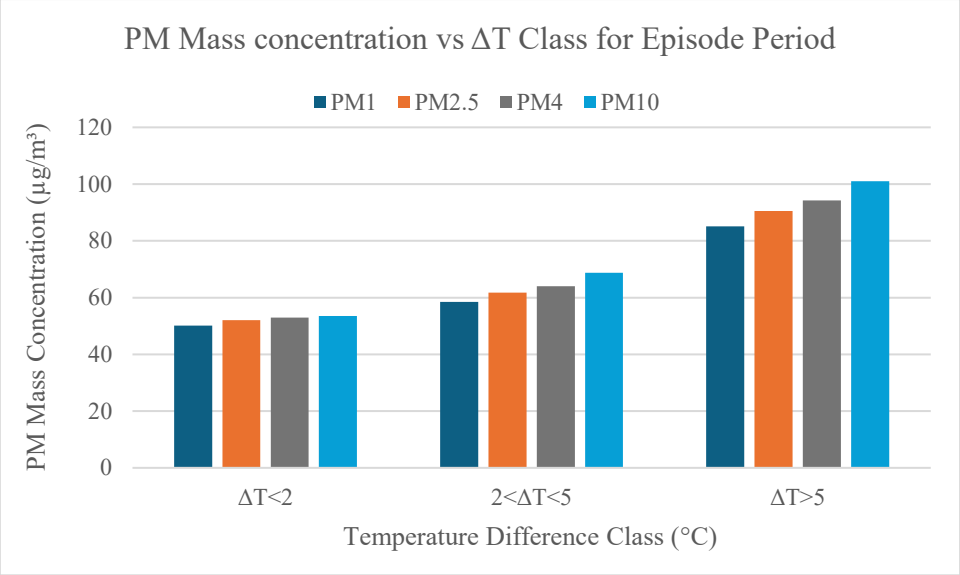

Fig. 27.PM concentrations versus ΔT during episode conditions

5.5.3. Air pressure

The figure illustrates a comparison of the average concentration levels of the mass of particulate matter (PM) for different size fractions of particles under high pressure (HighP) and low pressure (LowP) atmospheric regimes.

It is observed that for all size fractions of particles, the concentration levels of the mass of particulate matter are consistently higher under high pressure regimes than under low pressure regimes. This suggests that high pressure regimes favor the buildup of particles in the atmosphere. High pressure regimes are often associated with high levels of atmospheric stability and low vertical mixing rates, which favor the buildup of particles in the atmosphere.

The mass of particulate matter showed a similar behavior to that observed for relative humidity and temperature for the pressure regimes.

Hence, the pressure regimes merely scale the levels of the concentration of the mass of the particulate matter but preserve the size distribution of the particles. It is also observed that the differences in the levels of the concentration of the mass of the particulate matter for high and low pressure regimes are more pronounced for larger size fractions of particles (PM4 and PM10). This suggests that high pressure regimes not only favor the buildup of fine particles but also favor the buildup of larger particles in the atmosphere.

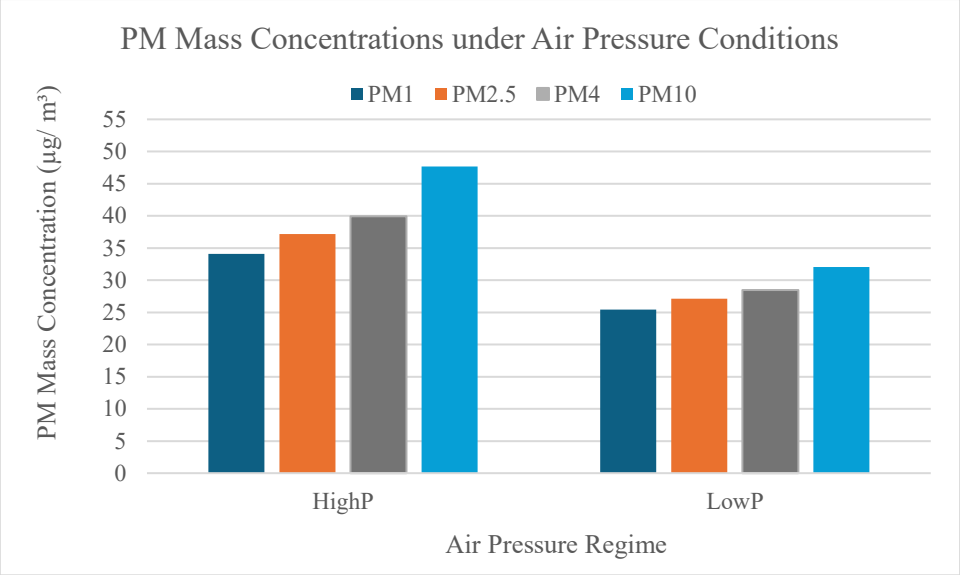

Fig. 28. PM mass concentrations under high- and low-pressure regimes

Based on the obtained results, the critical role of meteorological conditions in regulating PM mass concentrations cannot be excluded. The observed variability of humidity, stability, and pressure conditions affects the accumulation and dispersion of PM across all fractions. The similar sensitivity of different PM fractions to the observed meteorological conditions implies that the overall particle mass is affected rather than the specific size fraction.

5.6. Pollution Episode Characteristics

Here, pollution episodes were identified and characterized in terms of timing and type. Traffic and non-traffic episodes were compared.

The occurrence of pollution episodes shows a clear daily cycle. The highest number of episode hours is observed in the early morning (approximately 01:00–04:00), a period typically characterised by limited atmospheric mixing and stable boundary layer conditions that allow pollutants to accumulate.

Episode frequency reaches a minimum around midday, when enhanced dispersion favours dilution. A moderate increase later in the evening indicates that accumulation processes resume as atmospheric mixing weakens. Taken together, these observations highlight the strong influence of atmospheric stability on episode formation, in addition to emission-related factors such as traffic.

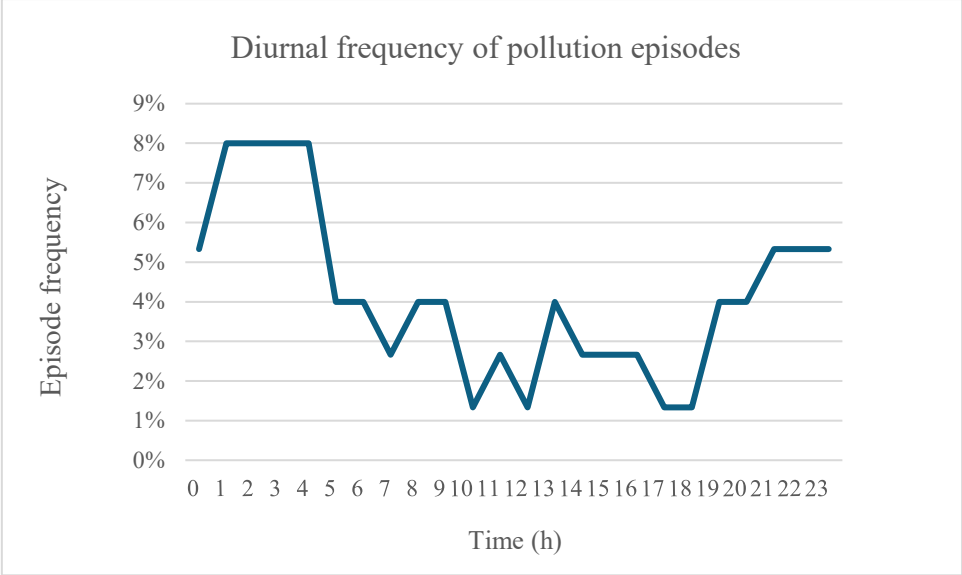

Fig. 29. Hourly frequency of pollution episode occurrence

Two different behaviours come out from the graph (fig. 30). Non-traffic episodes are mostly observed between midnight and early morning (00:00–05:00), which corresponds to periods of weak mixing and enhanced accumulation. Traffic-related episodes, on the other hand, are concentrated during the main commuting hours (07:00–09:00 and 18:00–21:00). This distribution suggests that pollution episodes result from the interaction between emission sources and the daily evolution of atmospheric mixing conditions.

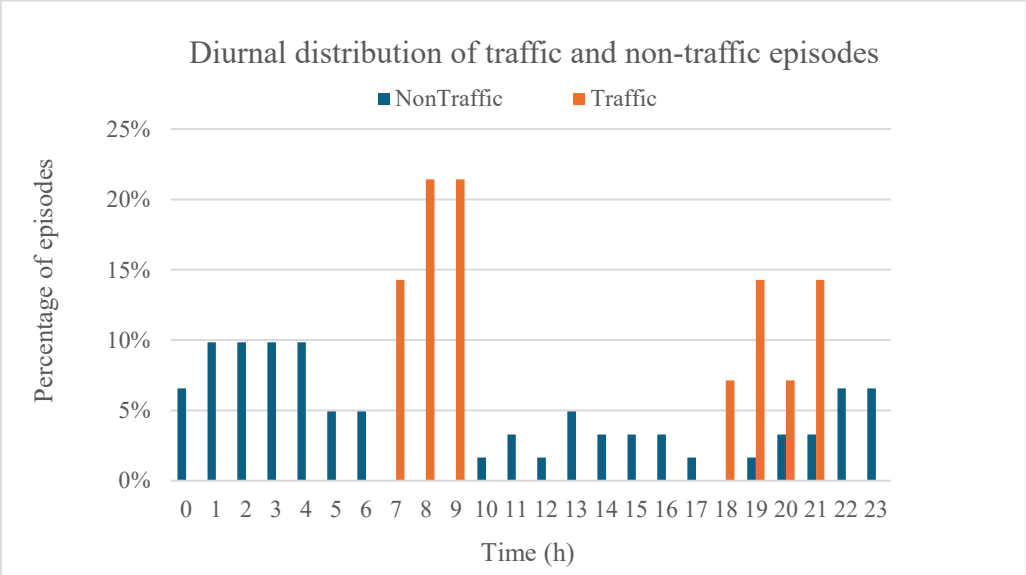

Fig. 30. Hourly distribution of traffic and non-traffic episodes

By comparing the episode and background conditions, a clear difference in the level of particle number concentration (CN) values is evident. For instance, during the background periods, the majority of data points show values corresponding to normal CN, while a small percentage show high CN values. However, during episode periods, high CN values dominate the data points, indicating that pollution episode periods are characterized by high particle mass as well as an increase in particle number concentration. This indicates that there is an increased rate of fine and ultrafine particles, as these particles are commonly linked to combustion processes.

Overall, these results show that episode periods are a result of the combined effect of increased emissions and reduced atmospheric dispersion, leading to an increase in particle mass as well as an increase in particle number concentration. The strong association between episode periods and particle number concentration values shows the importance of fine particle processes during high pollution periods.

The strong association observed between pollution episodes and elevated particle number concentrations provides important insight into the physical nature of episode formation. While background conditions are overwhelmingly characterised by normal CN levels, episode periods are dominated by high CN values, indicating that episodes are accompanied by a substantial increase in the abundance of fine and ultrafine particles.

When interpreted together with the diurnal analysis of episodes, this pattern suggests that multiple mechanisms contribute to episode development.

Episodes associated with traffic are concentrated during commuting hours and are consistent with increased combustion emissions that generate fine particles. In contrast, nighttime and early morning episodes occur under stable atmospheric conditions that favour local accumulation.

Together, these behaviours indicate that episode formation depends on both emission activity and the daily evolution of atmospheric mixing. Elevated CN during episode hours reflects this combination of stronger emissions and reduced dispersion.

This pattern highlights the importance of fine-particle processes in urban pollution events and suggests that mitigation efforts should consider sources of ultrafine particles in addition to overall mass concentrations.

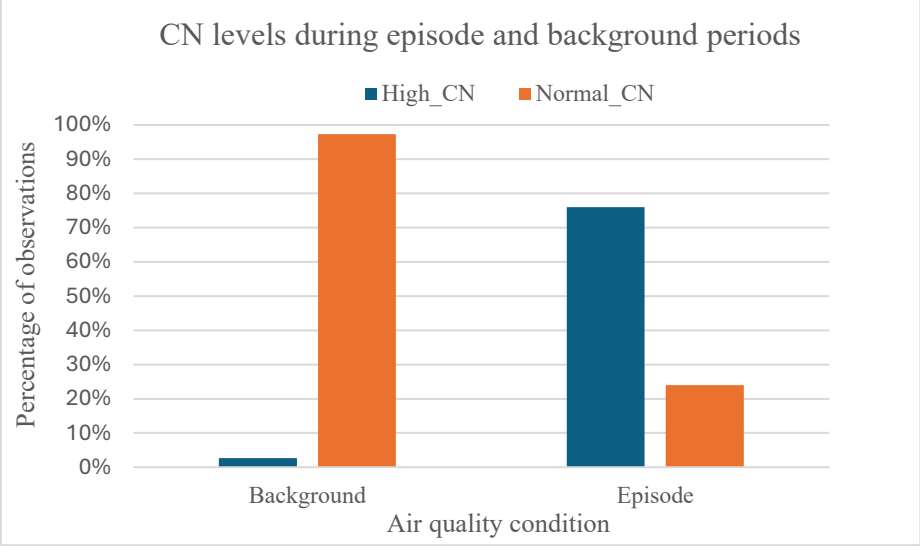

Fig. 31. Particle number concentration (CN) under background and episode conditions

Particle number concentration shows a well-defined daily pattern. CN values are highest during the late night and early morning hours, decrease gradually during the morning, and reach a minimum in the late afternoon. A secondary increase is observed in the evening. This behaviour is consistent with the daily evolution of the atmospheric boundary layer. During nighttime and early morning hours, limited vertical mixing favours the accumulation of particles near the surface, resulting in elevated CN levels. With increasing solar heating during the day, atmospheric mixing becomes more effective, and particle concentrations usually drop. The evening increase in CN appears to result from a combination of reduced mixing and fresh local emissions.

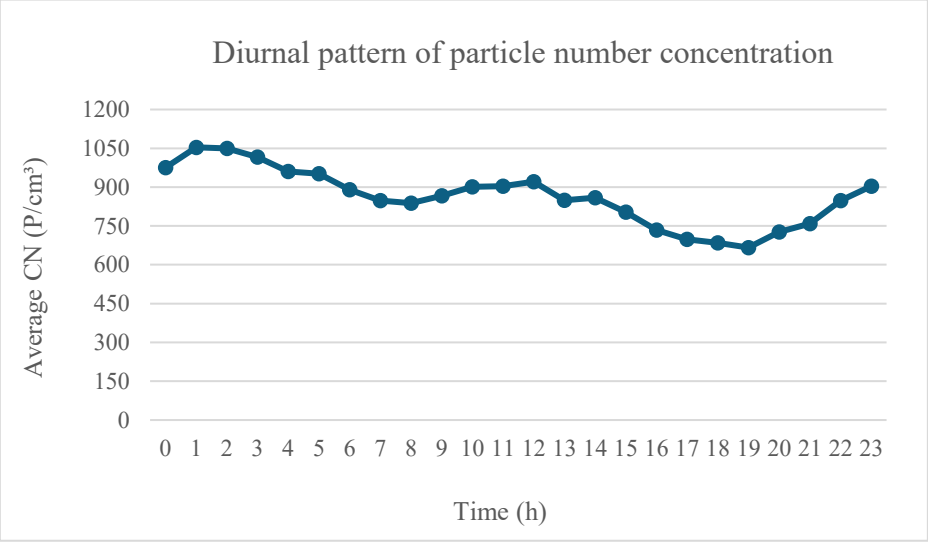

Fig. 32. Diurnal profile of particle number concentration (CN)

Episode CN reaches its highest values in the late morning. This peak may be associated with a combination of increased emissions and still-limited atmospheric dispersion. Afterward, concentrations decline toward midday and afternoon as vertical mixing becomes stronger, although episode values continue to exceed background levels.

The persistent gap between the two curves indicates that episode hours correspond to conditions in which particle accumulation is more pronounced. Rather than forming isolated spikes, episodes follow the same daily trend seen under background conditions but at consistently higher concentration levels. This behaviour points to the simultaneous action of stronger emissions and weaker dispersion.

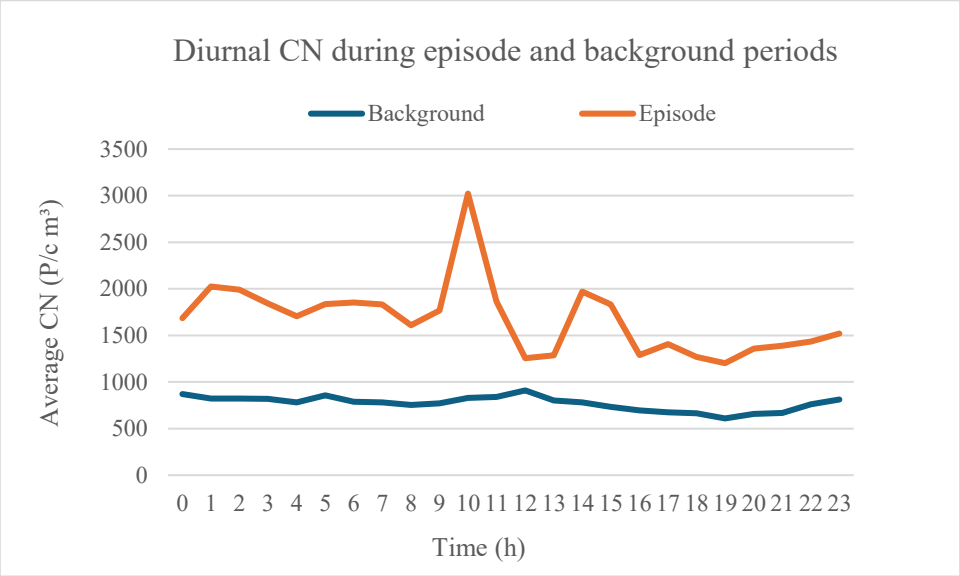

Fig. 33. Diurnal CN variation for episode and background periods

The comparison between traffic and non-traffic periods reveals a distinct temporal structure in particle number concentration. During the early morning hours, CN levels are generally higher under non-traffic conditions, suggesting that nocturnal accumulation and limited atmospheric mixing play a dominant role in controlling concentrations. As traffic activity begins in the morning, elevated CN values are observed during traffic hours, indicating a clear contribution from vehicular emissions.

There is a noticeable enhancement in CN during the main traffic windows, where concentrations during traffic periods approach or exceed those observed under non-traffic

conditions at adjacent hours. However, outside these windows, non-traffic concentrations remain relatively high, reflecting the influence of background accumulation processes in addition to direct emission sources.

Generally, the patterns suggest that urban CN variability results from the interaction between emission intensity and atmospheric dispersion. Traffic activity introduces short-term increases in particle number, while background meteorological conditions modulate the baseline concentration throughout the day.

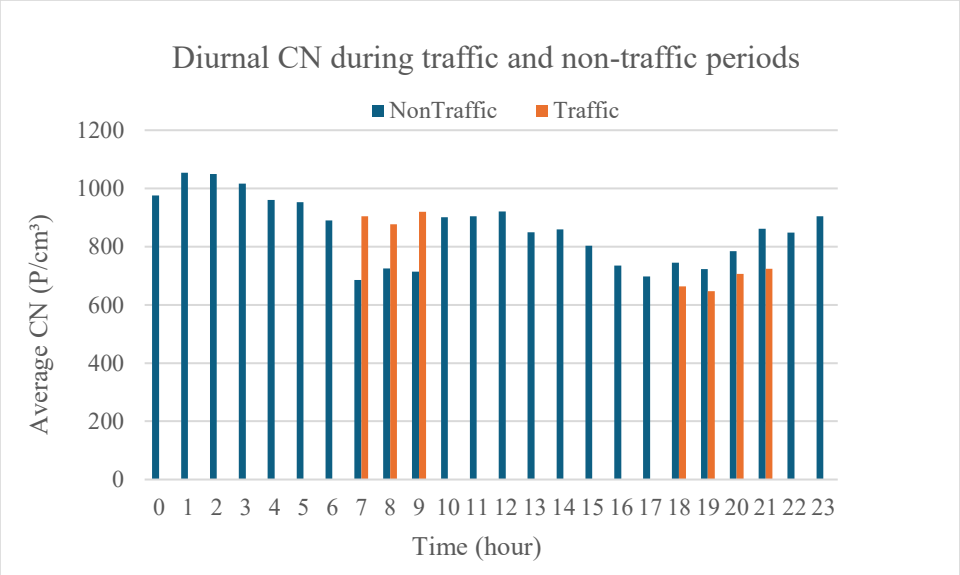

Fig. 34. Hourly CN levels for traffic and non-traffic periods

Traffic and non-traffic episodes are not evenly distributed over the day. Traffic-related episodes cluster around commuting hours, with the largest share occurring in the morning. Around 08:00–09:00 they represent roughly 21–22% of all traffic episodes. A smaller rise appears again in the evening, reaching about 14–15% near 20:00–21:00, which follows the usual daily pattern of urban traffic.

Non-traffic episodes show a different timing. They occur more often at night and in the early morning, with hourly contributions close to 8–10% between midnight and 04:00. Because these hours fall outside peak traffic activity, their frequency points to the importance of atmospheric accumulation. Under weak nighttime mixing, locally emitted particles can build up near the surface and increase the likelihood of episode conditions.

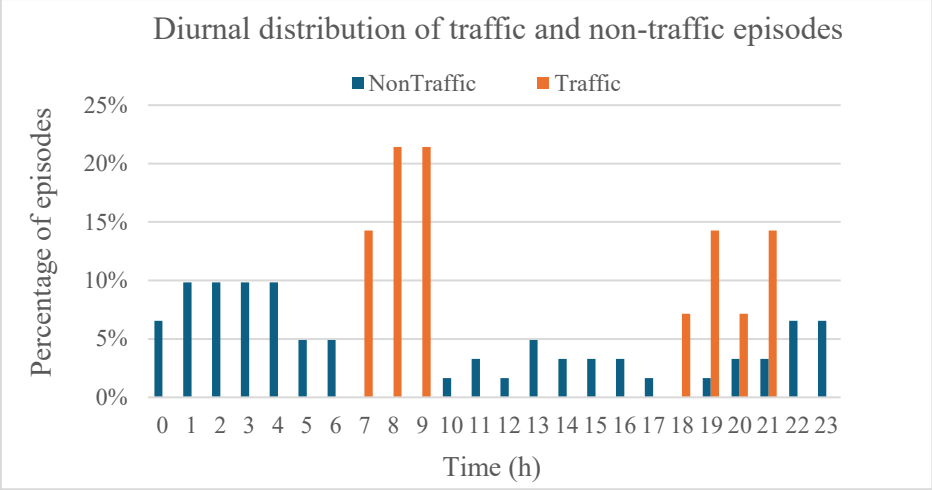

Fig. 35. Hourly frequency of traffic and non-traffic episodes

A comparison between weekdays and weekends shows a small but measurable difference in particle number concentration. The mean CN during weekdays is about 875 p m^{-3}, while weekend values fall to roughly 825 p m^{-3}, corresponding to a decrease of around 5–6%.

Weekend concentrations are slightly lower, which agrees with reduced traffic and activity. The difference is moderate, but it still reflects the contribution of everyday urban emissions. At the same time, weekday and weekend values remain relatively close. This similarity suggests that background processes and weather conditions also play an important role in shaping CN levels.

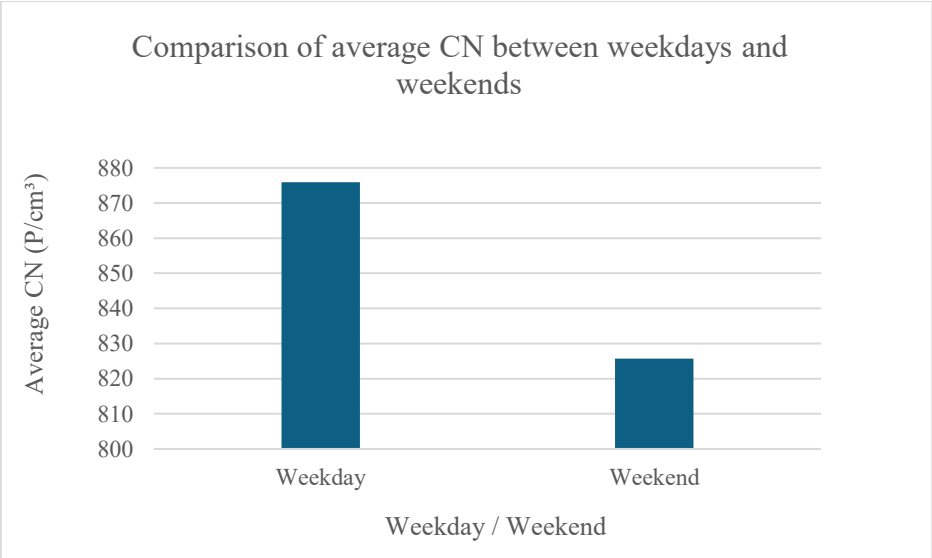

Fig. 36. Average CN levels on weekdays and weekends

During background periods, most measurements belong to the normal CN class (around 650 observations), while only a small number, about 15–20 cases, are classified as high CN. This indicates that elevated particle number concentrations are relatively rare under background conditions. In contrast, non-traffic episodes are primarily associated with high CN values. Roughly 45–50 observations fall into the high CN class, compared with only a small number of normal CN cases. Traffic episodes show a similar but weaker pattern, with high CN still more frequent than normal CN, although the total number of traffic episodes is limited.

As shown in the figure, CN levels are generally higher during episode hours than during background periods. Both traffic and non-traffic episodes are linked to elevated particle numbers, whereas background conditions are mainly associated with moderate concentrations. The separation between these groups suggests that CN provides a useful measure for distinguishing polluted from non-polluted conditions.

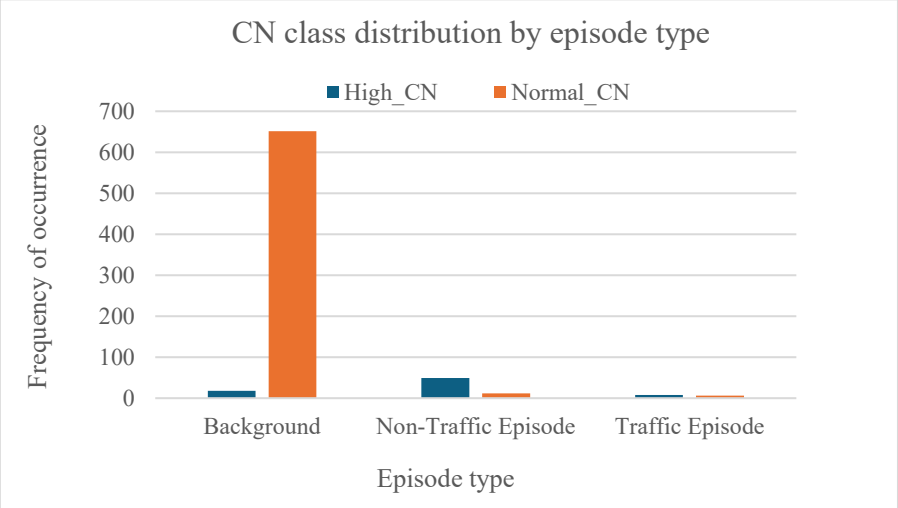

Fig. 37. Distribution of CN classes by episode type

The results of the analysis of pollution episodes indicate notable differences between the background and episode periods. Pollution episodes tend to be associated with higher PM concentration and occur more often when the atmosphere is less mixed. The pollution episodes tend to occur because of emission sources and the natural evolution of stability with time of day.

5.7 Effective Density (ρ_{eff}) Characteristics

Effective particle density, denoted by ρ_{eff}, is an essential parameter used to determine the physical characteristics of aerosol particles. This parameter takes into consideration the effects

of particle composition, structure, and size distribution. Studying ρ_{eff} provides a better comprehension of aerosol characteristics and properties.

5.7.1. Temporal Variability of Effective Particle Density

Effective density of aerosol particles may vary over a given period. Studying this aspect provides a better comprehension of the characteristics of aerosol properties over different periods of time. This section focuses on the daily and hourly variability of ρ_{eff}.

5.7.1. 1. Daily Variation of Effective Density

The average daily effective density for January 2025 is approximately in the range of 0.69 g/cm³ to 0.93 g/cm³. In the initial part of the month (days 1 to 6), the density is low and constant. Subsequently, on day 10, the density increases dramatically. It peaks at around 0.93 g/cm³. Following the peak, the density gradually decreases but remains at a reasonably high level. A significant fall is recorded on day 20. Here, the density decreases to around 0.71 g/cm³. In the later part of the month, there is a series of moderate increases in density, followed by a minor fall. It ends the month at around 0.73 g/cm³ on day 31.

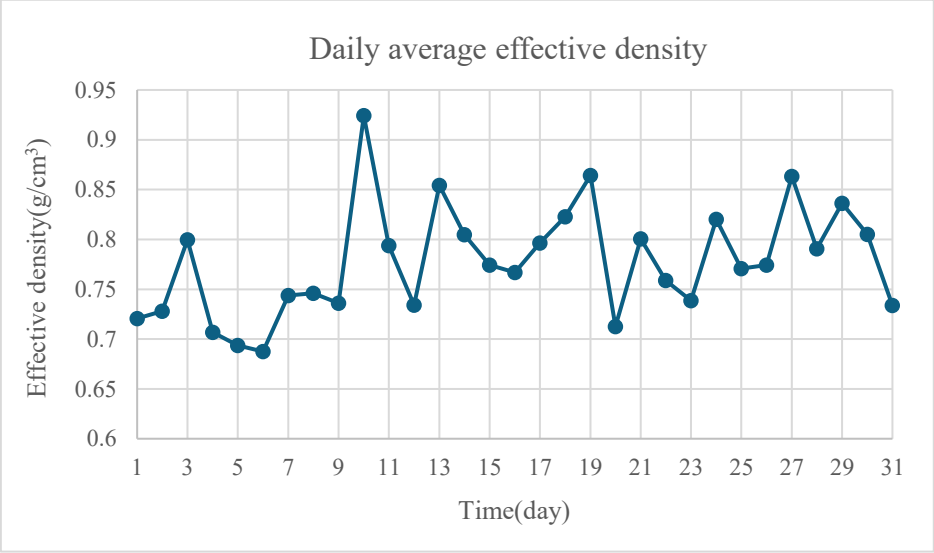

Fig. 38. Daily average effective density over the period

5.7.1. 2. Diurnal (Hourly) Variation of Effective Density

The variation in the mean effective particle density (ρ_{eff}) during the day ranges between 0.53 and 0.96 g/cm³ over a 24-hour cycle. In the early morning hours between 01:00 and 06:00, ρ_{eff} stays at moderate levels around 0.70–0.84 g/cm³. A strong minimum in ρ_{eff} around 07:00–08:00

corresponds to values around 0.53 g/cm³. Low values of effective density are usually associated with combustion particles such as soot and organic matter with relatively low material density. Values of ρ_{eff} increase steadily from around 09:00, reaching peak values almost 0.95 g/cm³ during midday and late afternoon between 12:00 and 18:00. High values of effective density usually indicate the presence of aged particles with secondary inorganic components such as sulfates and nitrates. After 18:00, ρ_{eff} decreases gradually to intermediate values around 0.74–0.80 g/cm³ during the evening and late-night hours.

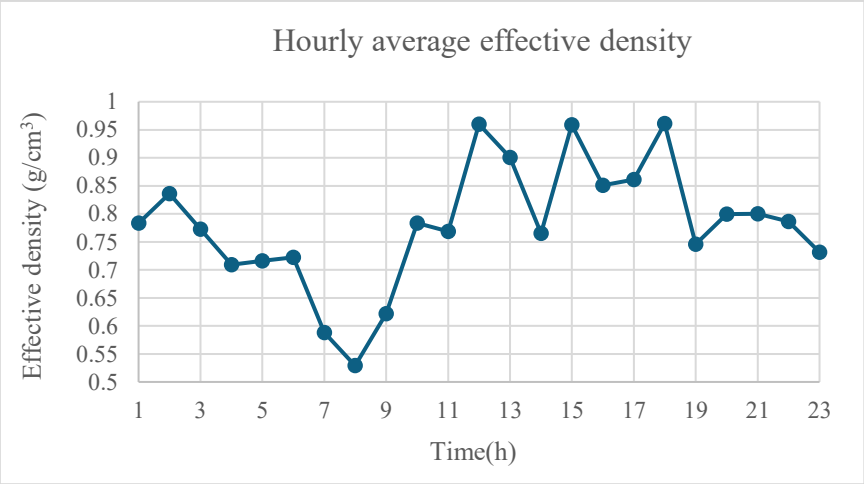

Fig. 39.Hourly average effective density over the 24-hour cycle

The hourly and daily average profiles of ρ_{eff} show the same aerosol system at two different timescales. The profile of ρ_{eff} during the hour shows clear day-to-day variations with low values during the morning hours and high values during midday. The profile of ρ_{eff} as an average over the day shows the same features but with the effects of the regimes dominating the day. For example, the peak around day 10 in the monthly profile corresponds to the periods when midday values of ρ_{eff} were likely to dominate the day, while the decrease around day 20 suggests periods when low-density values dominated the day.

5.7.2. Meteorological influence

Meteorological conditions affect aerosol particle characteristics by impacting aerosol formation, transformation, and dispersion. Some meteorological conditions include relative humidity and stability. Studying these conditions and their impact on ρ_{eff} can provide a better comprehension of aerosol characteristics.

5.7.2.1. Relative Humidity

The figure shows the range of variation of mean effective density (ρ_{eff}) for three classes of relative humidity (RH), which are RH < 60%, RH 60–80%, and RH ≥ 80%. The highest value of ρ_{eff} (approximately 0.91 g/cm³) was found for low humidity conditions (RH < 60%), whereas the lowest value of ρ_{eff} (approximately 0.74 g/cm³) was found for high humidity conditions (RH ≥ 80%), with the intermediate RH class (60–80%) showing moderate values of ρ_{eff} (approximately 0.77 g/cm³). The reduction of ρ_{eff} with increasing RH classes indicates changes to the particles under humid conditions. High RH values may cause hygroscopic growth and enhance the water content of the particles. In contrast, under low RH values, particles may show greater contributions of denser inorganic compounds. The pattern indicates that relative humidity influences aerosol physical characteristics, with lower RH conditions corresponding to higher effective density and higher RH conditions associated with reduced ρ_{eff} values.

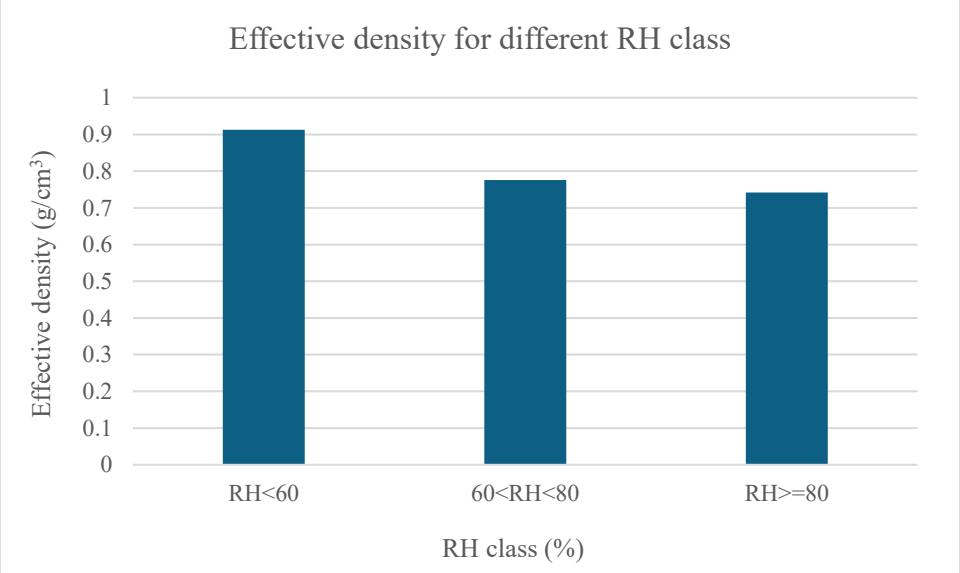

Fig. 40. Effective density across different RH classes

5.7. 2. 2. Atmospheric stability conditions

The figure shows the variation of average effective particle density (ρ_{eff}) under different atmospheric stability conditions: high (stable), medium, and weak stability (low ΔT). The highest ρ_{eff} value (almost 0.89 g/cm³) is observed under stable atmospheric conditions. In the regime of medium stability, ρ_{eff} decreases to approximately 0.77 g/cm³, while the lowest value of ρ_{eff} (approximately 0.70 g/cm³) occurs under weak stability conditions.

The relatively high values of ρ_{eff} during stable conditions may be related to suppressed vertical mixing and dispersion, which favor the presence of secondary particles with relatively higher density. In contrast, weak stability conditions are usually accompanied by enhanced mixing of the atmosphere, which facilitates dispersion of locally accumulated particles and may favour the presence of freshly emitted particles with relatively lower density.

The progressive reduction of ρ_{eff} with changing stability conditions from stable to weak stability suggests that atmospheric stability controls the ratio of aged and denser aerosol particles to relatively fresher and less dense particles.

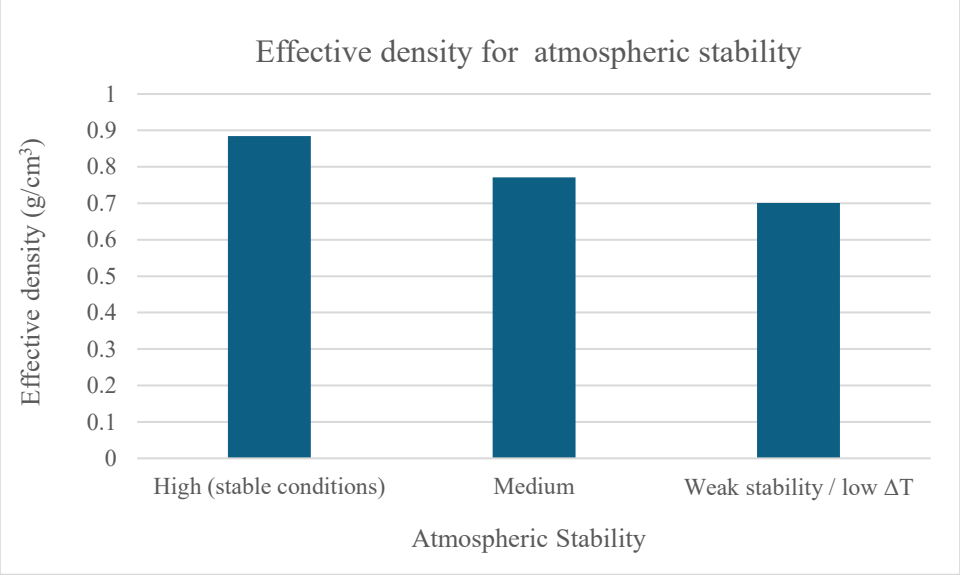

Fig. 41. Effective density under different atmospheric stability conditions

5.7. 2. 3. Air pressure

The mean effective particle densities have been shown under two different atmospheric pressure regimes: high pressure (High P) and low pressure (Low P) (Fig. 42). In comparison with low pressure (0.77 g/cm³), the values of densities are slightly higher in high pressure, at (0.79 g/cm³). However, this difference is minor, thus illustrating that atmospheric pressure affects effective particle density to a limited extent. The increase in density in high pressure may be explained by the stability of atmospheric conditions, which are common in high pressure and result in minimal vertical mixing and maximum settling of particles. In these

conditions, it may also be expected that older particles with higher effective densities, such as secondary aerosol, are present.

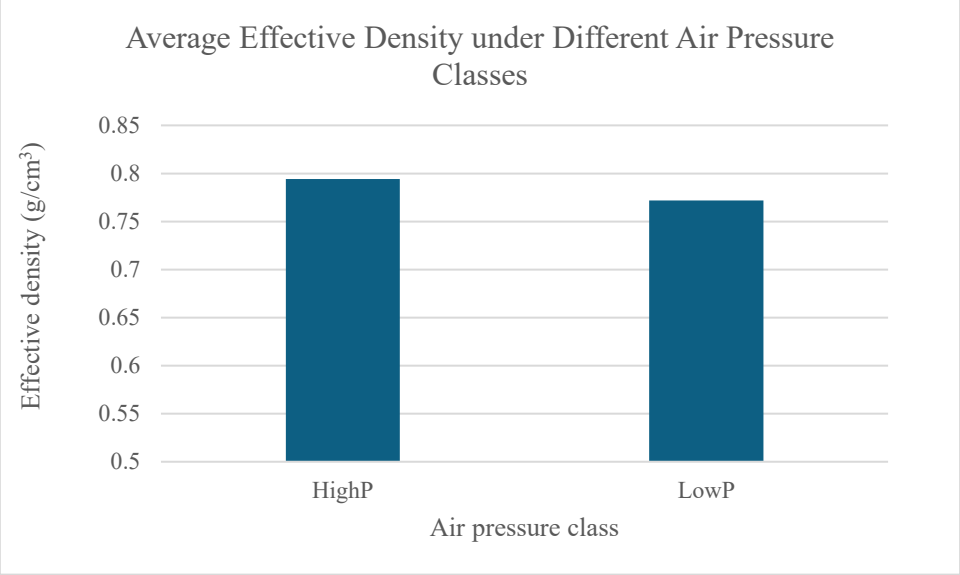

Fig. 42. Average effective particle density across high and low air pressure classes

5.7 .3. Aerosol Physical Characteristics and Effective Density

Aerosol physical characteristics include aerosol particle concentration and aerosol mass concentration. These characteristics are related to aerosol density. By studying these relationships, it is possible to comprehend how different aerosol populations affect aerosol density values.

5. 7. 3. 1. Particle number concentration (Cn)

The hourly variation is depicted between the concentration of particles (Cn) and the effective density (ρ_{eff}) by the scatter plot. There is a wide range of variation in the data points, indicating that there is no correlation between the two variables.

There is also a wide range of variation in the concentration of particles (400-1200 P/cm³) and the density (0.5-1.0 g/cm³) within a certain cluster. This implies that the increase in the number concentration is not necessarily associated with the increase in the density of the particles.

For the data points with lower values of number concentration (Cn) than approximately 600 P/cm³, the effective density (ρ_{eff}) is more dispersed. There are some data points with higher density than approximately 1.5 g/cm³ and even approaching approximately 3 g/cm³. For the data points with higher values of number concentration (Cn) than approximately 1500 P/cm³, the effective density (ρ_{eff}) is relatively stable in the range of approximately 0.5-0.8 g/cm³.

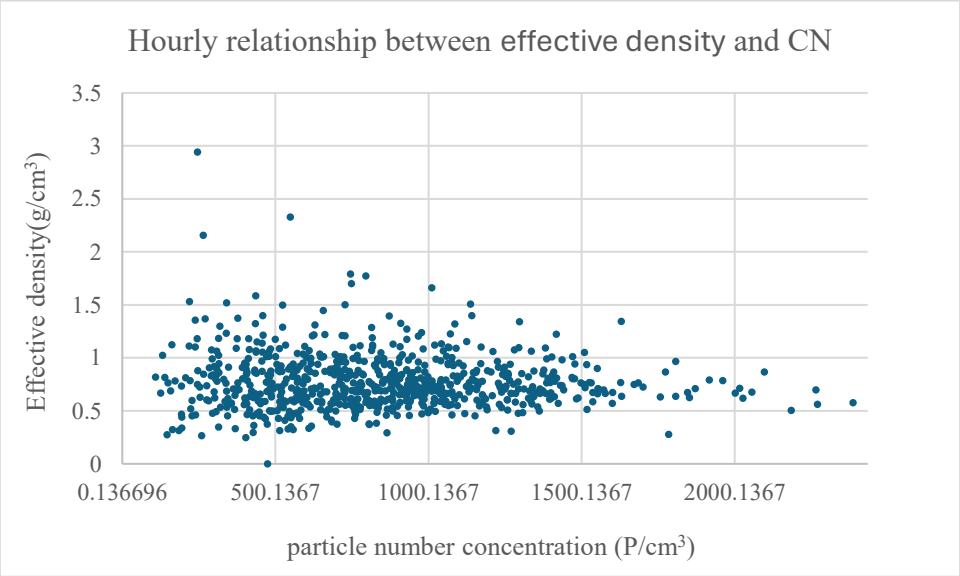

Fig. 43. particle number concentration and effective density relationship

5. 7. 3. 2. Effective Density and CN Relationship under different condition

The graph compares the relationship between number concentration (Cn) and effective density (ρeff) under episode and background conditions. The background data points are mostly found to be concentrated at lower values of Cn (usually below 1500 P/cm³) and have a somewhat wide range of ρeff values, approximately between 0.3 and above 1.5 g/cm³ with some higher-density outliers.

Episode conditions extend toward significantly higher Cn values (up to about 4000 P/cm³), while ρeff mostly remains within a narrower band, approximately between 0.4 and 1.1 g/cm³. Compared to background periods, episodes are characterized by higher particle numbers but not proportionally higher effective densities. The distribution indicates that during episode events, particle concentration increases substantially, whereas effective density varies within a

limited range, while background conditions exhibit greater variability in density at comparatively lower number concentrations.

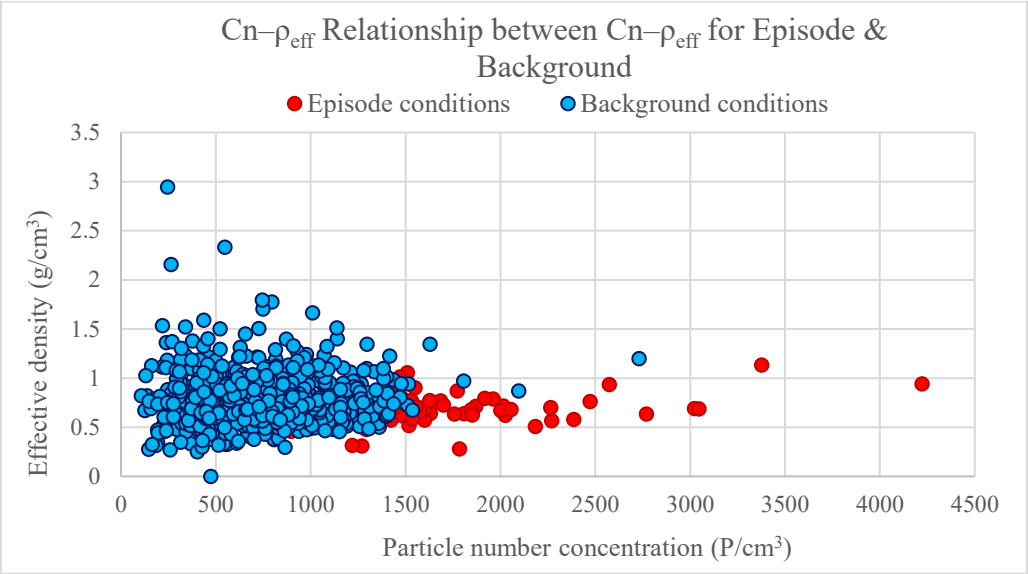

Fig. 44. Particle number concentration vs effective density during episode and background periods

5. 7. 3. 3. PM Mass Concentrations and Effective Density

As shown in the scatter plots presented in figures 45-48, the relationship between particulate matter mass concentrations, namely PM1, PM2.5, PM4, and PM10, and effective density ρeff, shows most of all data points falling into a range of relatively low to moderate concentrations, typically between 5 to 70 µg/m³. In this range, ρeff tends to stay within a range of 0.4 to 1.1 g/cm³, showing a stable density of particle populations despite variations in total mass concentration.

A common observation of all scatter plots is the lack of a clear relationship between PM concentrations and effective density ρeff. In other words, as particle mass concentration increases, effective density ρeff does not increase accordingly. Instead, at elevated PM concentrations, ρeff tends to stay within a relatively narrow range, typically between 0.5 to 0.9 g/cm³.

Another common observation of all scatter plots of particle size fractions is the increased variability of effective density ρeff at low PM concentrations. In some instances, a number of data points show relatively high effective densities, namely >2 g/cm³, occasionally even as high

as ~3 g/cm³, while the total particle mass concentration remains low. These data points likely represent episodic contributions of denser particle types, such as mineral or metallic particles, which become visible at low total particle mass concentrations. At elevated PM concentrations, such high values of effective density ρeff are not common, indicating a lack of contribution of denser particles to elevated PM mass concentrations.

Despite these broad similarities, some discernible differences can be observed in the different fractions of particles in the atmosphere. In the case of PM1, the majority of the results are contained in the range of approximately 5-60 µg/m³, with effective densities typically in the range of 0.4-1.2 g/cm³; a few results with low concentrations have effective densities close to 3 g/cm³. In the PM2.5 plot, many of the results are contained in the range of less than 60 µg/m³ with effective densities in the range of 0.3-1.5 g/cm³, whereas results with concentrations above 80 µg/m³ are contained in a more limited range of 0.5-0.9 g/cm³, indicating a relatively homogeneous particle composition.

In the PM4 plot, most values are contained in the range of approximately 5-70 µg/m³, with effective densities in the range of 0.4-1.1 g/cm³. Even for results with concentrations above about 80 µg/m³, the effective density is still relatively constrained (below 1.0 g/cm³), indicating that increases in PM4 concentration are not related to increases in particle density, but rather to the variable total contribution of different particle size fractions.

In the PM10 plot, it is evident that the majority of the results are contained in the range of the reported concentrations.

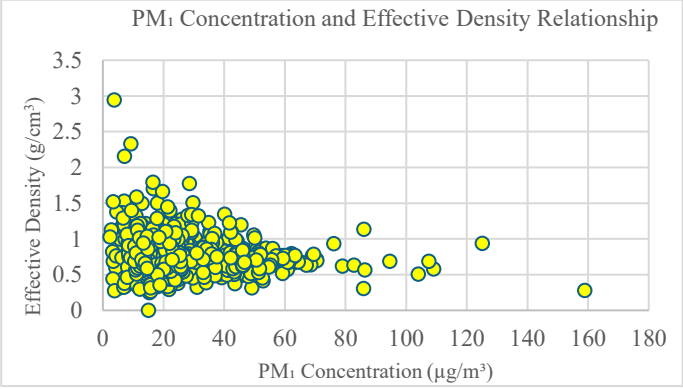

Fig. 45. Relationship between PM₁ concentration and effective density

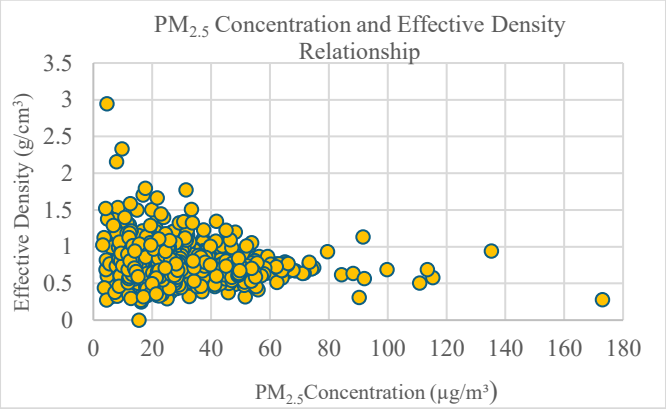

Fig. 46. Relationship between PM2.5 concentration and effective density

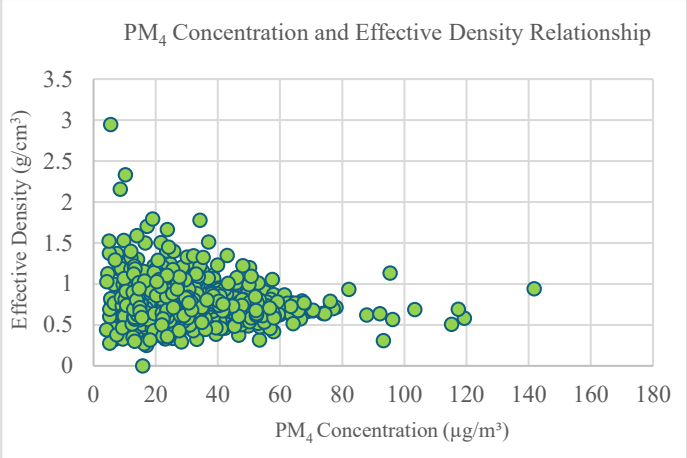

Fig. 47. Relationship between PM4 concentration and effective density

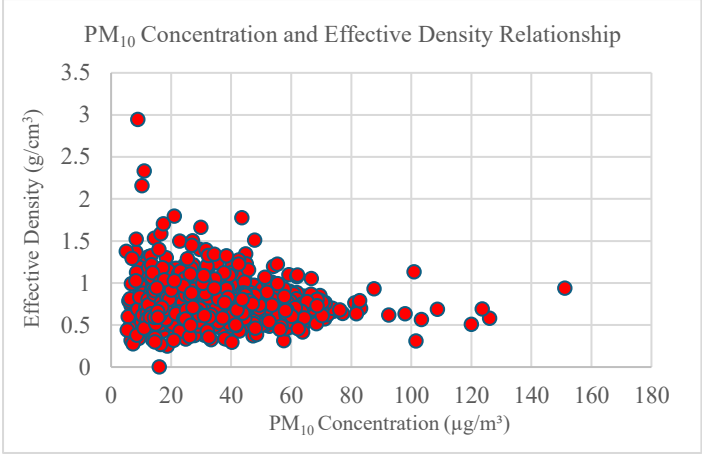

Fig. 48. Relationship between PM10 concentration and effective density

5. 7. 3. 4. Influence of Particle Size-Class Increments

The differences in the increments of the different size classes of the particles can also provide further information regarding the distribution of the particles in different ranges of the size spectrum. The increments of the different size classes of the particles can be studied in relation to the effective density of the aerosols to determine the presence of significant differences in the density of the particles in different ranges of the size spectrum.

The distribution of the fine-mode increment ($PM_{2.5} - PM_1$) shows that most observations are concentrated within a relatively narrow concentration interval, generally below 4–5 µg/m³. Within this range, effective density (ρ_{eff}) exhibits considerable vertical dispersion, spanning from low values (almost 0.3 g/cm³) to values exceeding 1.5 g/cm³. This widespread at low increment levels indicates that small variations in fine-mode mass do not correspond to a consistent density response.

As the increment increases, the number of observations decreases and the variability in ρ_{eff} becomes more restricted. Higher fine-mode increments are not associated with systematically higher density values; instead, ρ_{eff} tends to remain within moderate ranges. The absence of a clear directional pattern suggests that changes in the $PM_{2.5} - PM_1$ increment are not directly reflected in proportional changes in effective density.

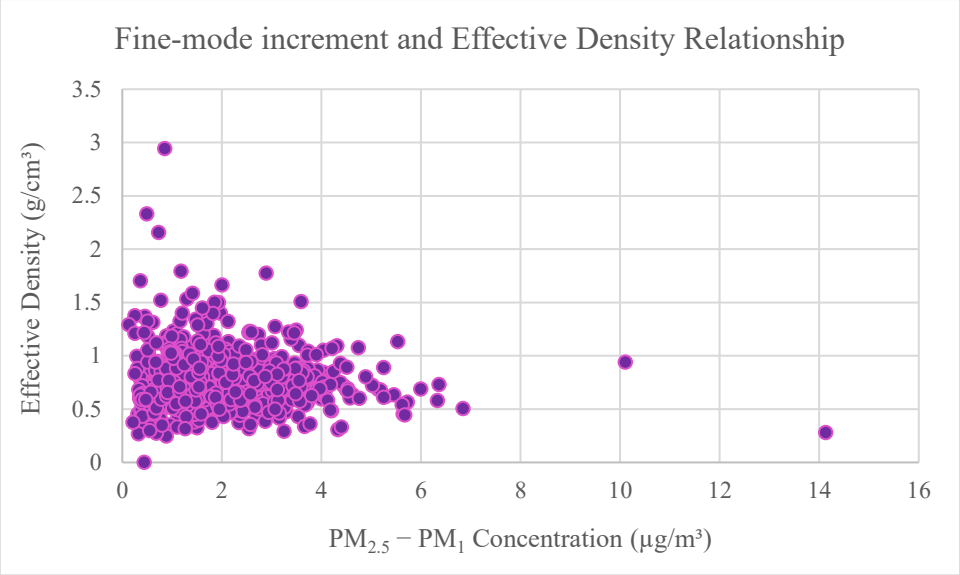

Fig. 49. Fine-mode increment vs effective density

The range of concentration for the coarse mode increment, defined as (PM_4 - $PM_{2.5}$), is broader than that of the fine increment. It reaches moderate and, in certain circumstances, high concentrations. Nevertheless, the range of the effective densities remains largely moderate, between 0.4 and 1.0 g/cm³.

This reveals that an increase in coarse mass concentration does not necessarily imply an increase in the density of the particles. Isolated occurrences of high densities are found in intermediate coarse mode increments, possibly resulting from episodic contributions of mineral or mechanically derived particles. Nevertheless, these do not reveal any particular trend. Overall, the findings reveal that the mere occurrence of coarse mode particles does not dominate the response of the effective densities, possibly indicating that internal mixing, as well as contributions of multiple particle sizes, are more important than the coarse mass concentration.

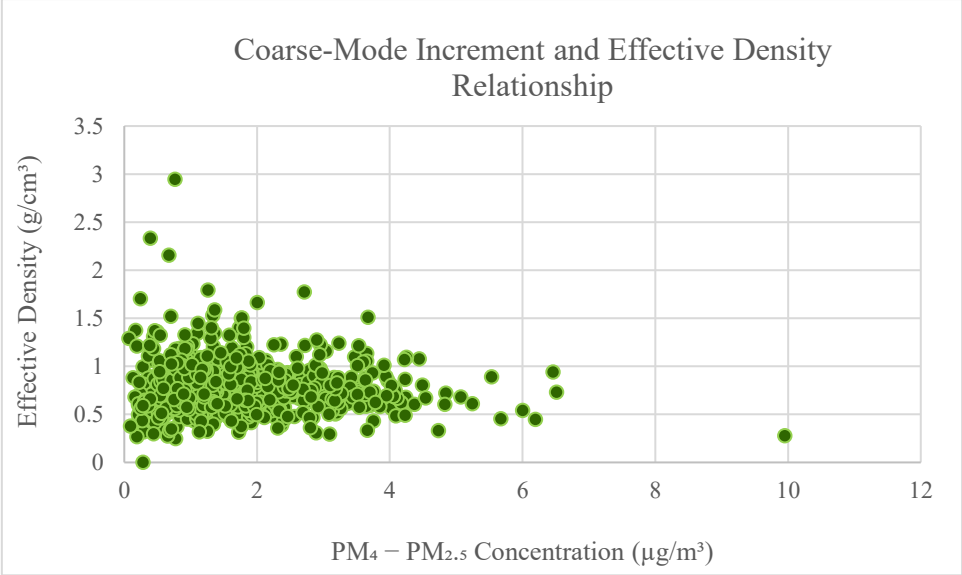

Fig. 50. Coarse-mode increment vs effective density

The super-coarse increment ($PM_{10} - PM_4$) exhibits substantial variability in concentration, including several high-mass events. However, this variability is not mirrored by proportional changes in effective density. Even at elevated $PM_{10} - PM_4$ values, ρ_{eff} remains predominantly within moderate levels, without progressive increase. High-density observations are mainly found at lower increment levels rather than during high super-coarse events. This indicates that increases in the largest particle fraction do not systematically shift the overall effective density upward. Instead, density variations appear to be influenced by the combined contribution of multiple particle size fractions rather than by the super-coarse component alone.

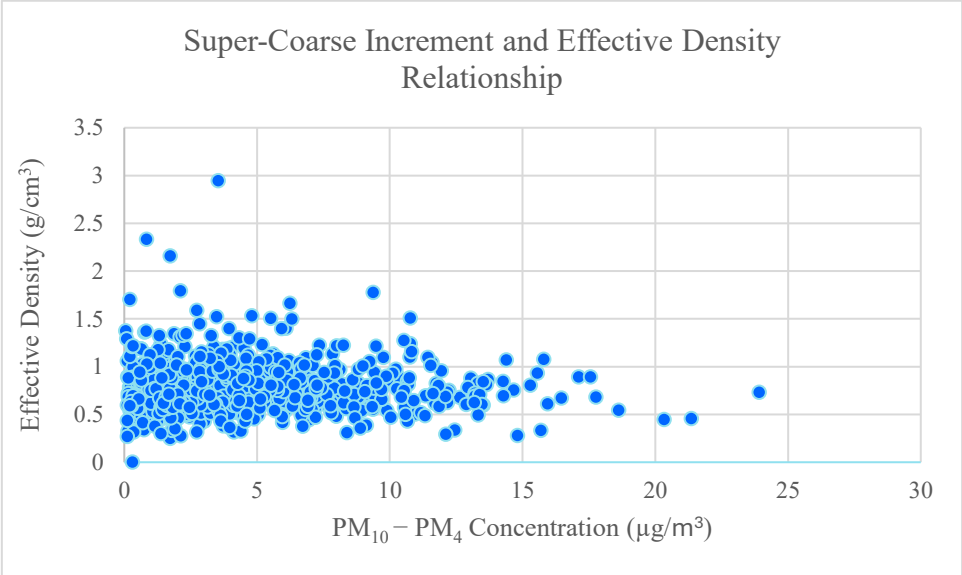

Fig. 51. Super-coarse increment vs effective density

5. 7. 3. 5. Influence of Particle Mass Fractions

The particle mass fractions can also be studied to determine the relative contribution of the different ranges of the size spectrum to the overall particle mass. The differences in the particle mass fractions can also be studied to determine the possible influence of the differences in the prevailing source of the atmospheric aerosols on the effective density of the aerosols.

5. 7. 3. 5. 1. Fine fraction

The scatter plot illustrates the association between fine mass fraction ($PM_{2.5}$ / PM_{10}) and effective density (ρ_{eff}). Most observations are concentrated within a fine fraction range of approximately 0.6–1.0, indicating that fine particles dominate the mass during the majority of measurement periods.

As the fine fraction increases toward unity, the vertical spread of ρ_{eff} becomes more confined, with most values clustering around moderate densities (approximately 0.5–0.9 g/cm³). Lower fine fraction values (below 0.6) are fewer but exhibit greater variability in ρ_{eff}, including some higher-density observations. The distribution does not indicate a strong linear dependence of effective density on fine mass fraction. Instead, density variations appear within a relatively stable interval even when the fine fraction changes, suggesting that compositional factors within the fine mode influence ρ_{eff} more than the fractional contribution alone.

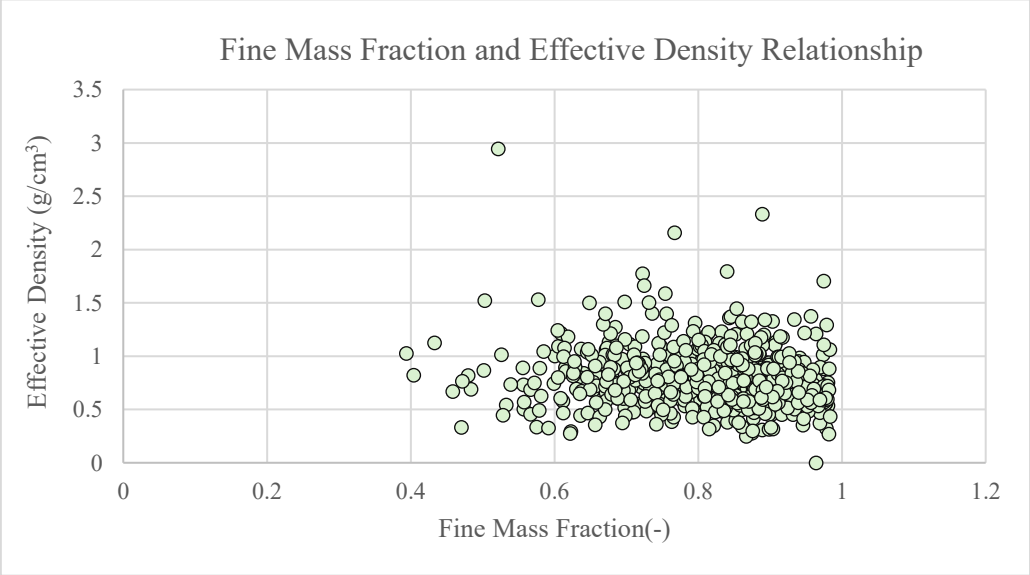

Fig. 52. Fine mass fraction vs effective density

5. 7. 3. 5. 2. Coarse fraction

The relationship between the coarse mass fraction and the effective density (ρ_{eff}) can be identified by a scatter plot. A large portion of the data are concentrated in a range of coarse fraction values between 0.05 and 0.35. This suggests that the coarse fraction of the total particulate mass remains limited and varied. Over this range of coarse mass fraction values, the ρ_{eff} values remain predominantly in the range of 0.4 and 1.1 g/cm³.

As the coarse mass fraction increases beyond this range of approximately 0.4, the number of points decreases. The effective density values do not tend to increase in this region. Several points have a density of more than 2 g/cm³ at a moderate coarse mass fraction. These points are isolated and do not indicate a trend.

The overall trend suggests that changes in the coarse mass fraction do not directly relate to changes in the effective density. The density values remain mostly in a moderate range over the entire range of coarse mass fraction values which explain the density of the particles is not solely a function of the coarse fraction.

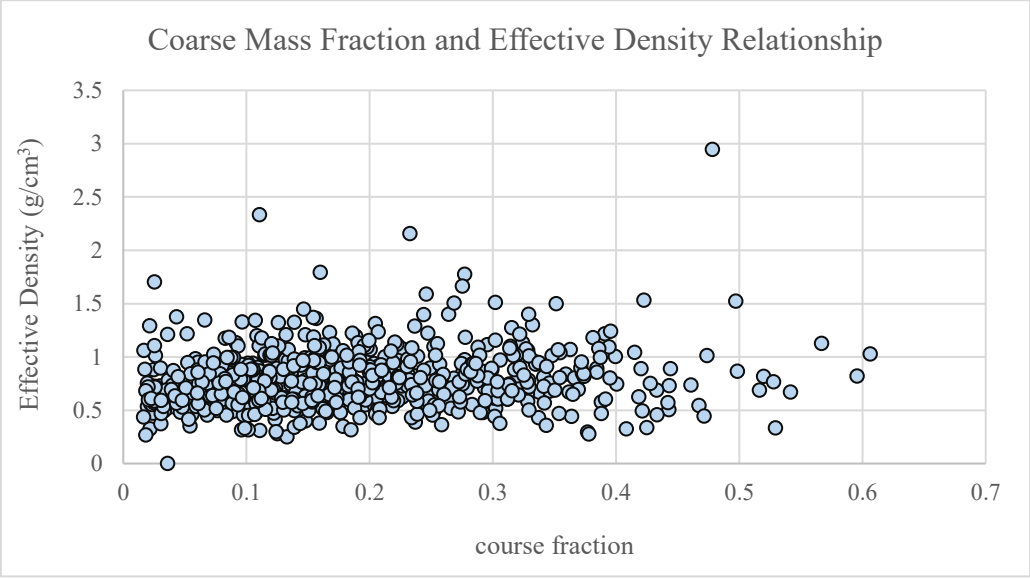

Fig. 53. Coarse mass fraction vs effective density

5. 7. 3. 5. 3. Super-fine fraction

The scatter plot illustrates the relationship between the super-coarse fraction (mass fraction in the size range 4-10 µm) and the effective density. The data points are concentrated in the range of low values of the super-coarse fraction, mainly below 0.30. The values of the effective

density are mainly concentrated in the range from 0.4 to 1.1 g/cm³, indicating a range of moderate effective density values for most of the data points.

As the values of the super-coarse fraction increase above about 0.30, the number of data points decreases. However, the values of the effective density do not show a trend of increase or decrease with the increase in the values of the super-coarse fraction. Even at high values of the super-coarse fraction in the range from 0.4 to 0.5, the values of the effective density are still concentrated in the range of moderate values. A similar pattern to that observed in the previous figure is found here, with a few scattered points above 2 g/cm³ at intermediate super-coarse fractions and no clear trend.

Overall, the data points show that the variation in the values of the 4-10 μm fraction is not related to the variation in the values of the effective density.

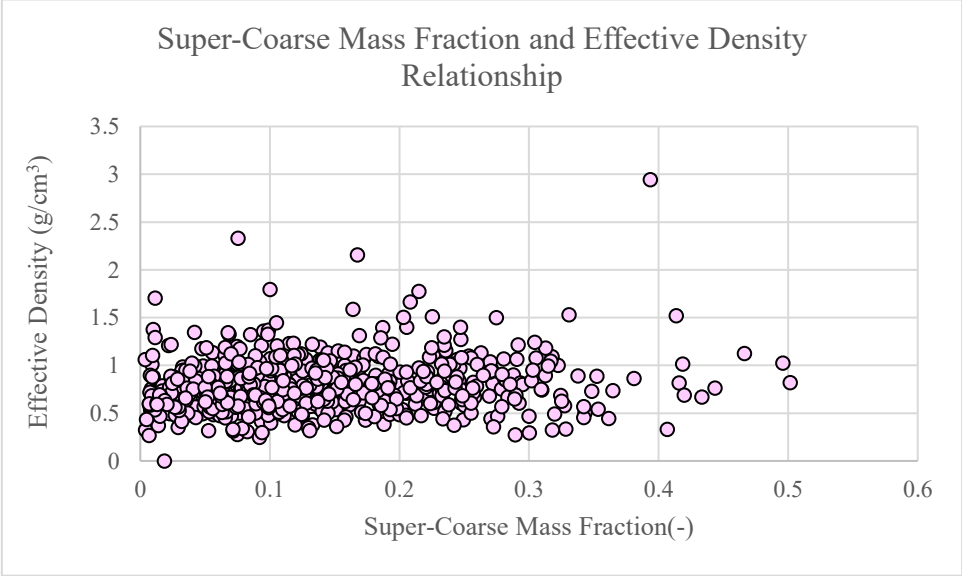

Fig. 54. Super-coarse mass fraction vs effective density

The figure demonstrates the behavior of mean effective density (ρ_{eff}) for different coarse fraction classes. The maximum ρ_{eff}, about 1.02 g/cm³, is observed for the high coarse class, whereas for the medium coarse class and the low coarse class is almost 0.83 and 0.76 g/cm³, respectively. Thus, the increasing trend in the value of ρ_{eff} from the low coarse class to the high coarse class indicates that the periods with higher coarse fraction values are associated with higher effective density values. Typically, coarse particles are associated with mechanically driven sources like resuspended materials, crustal materials, or minerals, which tend to have higher density values compared to the particles in the ultrafine mode.

Lower values of coarse fraction indicate higher values of particles in the ultrafine mode, which might be associated with combustion-driven particles with relatively lower values of effective density.

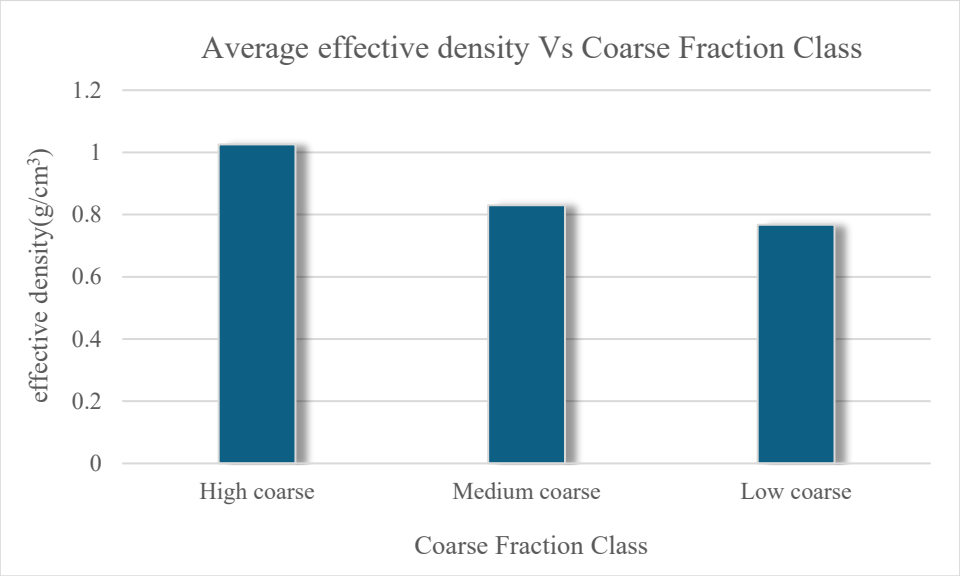

Fig. 55. Average effective density for different coarse fraction classes

5. 7. 4. Source-related factors

Human activities such as traffic can also influence the characteristics of the atmospheric aerosols. Differences in traffic and non-traffic conditions, as well as differences in weekdays and weekends, can also influence the characteristics of the aerosols in the atmosphere. The differences in the source of the atmospheric aerosols can also be studied to determine the possible role of the differences in the source of the aerosols in the prevailing patterns of the effective density of the aerosols.

5. 7. 4. 1. Traffic and non-traffic

The figure compares the hourly variation of the ρ_{eff} parameter under traffic and non-traffic conditions. For non-traffic periods, the analysis covers the entire day. In contrast, traffic-related values are mainly observed during the morning (07:00–09:00) and evening (18:00–21:00) rush hours. During non-traffic conditions, ρ_{eff} ranges from approximately 0.70 to 0.96 g/cm³. The highest values appear around midday, especially between 12:00 and 15:00. This pattern may be linked to particle aging processes or the formation of relatively denser aerosols during this period.

A different trend is observed during traffic hours. In the morning, ρ_{eff} decreases noticeably, reaching values between 0.55 and 0.62 g/cm³. In the evening, however, the parameter increases again and, in some cases, even exceeds the values recorded during non-traffic periods, particularly around 18:00.

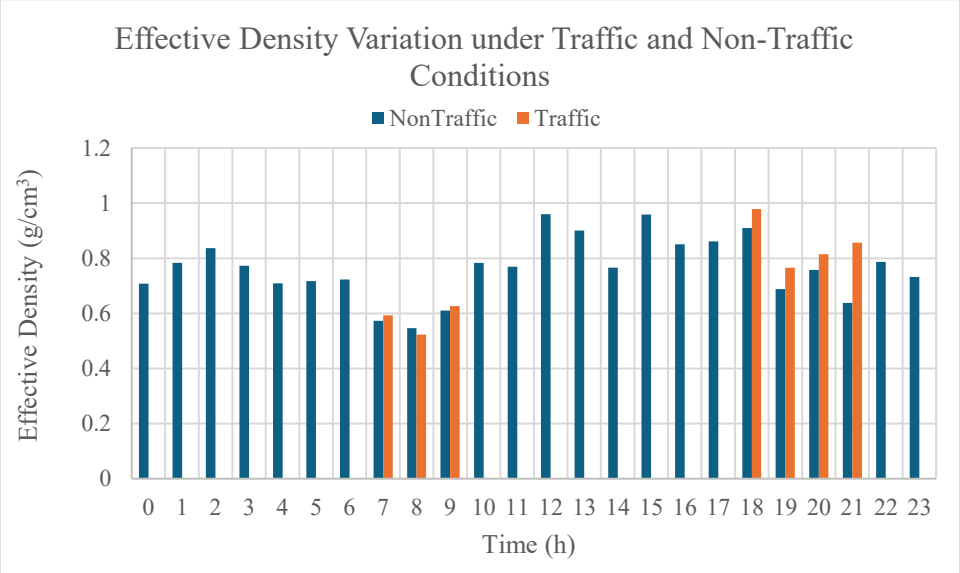

Fig. 56. Hourly variation of effective density under traffic and non-traffic conditions

5. 7. 4. 2. Weekend vs Weekday

The figure shows a comparison of mean effective particle density for weekdays and weekends. The results show that there are closely similar values between weekdays and weekends. The mean effective particle density for weekdays is 0.780 g/cm³, and for weekends, it is 0.770 g/cm³. The difference between weekdays and weekends is minimal at 0.01 g/cm³. This shows that effective particle density does not change significantly between weekdays and weekends. Although there are slightly higher values for weekdays than for weekends, they are not significant. This shows that there is no significant influence of weekday anthropogenic activities such as traffic emissions on effective particle density. The variability of data is also seen in a slightly higher standard deviation for weekdays (0.267) than for weekends (0.245), which is not significant.

In conclusion, it is seen that effective particle density is almost the same for weekdays and weekends. This shows that there is no significant influence of human activity levels between weekdays and weekends on effective particle density.

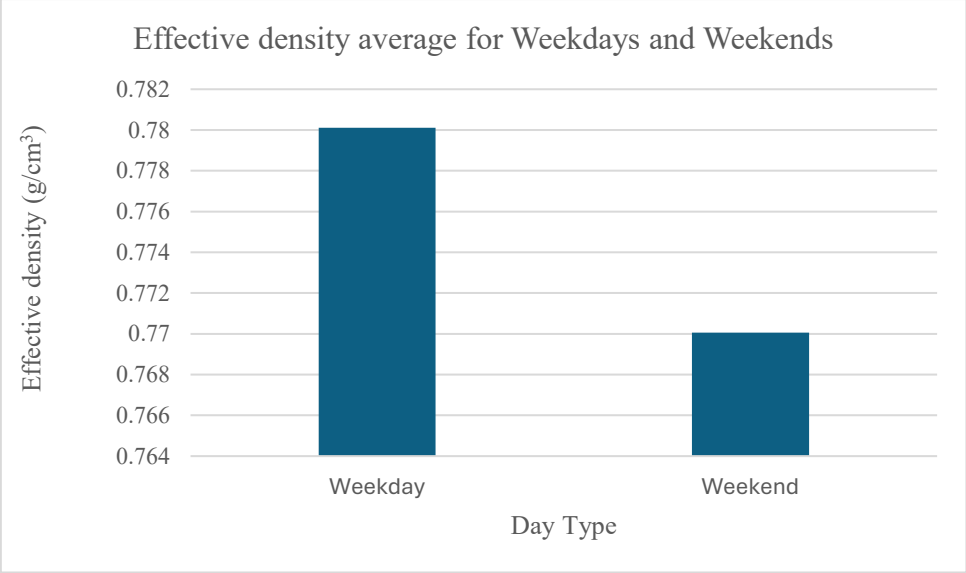

Fig. 57. Effective density for weekday and weekend periods

In general, the effective particle density (ρ_{eff}) is maintained in the moderate range with time and meteorological variability. High values of effective density are often observed near solar noon and during periods of strong stability in the atmosphere, while low values are more common in the mornings when the mixing in the atmosphere is less active. Comparisons of the particle number concentration, particulate matter mass concentrations, and particle size fractions indicate that the aerosol density is controlled neither by one dominant factor nor by the particle composition, the atmosphere, nor the relative contribution of the different particle size fractions.

5. 8. Particle Number Concentration (CN) Analysis

This section presents the behaviour of particle number concentration (CN). Its temporal patterns and relationship with $PM_{2.5}$ are analysed.

5. 8. 1. Particle Number Concentration (CN) in different conditions

The comparison between episode and background conditions shows a clear and consistent increase in both particle number concentration (CN) and $PM_{2.5}$ during episode periods. Average CN values are close to 780 particles m^{-3} during background hours and increase to about 1700 particles m^{-3} in episode conditions, which corresponds to more than a twofold rise. $PM_{2.5}$ shows

the same pattern, changing from roughly 25 µg/m³ to nearly 70 µg/m³. Both quantities therefore increase during episodes. In practical terms, episode hours are associated with higher particle mass as well as higher particle numbers. This behaviour is compatible with stronger emissions and/or weaker atmospheric mixing during these periods.

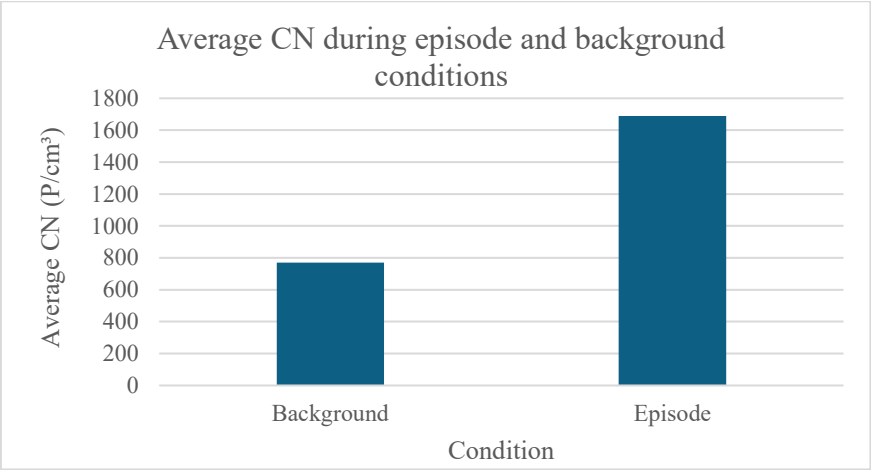

Fig. 58. CN distribution across pollution condition categories

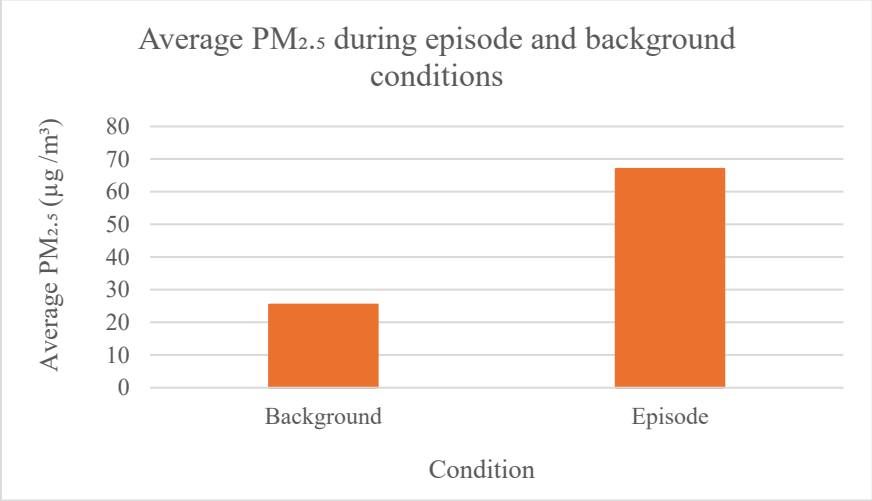

Fig. 59. $PM_{2.5}$ under background and episode regimes

The comparison between background conditions and the two types of conditions during pollution episodes reveals a consistent increase in both particle number concentration (CN) and $PM_{2.5}$ mass during episode periods.

Under background conditions, the average CN is approximately 770 P/cm³, whereas it rises sharply during episodes. The highest CN values are observed during non-traffic episodes (about

1700 P/cm³), followed by traffic episodes (about 1580 P/cm³). This represents more than a twofold increase relative to background levels. A similar pattern is observed for $PM_{2.5}$ mass concentration. Background $PM_{2.5}$ averages about 25 µg/m³. During non-traffic episodes it increases to roughly 68 µg/m³, while traffic episodes reach about 65 µg/m³.

The slightly higher values observed in non-traffic episodes show that the strongest pollution hours are not always tied to traffic peaks. They also occur during periods when particles accumulate under stagnant atmospheric conditions or when secondary aerosols build up. Traffic episodes remain clearly above background levels, but they are not the only situation in which high concentrations appear.

CN follows the same evolution as $PM_{2.5}$ in these episode hours. When mass concentrations rise, particle numbers rise as well. This means that episodes involve an increase in both particle mass and particle counts, reflecting a greater presence of fine particles in the urban air.

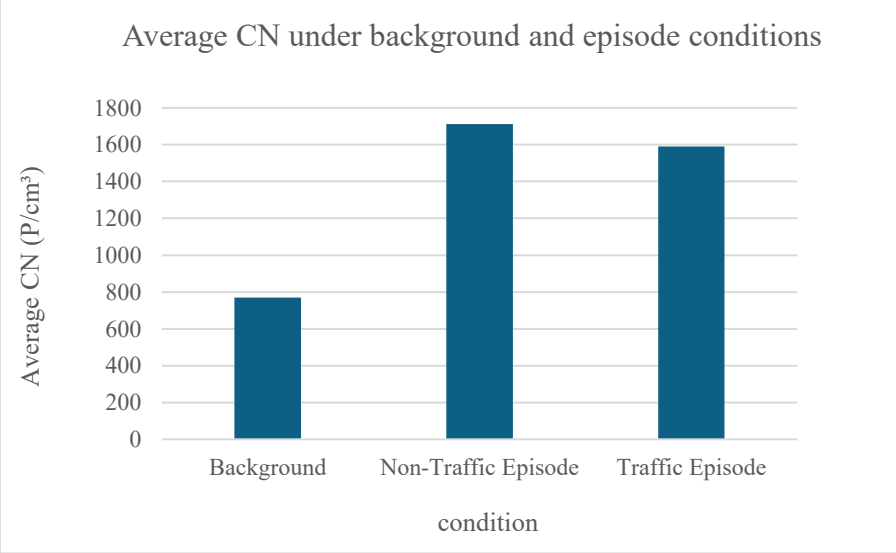

Fig. 60. CN under traffic classification

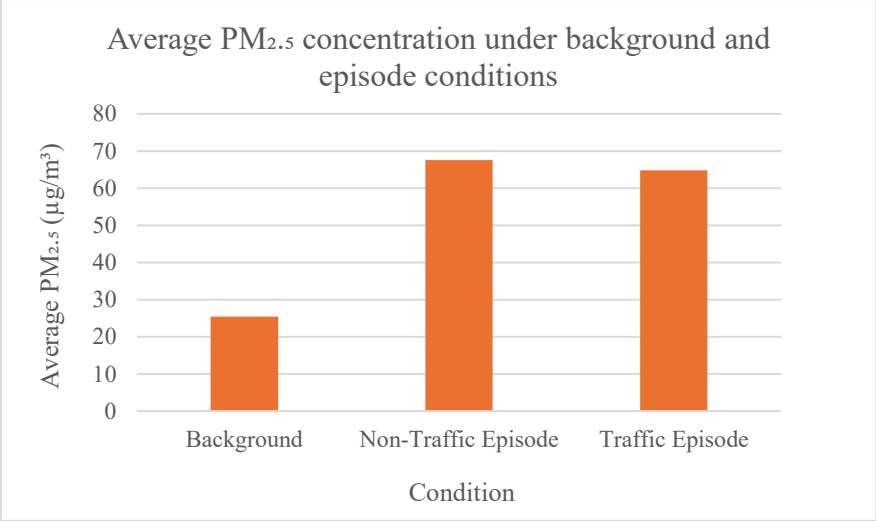

Fig. 61. $PM_{2.5}$ under traffic classification

5. 8. 2. Particle Number Concentration (CN) and $PM_{2.5}$

The scatter plot comparing CN and $PM_{2.5}$ shows that higher mass concentrations are generally associated with higher particle numbers. Most of the points follow an upward trend, although they do not align along a single straight line. A wide spread of values is visible in the graph. For similar $PM_{2.5}$ levels, CN can vary considerably, which suggests that the two quantities are not controlled by exactly the same mechanisms. $PM_{2.5}$ reflects the total accumulated mass, whereas CN responds more rapidly to fresh emissions such as traffic. A few points lie far from the main cluster and correspond to intense pollution events in which both variables reach high values. Taken as a whole, the distribution shows a positive but not perfectly tight link between particle number and mass.

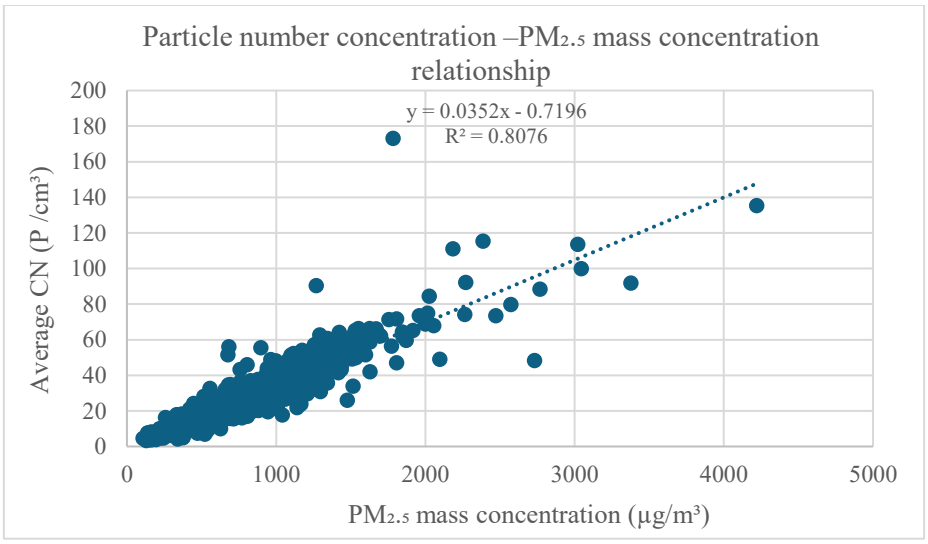

Fig. 62. CN–$PM_{2.5}$ relationship

Under background conditions, the scatter plot shows that CN tends to increase as $PM_{2.5}$ becomes higher. Most points form an upward pattern, so periods with larger mass concentrations usually coincide with larger particle numbers, even outside episode hours.

According to the linear regression of the data, a rise of 1 µg/m³ in $PM_{2.5}$ corresponds on average to about 26 additional P/cm³ in CN. The R^2 value of 0.79 means that a large share of the CN variation follows the behaviour of $PM_{2.5}$, although the points are not perfectly aligned. The remaining spread is likely related to changes in emissions and atmospheric mixing.

At higher $PM_{2.5}$ levels the scatter becomes slightly wider, which points to differences in particle characteristics and source contributions. Despite this variation, CN and $PM_{2.5}$ continue to evolve in the same direction during background periods.

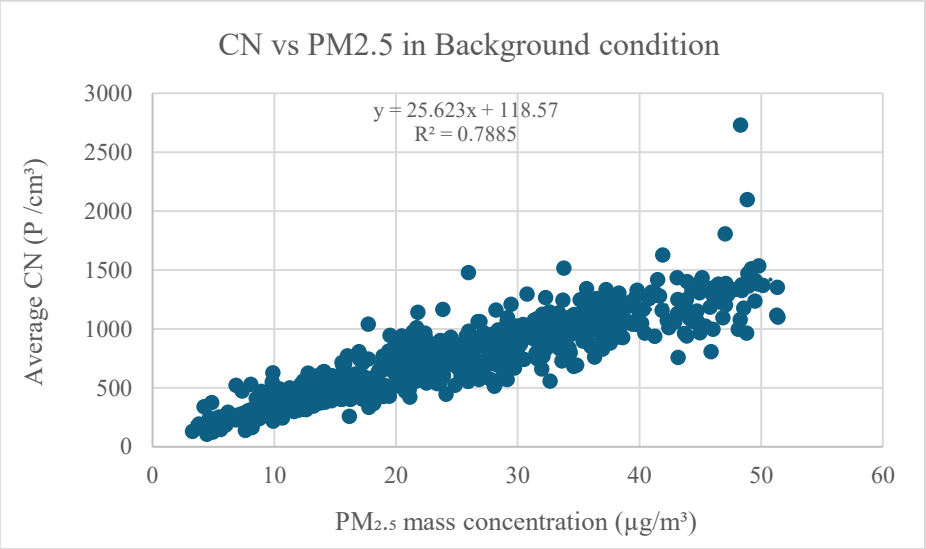

Fig. 63. CN–$PM_{2.5}$ relationship under background conditions

During episode conditions, the plot of CN versus $PM_{2.5}$ still shows an overall increase in particle number with increasing mass, but the points are more widely scattered than in background periods. This wider spread indicates stronger variability in particle behaviour during episodes.

From the equation, the positive slope means that higher $PM_{2.5}$ values are generally associated with higher CN. However, the coefficient of determination is $R^2 = 0.47$, so less than half of the CN variation follows the changes in $PM_{2.5}$. Compared with background conditions, the relationship is therefore weaker and less regular.

Several isolated points appear at high concentration levels where CN and $PM_{2.5}$ do not increase at the same rate. These cases are consistent with changes in particle sources and atmospheric processes during strong pollution events, including particle growth and shifts in size distribution. Even though CN and $PM_{2.5}$ remain positively related, their connection during episodes is more variable than under background conditions.

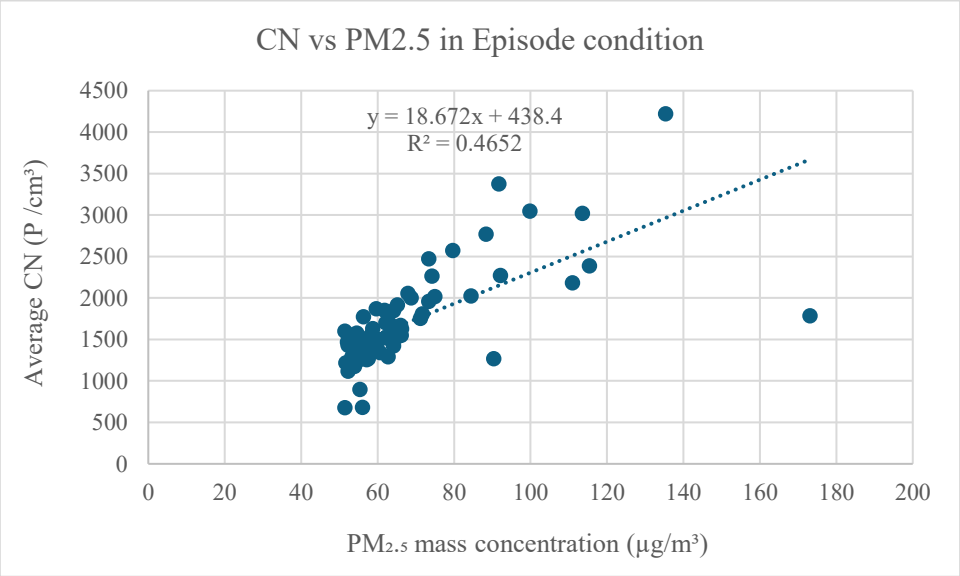

Fig. 64. CN–$PM_{2.5}$ relationship during episodes

The particle number concentration (CN) is also variable over time and shows clear enhancement during pollution episodes compared to background conditions. The enhancement of the particle number concentration is most pronounced during the night and early morning hours, while the concentration decreases during the day due to increased atmospheric mixing. Compared to $PM_{2.5}$, the enhancement of the particle number concentration is associated with increased mass concentration.

The figure.65 shows that $PM_{2.5}$ averages are higher in the High intensity of CN than in the Normal intensity one for both background and episode periods. For background periods, the mean value rises from about 25 µg/m³ in the Normal CN class to roughly 45 µg/m³ in the High CN class. This shows that larger particle numbers are associated with higher particulate mass even outside episode hours.

The same behaviour appears during episodes, but at higher concentration levels. Episode averages are around 57 µg/m³ for Normal CN and increase to nearly 70 µg/m³ for High CN. The difference between the two CN classes is therefore preserved, while the overall $PM_{2.5}$ baseline is shifted upward. Across both regimes, increases in CN occur together with increases in $PM_{2.5}$. The comparison also shows that episode conditions amplify this joint rise in number and mass.

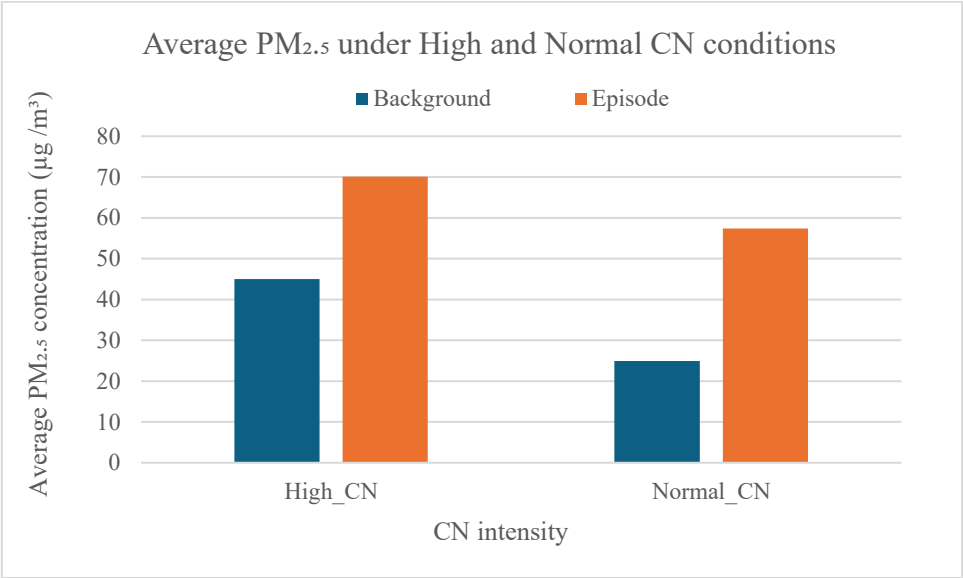

Fig. 65. $PM_{2.5}$ by CN intensity class

The figure compares the mean mass concentrations across two different levels of particle number concentration. For all particle mass concentrations, the levels are substantially higher in the high-intensity class than the normal one. In both particle number concentration levels, the expected cumulative order of particle fractions is maintained. The order suggests that the particle fraction sizes are distributed similarly across both levels. However, the levels are substantially higher in the case of the high-intensity level than the normal-intensity. The pattern suggests that the periods with high particle number concentration are the same as the periods with high particle mass concentration. The concurrent rise in particle number and particle mass suggests that the periods with high particle number concentration are the result of high particle accumulation.

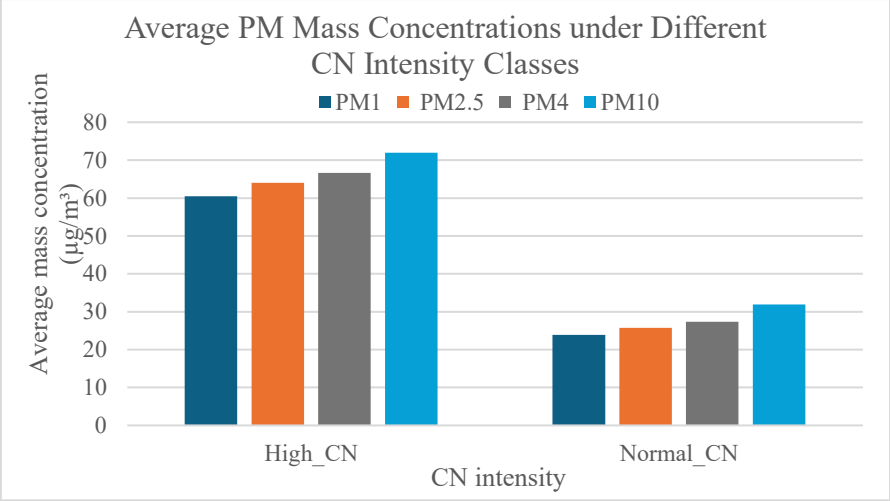

Fig. 66. Average mass concentrations across CN intensity classes

Generally, the particle number concentration (CN) increases significantly during pollution episodes when compared with the normal or background period. High values of CN are associated with high values of the mass concentration of $PM_{2.5}$, showing that the period of high particle numbers is associated with high particulate matter mass concentrations. Similar observations are made for the concentrations of other particulate matter fractions, namely, PM_1, $PM_{2.5}$, PM_4, and PM_{10}, which increase during high CN conditions, showing that high particle numbers are associated with the accumulation of particulate matter.

5. 8. 3. Impact of Meteorological Conditions on particle number concentration

The chart illustrates how the average particle number concentration (CN) behaves as it moves with different levels of relative humidity (RH). As seen on the chart, on increasing the levels of RH, the CN does not simply move up but does it in a non-linear manner. The maximum average particle number concentration appears to be around the RH value between 60% and 80%, where the concentration is about 1000 particles per cubic meter, suggesting that moderate levels of RH may result in the buildup of particles. Further, when RH levels reach about 80% and go even higher, the average particle number concentration dips to about 700–750 particles per cubic meter. This may suggest that at such high levels of humidity, hygroscopic growth may result in the deposition of particles.

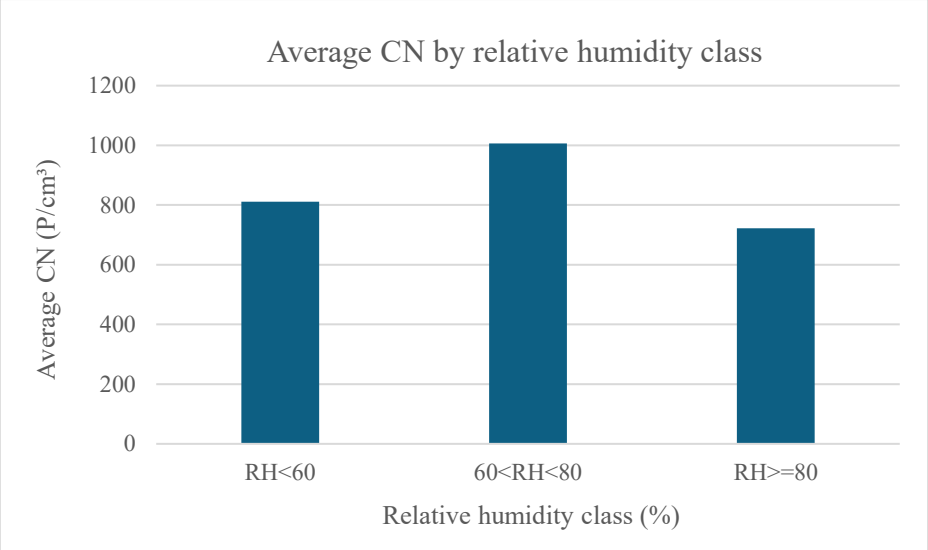

Fig. 67. CN across relative humidity classes

CN remains higher during episodes than during background periods for each class of relative humidity (RH). Under background conditions, CN is lowest in the high-humidity class (RH ≥ 80%). It increases at low humidity (RH < 60%) and reaches its maximum in the intermediate range (60–80%). This distribution shows that CN varies with humidity and that moderate RH is associated with higher particle numbers than very humid conditions. Episode hours follow a similar structure but at higher concentration levels. The largest CN values appear in the low-humidity class, close to 2000 p m^{-3}. At RH ≥ 80% the values decrease, although they remain above background levels. The intermediate RH class again lies between the low and high extremes. Taken together, the figure shows that RH influences the distribution of CN within each regime, while episode conditions correspond to consistently higher concentrations.

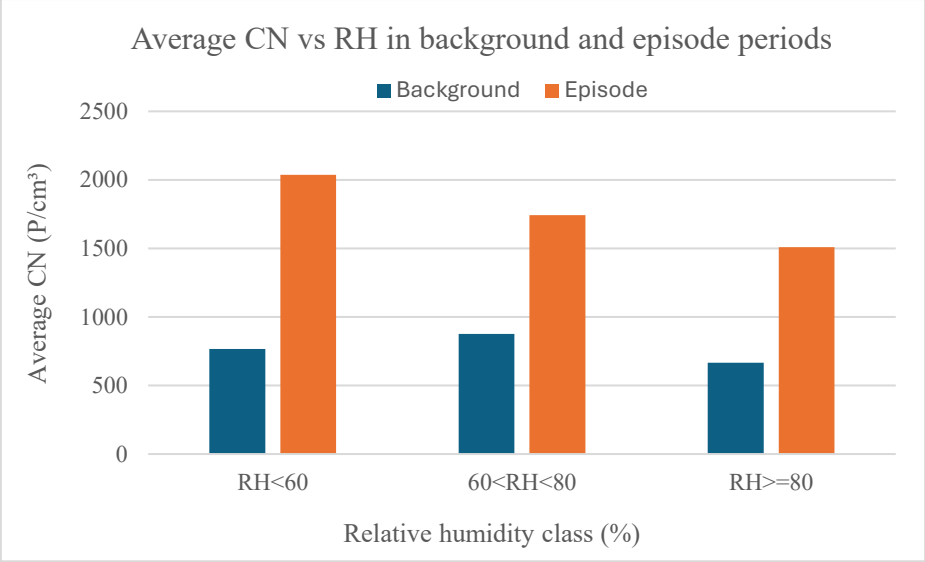

Fig. 68. CN versus relative humidity under different regimes

From the chart below, it can be seen that there is a distinct trend where the concentration increases with increasing ΔT. The lowest concentration of mean number concentration (CN) particles occurs when ΔT < 2 (approximately 600-650 P/cm³), which may be due to favourable conditions for particles to be dispersed or not to accumulate. Conversely, higher values are recorded for ΔT 2-5 and ΔT > 5 (approximately 900-950 P/m³). This shows that there are more structures within the atmosphere where particles tend to accumulate when there are larger ΔT values. The small difference between ΔT 2-5 and ΔT > 5 implies that after a certain ΔT value, the concentration of particles (CN) remains consistent at a higher value than before. This shows that there is a considerable effect of thermal stratification on particles within the atmosphere.

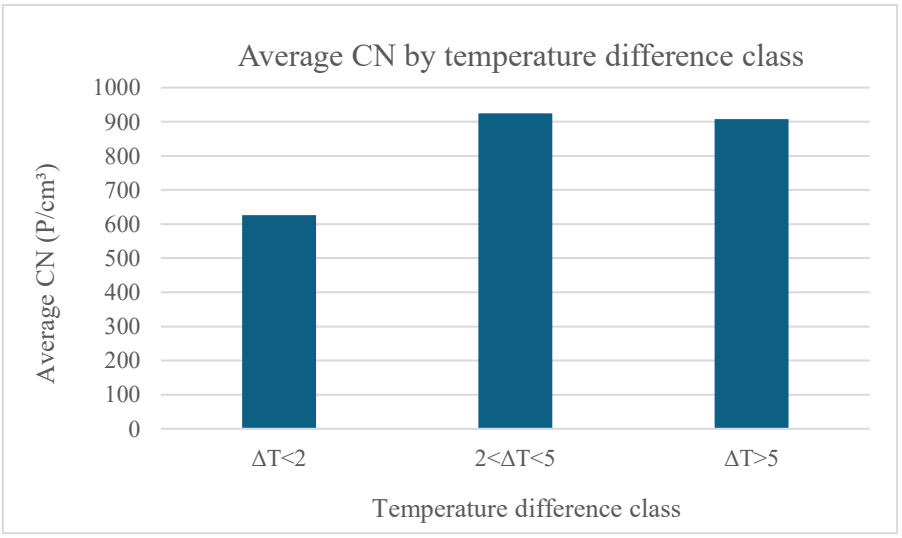

Fig. 69. CN across temperature difference classes

The chart compares average CN values for different temperature difference (ΔT) classes under background and episode conditions. In all classes, episode values remain higher than background values. The strongest contrast appears in the ΔT > 5 class, where episode CN reaches about 2200 particles m^{-3}, while the corresponding background level is close to 800 particles m^{-3}. In the intermediate ΔT range (2–5), episode CN is lower than in the highest class but still clearly above background concentrations. The smallest values in both regimes occur when ΔT is below 2. The figure shows that larger temperature differences are generally associated with higher CN during episodes, while background variations are more limited. This pattern points to an influence of atmospheric structure on particle accumulation.

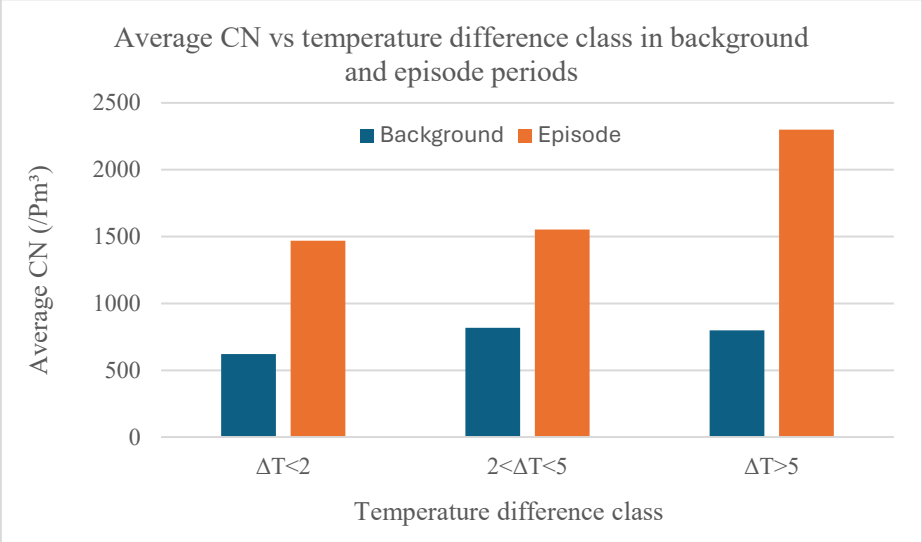

Fig. 70. CN versus ΔT under background and episode conditions

The figure below shows a comparison of the mean particle number concentration under high and low pressure. From the results, it can be noted that the values of the particle number concentration under high pressure conditions (almost 1100 P/cm³) are higher than those under low pressure conditions (almost 800 P/cm³).

These findings can be explained by the characteristic properties of high-pressure systems. High-pressure systems are normally associated with stable atmospheric conditions. The conditions of high pressure are normally associated with low vertical mixing. This implies that particles under these conditions have limited space for dispersion. Therefore, particles accumulate in large numbers near the surface, hence a higher number concentration.

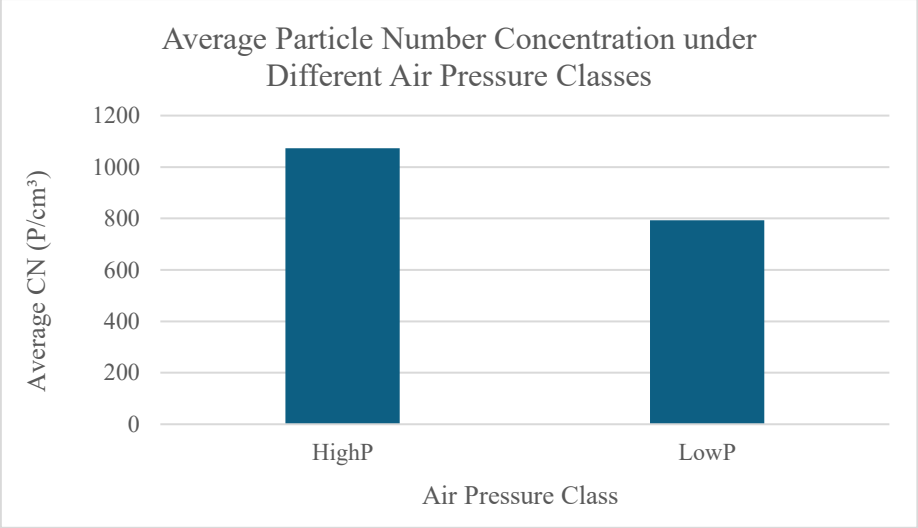

Fig. 71. Average CN values under high- and low-pressure conditions

The results show that meteorological conditions have a significant effect on particle number concentration. The particle number concentration increases under moderate relative humidity conditions, higher ΔT values, and high-pressure conditions. All these conditions are normally associated with higher stability in the atmosphere. Conversely, lower particle number concentration values occur under conditions of higher atmospheric mixing and dispersion. This implies that atmospheric stability plays a large role in determining the particles within the study region.

5. 9. Correlation

For the analysis of the relationships between the concentrations of particulate matter, the particle number concentration, the effective particle density, and the meteorological parameters, a correlation analysis was carried out. This analysis provides a way to identify possible relationships between the parameters of the atmosphere and the characteristics of the particles. The results of the correlation analysis are given in Tables 1-3.

5. 9. 1. Correlation between meteorological parameters and PM concentrations

The results presented in Table 1 indicate a negative correlation between relative humidity (RH) and all fractions of particulate matter. The strength of the negative correlation increases from PM1 to PM10. However, the strongest correlation was found for PM10 (r = -0.36). These

findings indicate that high levels of relative humidity may be responsible for the suppression of particulate matter concentrations.

On the other hand, the temperature difference (ΔT = T - Tdew) shows a positive correlation with all fractions of particulate matter. Moreover, the correlation coefficients for the temperature difference increase from PM1 to PM10, with the strongest correlation for the latter (r = 0.35). The drier atmospheric conditions, i.e., high levels of ΔT, are conducive to high levels of particulate matter concentrations. It can be understood because high levels of ΔT show drier air leading to more particulate matter since there is less moisture in the air.

Finally, there is a weak positive correlation between air pressure and all fractions of particulate matter (r = 0.12-0.26) showing that high air pressure levels contribute to high particulate matter concentrations because they indicate stable atmospheric conditions.

Table 1:Correlation between Meteorological Parameters and PM

Meteorological Parameters	PM_1	$PM_{2.5}$	PM_4	PM_{10}
RH	-0.16	-0.20	-0.24	-0.36
ΔT (T-Tdew)	0.14	0.18	0.22	0.35
Air pressure	0.12	0.15	0.18	0.26

5. 9. 2. Correlation between CN and other variables

As shown in Table 2, the particle number concentration is strongly and positively correlated with all fractions of the particulate matter. These coefficients vary from 0.88 to 0.93 and show a very strong positive relationship between the concentration of the particles in the atmosphere. The highest correlation is found for PM1 implying that the concentration of the particles in the atmosphere is largely controlled by fine particles. However, the concentration of the particles in the atmosphere is negatively correlated with relative humidity (-0.21). This shows that the level of humidity in the atmosphere is inversely proportional to the concentration of the particles in the atmosphere.

Furthermore, the concentration of the particles is weakly positively correlated with the temperature difference as well as the pressure in the atmosphere, 0.19 and 0.17, respectively. These coefficients imply that the concentration of the particles in the atmosphere is controlled by the level of dryness in the atmosphere.

Table 2: Correlation between CN and Other Variables

Variable	PM_1	$PM_{2.5}$	PM_4	PM_{10}	RH	ΔT ($T-T_{dew}$)	Air pressure
CN	0.93	0.92	0.92	0.88	-0.21	0.19	0.17

5. 9. 3. Correlation of effective density with other variables

The results obtained for effective particle density, as shown in Table 3, reveal that it has weak negative correlations with all the particulate matter concentrations, with the correlation coefficients ranging from -0.11 to -0.14. The mass concentration of particulate matter increases, the effective density of particles decreases slightly that may be due to the chemical composition or structural characteristics of the particles present in the atmosphere. In addition, effective density has a moderate negative correlation with relative humidity, where the correlation coefficient is -0.22. This may be due to the fact that the effective density of particles decreases because of the hygroscopic growth of the particles, where the particles tend to gain more moisture at high humidity conditions. However, effective density has a positive correlation with the temperature difference (0.23). It seems that the effective density of particles is high at low humidity conditions, as the particles tend to gain less moisture at low humidity conditions. In addition, the correlation coefficient for effective density and air pressure is very low, at 0.05 which indicates that the effective density of particles is almost independent of the air pressure and the correlation between effective density and particle number concentration (CN) is almost equal to zero, at -0.00093 so, it can be said the effective density of particles is almost independent of the particle number concentration. However, the results obtained indicate that the effective density of particles is more influenced by the humidity conditions of the atmosphere.

Table 3: Correlation of Effective Density with PM and Meteorological Parameters

Variable	PM_1	$PM_{2.5}$	PM_4	PM_{10}	RH	ΔT (T-Tdew)	Air pressure	CN
Effective Density	-0.14	-0.13	-0.13	-0.11	-0.22	0.23	0.05	-0.00093

The results of the correlation analysis confirm that the meteorological conditions have a considerable impact on the concentrations of the particles. The relative humidity shows a negative correlation with the concentrations of the particulate matter as well as the particle number concentration. This implies that the removal processes of the particles could be related

to the humidity. On the other hand, the conditions of low humidity in the atmosphere, indicated by the large values of the temperature difference ΔT, are associated with high concentrations of the particulate matter as well as the particle number. Finally, the effective particle density seems to be more influenced by the humidity than the particle number or the particle mass concentrations.

Chapter 6:

Discussion

6.1. Temporal Variations in PM Mass Concentrations

The present study carried out in Turin, Italy, by Politecnico di Torino, shows strong temporal dynamics in PM mass concentration in different fractions (PM1, PM2.5, PM4, and PM10) during January. The pattern is characterized by high concentration initially, strong reduction in concentration during the initial period, secondary peaks during the middle period, minima during days 19–22, and relatively steady levels during the last days. This is a non-monotonic pattern with simultaneous variation in concentration across all fractions with consistent ordering of PM10 > PM4 > PM2.5 > PM1. This is consistent with a cumulative distribution where total mass variation is primarily responsible for variation in concentration rather than changes in sizing. This is likely due to episodic pollution superposition on a consistent background. Particle mass ratios such as PM1/PM10, PM2.5/PM10, and PM4/PM10 vary moderately from day to day within narrow ranges with synchronized minima (for example, on day 21 due to transient dominance of coarse particles) and maxima favoring finer fractions during the month's margin. These are consistent with mass variation effects over source effects on sizing. These are consistent with global urban PM concentration patterns over long periods. For example, a study on particle number concentration during a decadal period in European cities showed similar episodic increases and non-monotonic monthly variation and suggested these were due to accumulation under stable meteorological conditions. Similarly, global analyses on PM2.5 concentration temporal trends from 2000 to 2020 classified urban trends into types such as single-peak (approximately 49% of cities) and gradual-decreasing types with variability driven by socioeconomic and meteorological factors. In Beijing, a similar study on PM2.5 concentration during the entire year showed three diurnal clusters without strictly weekly cycles, consistent with strong effects of weather on concentration. These are consistent with our episodic variation pattern. Stable ratios in particle sizing are consistent with urban-rural comparisons where temporal trends are similar across land types due to dominant effects of mass accumulation processes [98], [99], [100], [101].

6.2. Diurnal Profiles and Boundary Layer Dynamics

Diurnally, all particulate matter fractions show a synchronized temporal pattern with increased concentrations during late night/early morning, a gradual decrease in the morning, a small peak in late morning, minima in the afternoon (15:00-18:00), and increased concentrations during the evening and nighttime periods. This temporal pattern of particulate matter fractions is consistent with the development of the planetary boundary layer (PBL), with shallow and stable

nocturnal conditions keeping pollution near the surface and increased vertical mixing and dispersion during midday with the development of a deeper boundary layer. These diurnal trends appear consistent with a common cause related to the development of the planetary boundary layer rather than fraction-specific mechanisms. Mass ratios show a small decrease during the afternoon (with coarser fractions dominating under mixing conditions) and an increase during the evening (with finer fractions dominating under low-mixing conditions), with smooth diurnal curves without intersections. These diurnal trends show no evidence of marked bimodal traffic-related peaks. During pollution episodes, the ratios remain high (for PM1/PM10>0.85 and for the other fractions >0.90), uniformly shifted upward without any reshaping of the diurnal pattern. These trends suggest the presence of fine particles during periods of adverse conditions. Global fine PM analyses report median 13.1% diurnal variability related to PBL heights, with nocturnal rises under low mixing matching Turin's profiles [102]. In low/middle-income cities (LMICs), PM2.5 peaks 26% higher nocturnally than midday, linked to PBL collapse and morning emissions, absent strict double peaks if meteorology dominates traffic [103]. European street-canyon studies confirm smoother variations under PBL control, with fine ratios peaking in stable hours, validating the absence of rush-hour dominance here despite the traffic proximate site [104].

6.3. Weekly Cycles and Anthropogenic Influences

Weekly patterns show coherent midweek peaks (Wednesday highest across fractions), Thursday-Friday declines, Saturday rises, and slight Sunday dips, with ratios higher weekends and lower midweek, suggesting anthropogenic buildup (e.g., cumulative emissions) modulated by weekly meteorology. Week-to-week mass variability is substantial (e.g., Monday PM10: 12-50 $\mu g/m^3$) while ratios remain stable, implying episodic overlays on repeatable cycles without strict day-of-week determinism. Site analysis near Corso Castelfidardo—a major commuting route—reveals persistent traffic (morning/evening congestion via Google Maps), loosely correlating with PM morning highs, yet nocturnal fine surges implicate meteorology as co-equal or dominant.

Such findings are in conformity with the literature on urban studies that highlights the importance of emission accumulation over a weekend period. A calendar of PM2.5 concentration levels for the year 2014 in Beijing revealed that there were no universal weekly concentration levels, with about half the weeks showing weekday peaks and Mondays being

the lowest concentration levels in only 13 weeks. The variations were attributed to meteorological influences. There are mid-week peaks in PM10 concentration levels (15–25 μg/m³) and weekend reductions of 10–20%, corresponding to reduced activity levels. These are European canyon monitoring findings. Such findings are in conformity with the observed trends in Turin. The spatiotemporal attributions of PM2.5 concentration levels globally reveal the fluctuating-to-decreasing concentration levels over the year in Chinese urban agglomerations. Mid-week increases are attributed to anthropogenic influences. The qualitative imprint of traffic flow without quantified flow rates serves to highlight the combined influence of local sources and PBL dynamics as the principal modulators.

From a diurnal and meteorological point of view, mass concentrations of all fractions of PM, namely PM1, PM2.5, PM4, and PM10, show a parallel trend, with peak mass concentrations under stable conditions characterized by intermediate relative humidity ranging from 60 to 80%, significant temperature change $\Delta T > 5°C$, and high pressure. On the other hand, low mass concentrations are recorded under dispersive and/or wet conditions, with relative humidity >80%, small temperature change $\Delta T < 2°C$, and low pressure. This consistent trend in mass concentration for all fractions of PM, with no alteration in peak and trough levels, implies that mass concentration is controlled by broad scale rather than specific conditions, contrary to some previous research findings [105], [106].

6.4. Meteorological parameters and particle mass concentrations

The results from this research revealed that temporal changes in particulate matter mass concentration levels for all particle sizes (PM1, PM2.5, PM4, and PM10) are primarily driven by the accumulation or dispersion of total particle mass and not by changes in particle sizes. The negative relationship between relative humidity and PM concentration levels, as well as the positive relationship between temperature-inversion intensity (ΔT) and atmospheric pressure, indicates that stability and vertical mixing were likely to be the major drivers of particulate matter concentration levels in the research area. For instance, during dry and stable atmospheric conditions, particles tend to accumulate on the surface, hence causing increases in all PM concentration levels. This indicates that boundary layer effects are likely to be more dominant in dictating particulate matter behavior in this research area as opposed to individual emission sources. These research findings are consistent with those from earlier research carried out in Turin and the Po Valley region. Based on a multi-year research project on the

PM1, PM2.5, and PM10 concentration levels in Turin, concentration levels showed a high degree of variability in terms of seasons and diurnal variations due to stability conditions and the PBL height, especially during the winter season when unfavorable meteorological conditions prevail in the region. The research findings have shown a high degree of consistency with the present results [107].

Another interesting feature that is observed in the present data is the similar behavior in variation across the PM fractions along with relatively stable particle mass ratios. This shows that increases in total particulate mass are more significant than changes in particle size distribution. Such behavior is usually seen in situations where a persistent pollution background is present due to stagnant atmospheric conditions, during which additional local or regional pollution emissions accumulate. Similar behavior has been observed in international research on particulate matter in urban areas. For example, Liu et al. studied long-term time series data on $PM_{2.5}$ in Beijing and showed that temporal variability in particulate pollution is more related to meteorological conditions than to weekly activity cycles [99]. This is similar to the present research data, in which meteorological conditions are seen to be more effective in modulating particulate matter concentration than daily activity cycles.

6.5. Particle number concentration

The results further reveal that the particle number concentration (CN) increases significantly during pollution episodes and shows strong positive correlations with the mass concentration of PM. This highlights the importance of ultrafine and fine mode particles during pollution episodes. However, the value of the coefficient of determination between CN and the mass concentration of PM is reduced during severe episodes compared to background conditions. This implies that during severe pollution episodes, the relationship between the mass concentration of particles and the number concentration of particles is more complex. A similar result was observed by Mikkonen et al., who analyzed a decade of measurements of the number concentration of particles in a European urban area. Their study revealed that the temporal variations in the number concentration of particles are significantly affected by emission activities and atmospheric conditions, and also the time and magnitude of the peak in the number concentration of particles may not coincide with the peak in the mass concentration of PM. This is due to the complex dynamics of urban aerosols [108]. Hence, the simultaneous increases in the number concentration of particles and the mass concentration of PM may result

from the enhancement of emissions and atmospheric accumulation. Moreover, relative humidity had an effect on aerosol properties in the present study. The negative correlation between relative humidity and PM/CN concentration, as well as the decrease in effective particle density with increasing relative humidity values, can be explained by hygroscopic growth mechanisms. In humid environments, aerosol particles tend to grow by incorporating more water into their composition. The effective density of particles may decrease as a result of changes in their structure. In contrast, drier atmospheric conditions may cause aerosol particles to become more compact, thus leading to an increase in effective density. These findings are consistent with those of Rissler et al., who studied effective particle density within a near-traffic urban environment. They found that urban aerosol particles are a mixture of porous soot aggregates and more compact aged particles whose physical properties vary depending on atmospheric processing and relative humidity levels [109].

Atmospheric pressure finds a weak positive correlation with PM/CN concentration within this investigation. The effect of atmospheric pressure on effective particle density is minimal. It seems that pressure acts primarily as an indicator of stable atmospheric conditions rather than a direct driver of particle physical properties.

The results of this thesis have shown that the variability of PM mass concentration, particle number concentration, and effective particle density at the site under investigation depends on the interplay of local emissions, especially those of traffic, and strong meteorological effects related to atmospheric stability and the boundary layer. Although the impact of traffic emissions on particle formation is evident, the most severe pollution events appear during periods of unfavorable meteorological conditions, reducing the dispersion of pollutants. Therefore, the results of this work point to the importance of taking into account the effects of atmospheric stability, humidity, and the boundary layer in understanding and managing urban air pollution. It appears that in cities such as Turin, reducing emissions may not be sufficient in preventing pollution events without additional forecasting and management techniques based on meteorological parameters and the boundary layer.

Chapter 7:

Conclusion

Conclusion

Urban air pollution and, specifically, fine particulate matter (PM) are known to pose considerable health hazards and are of particular concern during winter months due to stable atmospheric conditions that tend to trap pollutants in larger quantities. In Turin, which is part of the Po Valley known for its poor air quality due to its topography and meteorological conditions, it is known that PM levels tend to exceed maximum permissible limits. For effective mitigation of such pollution and formulation of public health policies, it is crucial to understand the temporal variations and meteorological influences of PM of different size fractions and effective density in terms of number concentration. From the results of the study, it is observed that mass concentration of PM of various size fractions ranging from ultrafine to coarse modes tends to vary in a synchronized manner with respect to time and is primarily governed by mixing conditions in the atmosphere. In particular, it is observed that day-to-day and hour-to-hour variations in PM concentration tend to peak during night hours and decrease in the subsequent afternoon hours. These variations do not specifically show bimodal peaks associated with traffic activity. The observations tend to indicate that boundary layer dynamics and stability conditions dominate over local influences of traffic activity. Similar trends were observed for weekly variations in PM concentration levels, where it was observed that variations in total particle mass concentration occurred, but ratios of size distribution tend to remain constant. These observations tend to indicate that bulk variations in concentration levels were observed and that meteorological influences tend to govern in uniform conditions over all fractions of PM. The order of PM fractions observed in all temporal variations is PM10 > PM4 > PM2.5 > PM1.

Following this idea of temporal coherence, the observed stability of size ratios over nighttime and daytime and over the week implies that all fractions of particulate matter experience uniform influences of meteorological variables like relative humidity, temperature gradients, and pressure. Sufficient humidity and high thermal stability favour the accretion of aerosol particles, while excessive humidity causes more scavenging and mixing, thus favouring dispersion through boundary layer growth. This uniform influence of meteorological variables is seen in the control over total PM mass and not over size fractions of aerosols. The diurnal variation of fine fractions of particulate matter, such as their enhancement during the night, underlines the effect of stability in preferentially increasing the fraction of combustion-derived aerosol in total PM mass.

Under this meteorological regime, episodes of enhanced pollution, predominantly occurring during low-mixing nighttime and early morning hours, not only increase PM mass but also enhance ultrafine particle number concentrations (CN) by several orders of magnitude, with clear distinctions between traffic-influenced episodes during commuting hours and non-traffic episodes under stagnant conditions. The effective density of the aerosol particles (ρeff) varies systematically during the day, following hygroscopic growth and aging, with lower values in the morning hours corresponding to freshly emitted combustion-derived aerosol and higher values in the middle of the day corresponding to processed urban aerosol. This underlines the close relationship between PM mass and CN, both of which are influenced by common meteorological variables, such as negative correlations with humidity and positive correlations with stability, although the variability of these relationships underlines the diversity of their sources, including both primary traffic-derived aerosol and secondary aerosol formation.

The location of the measurement site, strategically placed close to major traffic routes such as Corso Castelfidardo, offers valuable context to explain the results. From the data provided, it is evident that although local influences play a role in establishing a level of background PM concentrations, the lack of peak concentrations during rush hour periods suggests that regional-scale meteorological influences dominate local-scale variations. Such dual influences of local-scale aerosol precursors and regional-scale meteorological influences on aerosol formation and accumulation are characteristic of wintertime pollution events within the Po Valley basin.

Overall, it is evident from the results provided that wintertime atmospheric influences play a critical role in urban environments such as Turin, where atmospheric stability is a dominant feature of wintertime weather patterns. Although proximity to major traffic routes highlights the significance of local-scale influences on aerosol formation through combustion-based precursors, it is evident from the data provided that local influences on PM concentrations are subject to regional-scale meteorological influences on atmospheric stability. Such results are characteristic of urban-scale PM variability and are consistent with analogous studies of PM concentrations within other urban environments with similar topographic influences. Such results highlight that PM concentrations vary with diurnal and weekly mixing cycles rather than with sudden changes to emission inventories.

Finally, the study offers basic information on the intricate relationships between the pollutants, chemical compounds, and meteorological elements, which are the basis of urban air pollution. It is recommended that future studies should be directed towards: (1) the chemical analysis of

the particulate matter to identify primary and secondary components, (2) numerical models of the mechanisms of accumulation and transport, and (3) monitoring during additional seasons to assess the effectiveness of the mitigation strategies for urban air pollution. These lines of research would be useful in the development of policies, such as the restriction of traffic during high levels of atmospheric stability, or the coordination of the reduction of emissions, with the objective of ensuring the health of the population in urban areas with episodes of urban air pollution, particularly during the winter season.

Reference

[1] A. Isidro, A. Malgosa, and G. Prats-Muñoz, “Anthracosis in a Coptic Mummy,” Archivos de Bronconeumología, vol. 50, no. 8, pp. 368–369, 2014, doi: 10.1016/j.arbr.2014.06.006.

[2] J. T. Pryor, L. O. Cowley, and S. E. Simonds, “The physiological effects of air pollution: Particulate matter, physiology and disease,” Frontiers in Public Health, vol. 10, art. 882569, pp. 1–18, Jul. 2022, doi: 10.3389/fpubh.2022.882569.

[3] D. Fowler et al., “A chronology of global air quality,” Philosophical Transactions of the Royal Society A: Mathematical, Physical and Engineering Sciences, vol. 378, no. 2183, art. 20190314, pp. 1–20, Sep. 2020, doi: 10.1098/rsta.2019.0314.

[4] W. G. Christy, “History of the Air Pollution Control Association,” Journal of the Air Pollution Control Association, vol. 10, no. 2, pp. 126–174, 1960, doi: 10.1080/00022470.1960.10467911.

[5] W. W. Hanlon, “Coal Smoke, City Growth, and the Costs of the Industrial Revolution,” The Economic Journal, vol. 130, no. 626, pp. 462–488, Feb. 2020, doi: 10.1093/ej/uez055.

[6] L. M. Cook, “The Rise and Fall of the Carbonaria Form of the Peppered Moth,” The Quarterly Review of Biology, vol. 78, no. 4, pp. 399–417, Dec. 2003, doi: 10.1086/378925.

[7] N. Morag-Levine, “The Case of Proclamations (1610), Aldred’s Case (1610), and the Origins of the Sic Utere / Salus Populi Antithesis,” Law and History Review, vol. 40, no. 2, pp. 295–328, Jun. 2022, doi: 10.1017/S0738248022000097.

[8] R. A. Smith, Air and Rain: The Beginnings of a Chemical Climatology. London: Longmans, Green, and Co., 1872.

[9] R. Stone, “Counting the Cost of London’s Killer Smog,” Science, vol. 298, no. 5601, pp. 2106–2107, Dec. 2002, doi: 10.1126/science.298.5601.2106.

[10] T. Williamson, S. Moorcroft, H. Pearce, and B. Marner, 1952 Air Quality in a Modern Context: 70 Years Since the Great London Smog, Air Quality Consultants Ltd. for the Greater London Authority, Dec. 2022.

[11] J. Cao, S. C. Lee, J. C. Chow, and J. G. Watson, “Evolution of $PM_{2.5}$ Measurements and Standards in the USA,” Aerosol and Air Quality Research, vol. 13, no. 4, pp. 1197–1211, 2013.

[12] U.S. Environmental Protection Agency, Review of the National Ambient Air Quality Standards for Particulate Matter: Policy Assessment of Scientific and Technical Information (OAQPS Staff Paper), EPA-452/R-96-013, Office of Air Quality Planning and Standards, Research Triangle Park, NC, USA, Jul. 1996, pp. II-1–II-2.

[13] U.S. Environmental Protection Agency, "Revisions to the National Ambient Air Quality Standards for Particulate Matter," Federal Register, vol. 52, no. 126, pp. 24634–24664, Jul. 1, 1987.

[14] European Commission, Council Directive 1999/30/EC relating to limit values for sulphur dioxide, nitrogen dioxide and oxides of nitrogen, particulate matter and lead in ambient air, Official Journal of the European Communities, 1999.

[15] Amended by Commission Decision 2001/744/EC, Official Journal of the European Communities, L 278, p. 35, Oct. 23, 2001; and Directive 2008/50/EC, Official Journal of the European Union, L 152, p. 1, Jun. 11, 2008.

[16] P. Kumar, L. Morawska, W. Birmili, P. Paasonen, M. Hu, M. Kulmala, R. M. Harrison, L. Norford, and R. Britter, "Ultrafine particles in cities," Environment International, vol. 66, pp. 1–10, 2014. doi: 10.1016/j.envint.2014.01.013.

[17] World Health Organization, WHO Global Air Quality Guidelines: Particulate Matter ($PM_{2.5}$ and PM_{10}), Ozone, Nitrogen Dioxide, Sulfur Dioxide and Carbon Monoxide, Geneva, 2021.

[18] I. Manisalidis, E. Stavropoulou, A. Stavropoulos, and E. Bezirtzoglou, "Environmental and health impacts of air pollution: A review," Frontiers in Public Health, vol. 8, art. 14, Feb. 2020, doi: 10.3389/fpubh.2020.00014.

[19] World Health Organization, Air Pollution. Geneva, Switzerland: World Health Organization, 2022. [Online]. Available: https://www.who.int/health-topics/air-pollution

[20] A. A. Almetwally, M. Bin-Jumah, and A. A. Allam, "Ambient air pollution and its influence on human health and welfare: an overview," Environmental Science and Pollution Research, vol. 27, no. 22, pp. 24815–24830, May 2020, doi: 10.1007/s11356-020-09042-2.

[21] J. Yang, B. Shi, Y. Zheng, Y. Shi, and G. Xia, "Urban form and air pollution disperse: Key indexes and mitigation strategies," Sustainable Cities and Society, vol. 57, p. 101955, 2020, doi: 10.1016/j.scs.2019.101955.

[22] S. Sun, C. Sarkar, S. Kumari, P. James, W. Cao, R. S.-y. Lee, L. Tian, and C. Webster, "Air pollution associated respiratory mortality risk alleviated by residential greenness in the Chinese Elderly Health Service Cohort," Environmental Research, vol. 183, p. 109139, 2020, doi: 10.1016/j.envres.2020.109139.

[23] M. Michetti, M. Gualtieri, A. Anav, M. Adani, B. Benassi, C. Dalmastri, I. D'Elia, A. Piersanti, G. Sannino, G. Zanini, and R. Uccelli, "Climate change and air pollution: Translating their interplay into present and future mortality risk for Rome and Milan municipalities," Science of the Total Environment, vol. 830, p. 154680, 2022, doi: 10.1016/j.scitotenv.2022.154680.

[24] World Health Organization, WHO Global Air Quality Guidelines: Particulate Matter ($PM_{2.5}$ and PM_{10}), Ozone, Nitrogen Dioxide, Sulfur Dioxide and Carbon Monoxide. Geneva, Switzerland: World Health Organization, 2021. [Online]. Available: https://www.who.int/publications/i/item/9789240034228

[25] J. A. Bernstein, N. Alexis, C. Barnes, I. L. Bernstein, A. Nel, D. Peden, D. Diaz-Sanchez, S. M. Tarlo, and P. B. Williams, "Health effects of air pollution," Journal of Allergy and Clinical Immunology, vol. 114, no. 5, pp. 1116–1123, 2004, doi: 10.1016/j.jaci.2004.08.030.

[26] R. R. R. Appannagari, "Environmental pollution causes and consequences: A study," North Asian International Research Journal of Social Science & Humanities, vol. 3, no. 8, pp. 151–161, Aug. 2017. [Online]. Available: https://www.researchgate.net/publication/323944189

[27] M. K. Khallaf, The Impact of Air Pollution on Health, Economy, Environment and Agricultural Sources. Rijeka, Croatia: InTech Publishing, 2011.

[28] Y. Bian, Z. Huang, J. Ou, Z. Zhong, Y. Xu, Z. Zhang, X. Xiao, X. Ye, Y. Wu, X. Yin, C. Li, L. Chen, M. Shao, and J. Zheng, "Evolution of anthropogenic air pollutant emissions in Guangdong Province, China, from 2006 to 2015," Atmospheric Chemistry and Physics, vol. 19, no. 18, pp. 11701–11719, 2019, doi: 10.5194/acp-19-11701-2019.

[29] F. J. Kelly and J. C. Fussell, "Air pollution and public health: Emerging hazards and improved understanding of risk," Environmental Geochemistry and Health, vol. 37, no. 4, pp. 631–649, 2015, doi: 10.1007/s10653-015-9720-1.

[30] S. Fuzzi et al., “Particulate matter, air quality and climate: Lessons learned and future needs,” Atmospheric Chemistry and Physics, vol. 15, no. 14, pp. 8217–8299, 2015, doi: 10.5194/acp-15-8217-2015.

[31] Y. Yan, Y. Li, M. Sun, and Z. Wu, “Primary pollutants and air quality analysis for urban air in China: Evidence from Shanghai,” Sustainability, vol. 11, no. 7, p. 2319, 2019, doi: 10.3390/su11082319.

[32] M. Mao, X. Zhang, and Y. Yin, “Particulate matter and gaseous pollutions in three metropolises along the Chinese Yangtze River: Situation and implications,” International Journal of Environmental Research and Public Health, vol. 15, no. 6, p. 1102, 2018, doi: 10.3390/ijerph15061102.

[33] American Lung Association, State of the Air 2013: Health Effects of Ozone and Particle Pollution. Washington, DC, USA: American Lung Association, 2013. [Online]. Available: https://www.lung.org/getmedia/776a9086-2e73-4c76-9259-7018069cf28f/State-of-the-Air-2013.pdf

[34] L. Samek, Z. Stegowski, K. Styszko, L. Furman, and J. Fiedor, “Seasonal contribution of assessed sources to submicron and fine particulate matter in a Central European urban area,” Environmental Pollution, vol. 241, pp. 406–411, 2018, doi: 10.1016/j.envpol.2018.05.082.

[35] World Health Organization, Regional Office for Europe, Review of Evidence on Health Aspects of Air Pollution – REVIHAAP Project: Technical Report. Copenhagen, Denmark: WHO Regional Office for Europe, 2013. [Online]. Available: https://www.euro.who.int/en/health-topics/environment-and-health/air-quality/publications/2013/review-of-evidence-on-health-aspects-of-air-pollution-revihaap-project-technical-report

[36] W. Dai, J. Gao, G. Cao, and F. Ouyang, “Chemical composition and source identification of PM2.5 in the suburb of Shenzhen, China,” Atmospheric Research, vol. 122, pp. 391–400, 2013, doi: 10.1016/j.atmosres.2012.12.004.

[37] J. O. Babayemi, M. B. Ogundiran, and O. Osibanjo, “Overview of environmental hazards and health effects of pollution in developing countries: A case study of Nigeria,” Environmental Quality Management, vol. 26, no. 1, pp. 51–65, 2016, doi: 10.1002/tqem.21480.

[38] X. Chen, “A spatial and temporal analysis of the socioeconomic factors associated with breast cancer in Illinois using geographically weighted generalized linear regression,” Journal of Geovisualization and Spatial Analysis, vol. 2, no. 1, p. 5, 2018, doi: 10.1007/s41651-017-0011-5.

[39] M. K. Onabowale and O. K. Owoade, “Assessment of residential indoor–outdoor airborne particulate matter in Ibadan, Southwestern Nigeria,” Donnish Journal of Physical Sciences, vol. 1, no. 1, pp. 1–7, Oct. 2015.

[40] World Health Organization, 7 Million Premature Deaths Annually Linked to Air Pollution. Geneva, Switzerland: World Health Organization, 2014. [Online]. Available: https://www.who.int/news/item/25-03-2014-7-million-premature-deaths-annually-linked-to-air-pollution

[41] E. A. Moses and U. B. Orok, “Contamination and health risk assessment of suspended particulate matter (SPM) in Uyo, Niger Delta, Nigeria,” Journal of Scientific Research & Reports, vol. 6, no. 4, pp. 276–286, Mar. 2015, doi: 10.9734/JSRR/2015/16296.

[42] S. Gourdji, “Review of plants to mitigate particulate matter, ozone as well as nitrogen dioxide air pollutants and applicable recommendations for green roofs in Montreal, Quebec,” Environmental Pollution, vol. 241, pp. 378–387, 2018, doi: 10.1016/j.envpol.2018.05.053.

[43] World Health Organization, WHO Global Air Quality Guidelines: $PM_{2.5}$, PM_{10}, O_3, NO_2, SO_2, CO, WHO Regional Office for Europe, 2021.

[44] P. Pokorná, N. Zíková, P. Vodička, R. Lhotka, S. Mbengue, A. Holubová Šmejkalová, V. Riffault, J. Ondráček, J. Schwarz, and V. Ždímal, “Chemically speciated mass size distribution, particle density, shape and origin of non-refractory PM_1 measured at a rural background site in central Europe,” Atmos. Chem. Phys., vol. 22, pp. 5829-5858, 2022, doi:10.5194/acp-22-5829-2022.

[45] Y. Wu, Z. Liu, L. Wang, D. Zhang, X. Ji, J. Zhang, and Z. Hu, “A study of the morphology and effective density of externally mixed black carbon aerosols,” Atmospheric Measurement Techniques, vol. 12, no. 6, pp. 3443–3456, 2019, doi: 10.5194/amt-12-3443-2019.

[46] B. X. Liao, L. G. Zhang, W. Y. Li, Y. J. Luo, Y. J. Chen, J. Z. Liu, and Z. Q. Wang, “A mass correction method for the aerosol particle mass analyzer and implications for effective density,” Aerosol Science and Technology, vol. 53, no. 10, pp. 1109–1124, 2019, doi: 10.1080/02786826.2019.1623153.

[47] R. P. Pokhrel, T. Moosmüller, G. W. Fuller, M. N. Dubey, and C. E. Corrigan, “Impact of combustion conditions on physical properties of aerosols,” Aerosol Science and Technology, vol. 55, no. 3, pp. 256–270, 2021, doi: 10.1080/02786826.2020.1858748.

[48] M. Kazemimanesh, M. V. Zanatta, J. Z. Li, C. Liu, and J. L. Jimenez, “A comparative study on effective density, shape factor, and volatile mixing of particles by mobility/optical techniques,” Journal of Aerosol Science, vol. 161, p. 105940, 2022, doi: 10.1016/j.jaerosci.2022.105940.

[49] H. C. Cheung, J. Li, L. Wang, H. Hu, and M. Hu, “Hygroscopic properties and CCN activity of ambient aerosols,” Atmospheric Chemistry and Physics, vol. 20, no. 18, pp. 11907–11921, 2020, doi: 10.5194/acp-20-11907-2020.

[50] K. Hu, J. Zhang, Q. Zhao, Y. Zhang, and Z. Zheng, “Diversity of particle shape and mixing state from single-particle observations,” Geophysical Research Letters, vol. 48, no. 10, p. e2021GL093447, 2021, doi: 10.1029/2021GL093447.

[51] P. E. Saide, G. R. Carmichael, A. B. Nenes, M. J. Cubison, J. L. Jimenez, and S. N. Pandis, “Understanding and improving model representation of aerosol hygroscopic growth and density,” Atmospheric Chemistry and Physics, vol. 20, no. 5, pp. 2765–2783, 2020, doi: 10.5194/acp-20-2765-2020.

[52] R. G. McFiggans, P. F. Liu, T. W. Wilson, and M. D. Petters, “Physical and chemical properties controlling the interaction of aerosols with water vapour,” Atmospheric Chemistry and Physics, vol. 21, no. 15, pp. 11689–11727, 2021, doi: 10.5194/acp-21-11689-2021.

[53] M. D. Petters, A. Zieger, J. P. Schwarz, and J. H. Seinfeld, “Kappa distributions in global aerosol models,” Atmospheric Chemistry and Physics, vol. 23, no. 1, pp. 595–610, 2023, doi: 10.5194/acp-23-595-2023.

[54] D. W. Fahey, S. Solomon, T. Storelvmo, M. Krämer, and J. Fan, “Advances in understanding aerosol–cloud–climate interactions,” Reviews of Geophysics, vol. 61, no. 2, p. e2022RG000783, 2023, doi: 10.1029/2022RG000783.

[55] A. Dinoi, G. Pavese, M. Calvello, D. Chirizzi, A. Pennetta, G. E. De Benedetto, F. Esposito, C. Mapelli, and D. Contini, “Characterization of aerosol and its oxidative potential in a coastal semi-rural site of Southern Italy,” Atmospheric Environment, vol. 333, p. 120656, 2024, doi: 10.1016/j.atmosenv.2024.120656.

[56] A. Font, J. F. de Brito, V. Riffault, S. Conil, J.-L. Jaffrezo, and A. Bourin, “Long-term measurements of aerosol composition at rural background sites in France: Sources, seasonality and mass closure of $PM_{2.5}$,” Atmospheric Environment, vol. 334, p. 120724, 2024, doi: 10.1016/j.atmosenv.2024.120724.

[57] A. Naseri, T. A. Sipkens, S. N. Rogak, and J. S. Olfert, “Optimized instrument configurations for tandem particle mass analyzer and single particle-soot photometer experiments,” Journal of Aerosol Science, vol. 160, p. 105897, 2022, doi: 10.1016/j.jaerosci.2021.105897.

[58] V. S. Moorchilot, U. K. Aravind, S. P. M. Menacherry, and C. T. Aravindakumar, “Single-Particle Analysis of Atmospheric Aerosols: Applications of Raman Spectroscopy,” Atmosphere, vol. 13, no. 11, p. 1779, 2022, doi: 10.3390/atmos13111779.

[59] E. T. Vokes, E. R. Lewis, A. L. Johnson, and M. I. Cotterell, “Densities of internally mixed organic–inorganic particles from mobility diameter measurements of aerodynamically classified aerosols,” Aerosol Science and Technology, vol. 56, no. 8, pp. 688–710, 2022, doi: 10.1080/02786826.2022.2062293.

[60] L. Peng and Y. Liu, “Theoretical foundation of the relationship between three definitions of effective density and particle size,” Atmosphere, vol. 13, no. 4, p. 564, 2022, doi: 10.3390/atmos13040564.

[61] A. Du, J. Sun, H. Liu, W. Xu, W. Zhou, Y. Zhang, L. Li, X. Du, Y. Li, X. Pan, Z. Wang, and Y. Sun, “Mixing state and effective density of aerosol particles during the Beijing 2022 Olympic Winter Games,” Atmospheric Chemistry and Physics, vol. 23, pp. 13597–13611, 2023, doi: 10.5194/acp-23-13597-2023.

[62] S. Wang, K. Zhou, X. Lu, H. Chen, F. Yang, Q. Li, X. Yang, and X. Wang, “Measurement of Density and Shape for Single Black Carbon Aerosols in a Heavily Polluted Urban Area,” Aerosol and Air Quality Research, vol. 21, no. 12, article 210162, 2021, doi: 10.4209/aaqr.210162.

[63] T. Wu and B. E. Boor, “Urban aerosol size distributions: a global perspective,” Atmospheric Chemistry and Physics, vol. 21, pp. 8883–8914, 2021, doi: 10.5194/acp-21-8883-2021.

[64] X. Gong, H. Wex, J. Voigtländer, K. W. Fomba, K. Weinhold, M. van Pinxteren, S. Henning, T. Müller, H. Herrmann, and F. Stratmann, “Characterization of aerosol particles at Cabo Verde close to sea level and at the cloud level – Part 1: Particle number size distribution, cloud condensation nuclei and their origins,” Atmospheric Chemistry and Physics, vol. 20, pp. 1431–1449, 2020, doi: 10.5194/acp-20-1431-2020.

[65] J. L. Jimenez, M. R. Canagaratna, N. M. Donahue, A. S. H. Prevot, Q. Zhang, J. H. Kroll, P. F. DeCarlo, J. D. Allan, H. Coe, N. L. Ng, A. C. Aiken, K. S. Docherty, I. M. Ulbrich, A. P. Grieshop, A. L. Robinson, J. Duplissy, J. D. Smith, K. R. Wilson, V. A. Lanz, C. Hueglin, Y. L. Sun, J. Tian, A. Laaksonen, T. Raatikainen, J. Rautiainen, P. Vaattovaara, M. Ehn, M. Kulmala, J. M. Tomlinson, D. R. Collins, M. J. Cubison, E. J. Dunlea, J. A. Huffman, T. B. Onasch, M. R. Alfarra, P. I. Williams, K. Bower, Y. Kondo, J. Schneider, F. Drewnick, S. Borrmann, S. Weimer, K. Demerjian, D. Salcedo, L. Cottrell, R. Griffin, A. Takami, T. Miyoshi, S. Hatakeyama, A. Shimono, J. Y. Sun, Y. M. Zhang, K. Dzepina, J. R. Kimmel, D. Sueper, J. T. Jayne, S. C. Herndon, A. M. Trimborn, L. R. Williams, E. C. Wood, A. M. Middlebrook, C. E. Kolb, U. Baltensperger, and D. R. Worsnop, “Evolution of Organic Aerosols in the Atmosphere,” Science, vol. 326, no. 5959, pp. 1525–1529, 2009, doi: 10.1126/science.1180353.

[66] E. Marinou, V. Amiridis, I. Binietoglou, A. Tsikerdekis, S. Solomos, E. Proestakis, D. Konsta, N. Papagiannopoulos, A. Tsekeri, G. Vlastou, P. Zanis, D. Balis, U. Wandinger, and A. Ansmann, “Three-dimensional evolution of Saharan dust transport towards Europe based on a 9-year EARLINET-optimized CALIPSO dataset,” Atmospheric Chemistry and Physics, vol. 17, pp. 5893–5919, 2017, doi: 10.5194/acp-17-5893-2017.

[67] L. Wang, W. Wang, B. Lyu, J. Zhang, Y. Han, Y. Bai, and Z. Guo, “The Identification and Analysis of Long-Range Aerosol Transport Pathways with Layered Cloud-Aerosol Lidar with Orthogonal Polarization Datasets from 2006 to 2016,” Remote Sensing, vol. 15, no. 18, article 4537, 2023, doi: 10.3390/rs15184537.

[68] R. Stevens and A. Dastoor, “A review of the representation of aerosol mixing state in atmospheric models,” Atmosphere, vol. 10, no. 4, article 168, 2019, doi: 10.3390/atmos10040168.

[69] C. ChooChuay, S. Pongpiachan, D. Tipmanee, W. Deelaman, O. Suttinun, Q. Wang, L. Xing, G. Li, Y. Han, J. Palakun, S. Poshyachinda, S. Aukkaravittayapun, V. Surapipith, and J. Cao, “Long-range transboundary atmospheric transport of polycyclic aromatic hydrocarbons,

carbonaceous compositions, and water-soluble ionic species in southern Thailand," Aerosol and Air Quality Research, vol. 20, pp. 1591–1606, 2020, doi: 10.4209/aaqr.2020.0120.

[70] Commissione parlamentare di inchiesta sulle condizioni di sicurezza e sullo stato di degrado delle città e delle loro periferie, Report Comune di Torino. Rome, Italy, Jun. 26, 2024.

[71] A. Bigi and G. Ghermandi, "Long-term trend and variability of atmospheric PM10 concentration in the Po Valley," Atmospheric Chemistry and Physics, vol. 14, pp. 4895–4907, 2014, doi: 10.5194/acp-14-4895-2014.

[72] Turin climate data: Climate-Data.org, Climate and average weather – Turin, Italy. [Online]. Available: https://en.climate-data.org/europe/italy/piemont/turin-1108/ (Accessed: Dec. XX, 2025).

[73] L. Ferrero, D. Cappelletti, B. Moroni, G. Sangiorgi, M. G. Perrone, S. Crocchianti, and E. Bolzacchini, "Wintertime aerosol dynamics and chemical composition across the mixing layer over basin valleys," Atmospheric Environment, vol. 56, pp. 143–153, 2012, doi: 10.1016/j.atmosenv.2012.03.071.

[74] A. Robotto, S. Barbero, P. Bracco, R. Cremonini, M. Ravina, and E. Brizio, "Improving Air Quality Standards in Europe: Comparative Analysis of Regional Differences, with a Focus on Northern Italy," Atmosphere, vol. 13, no. 5, art. no. 642, 2022, doi: 10.3390/atmos13050642.

[75] ARPA Piemonte, Uno sguardo all'aria 2023: Relazione annuale sui dati rilevati dalla rete regionale di monitoraggio della qualità dell'aria, Agenzia Regionale per la Protezione Ambientale del Piemonte, Turin, Italy, 2024. [Online]. Available: https://www.arpa.piemonte.it/sites/default/files/media/2024-10/Uno%20Sguardo%20all%27Aria%202023.pdf

[76] D. Gallione, N. Mastromatteo, and M. Clerico, "Analysis of PM concentrations in Turin: Annual trend and monthly and daily mean concentration," International Journal of Environmental Pollution and Remediation, vol. 13, 2025, doi: 10.11159/ijepr25.004.

[77] PALAS GmbH, *Operating Manual: Fine Dust Monitor System Fidas® (Models 100, 200, 200 S, 300, 300 S)*, Version V0020312. Karlsruhe, Germany: PALAS GmbH, n.d. [Online]. Available: https://www.palas.de

[78] N. Mastromatteo, L. Drudi, D. Gallione, R. Bellopede, and M. Clerico, "Assessment of environmental parameters in natural coastal scenery and compositional by means of an

innovative approach," Atmosphere, vol. 15, no. 11, p. 1379, 2024, doi: 10.3390/atmos15111379.

[79] ParteQ GmbH, Product Data Sheet: Palas® Fidas® 200 S. Malsch, Germany: ParteQ GmbH, n.d. [Online]. Available: https://www.parteq.net

[80] PALAS GmbH, *User Manual: PDAnalyze Software (for use with the Promo® series, Fidas® series, UF-CPC, U-SMPS, and U-RANGE)*, Version V0030112. Karlsruhe, Germany: PALAS GmbH, n.d. [Online]. Available: https://www.palas.de

[81] Palas GmbH, *Fine Dust Measurement Device Fidas® 200 S*. Karlsruhe, Germany: Palas GmbH, Mar. 13, 2021. [Online]. Available: https://www.palas.de

[82] J. Kukkonen, R. Sokhi, L. H. Slørdal, S. Finardi, B. Fay, M. Millan, R. Salvador, A. Rasmussen, G. Schayes, and E. Berge, "Analysis and evaluation of European air pollution episodes," in Meteorology Applied to Urban Air Pollution Problems, COST Action 715 Final Report, B. Fisher et al., Eds. Sofia, Bulgaria: Demetra Ltd Publishers, 2005, pp. 99–114.

[83] J. L. Schnell and M. J. Prather, "Co-occurrence of extremes in surface ozone, particulate matter, and temperature over eastern North America," Proceedings of the National Academy of Sciences, vol. 114, no. 11, pp. 2854–2859, Mar. 2017, doi: 10.1073/pnas.1614453114.

[84] A. P. K. Tai, L. J. Mickley, D. J. Jacob, E. M. Leibensperger, L. Zhang, J. A. Fisher, and H. O. T. Pye, "Meteorological modes of variability for fine particulate matter (PM2.5) air quality in the United States: Implications for PM2.5 sensitivity to climate change," Atmospheric Chemistry and Physics, vol. 12, pp. 3131–3145, 2012, doi: 10.5194/acp-12-3131-2012.

[85] J.-P. Putaud et al., "A European aerosol phenomenology – 3: Physical and chemical characteristics of particulate matter from 60 rural, urban, and kerbside sites across Europe," Atmospheric Environment, vol. 44, no. 10, pp. 1308–1320, 2010, doi: 10.1016/j.atmosenv.2009.12.011.

[86] U.S. Environmental Protection Agency, "Review of the National Ambient Air Quality Standards for Particulate Matter," Federal Register, vol. 85, no. 84, pp. 24094–24144, Apr. 30, 2020.

[87] M. Kuwata, S. R. Zorn, and S. T. Martin, “Using Elemental Ratios to Predict the Density of Organic Material Composed of Carbon, Hydrogen, and Oxygen,” Environmental Science & Technology, vol. 46, no. 2, pp. 787–794, 2012.

[88] P. F. DeCarlo, J. G. Slowik, D. R. Worsnop, P. Davidovits, and J. L. Jimenez, “Particle morphology and density characterization by combined mobility and aerodynamic diameter measurements. Part 1: Theory,” Aerosol Science and Technology, vol. 38, no. 12, pp. 1185–1205, 2004.

[89] J. Rissler, E. Z. Nordin, A. C. Eriksson, P. T. Nilsson, M. Frosch, M. K. Sporre, A. Wierzbicka, B. Svenningsson, J. Löndahl, M. E. Messing, S. Sjögren, J. G. Hemmingsen, S. Loft, J. H. Pagels, and E. Swietlicki, “Effective Density and Mixing State of Aerosol Particles in a Near-Traffic Urban Environment,” Environmental Science & Technology, vol. 48, no. 11, pp. 6300–6308, 2014.

[90] J. L. Jimenez, M. R. Canagaratna, N. M. Donahue, A. S. H. Prevot, Q. Zhang, J. H. Kroll, P. F. DeCarlo, J. D. Allan, H. Coe, N. L. Ng, A. C. Aiken, K. S. Docherty, I. M. Ulbrich, A. P. Grieshop, A. L. Robinson, J. Duplissy, J. D. Smith, K. R. Wilson, V. A. Lanz, C. Hueglin, Y. L. Sun, J. Tian, A. Laaksonen, T. Raatikainen, J. Rautiainen, P. Vaattovaara, M. Ehn, M. Kulmala, J. M. Tomlinson, D. R. Collins, M. J. Cubison, E. J. Dunlea, J. A. Huffman, T. B. Onasch, M. R. Alfarra, P. I. Williams, K. Bower, Y. Kondo, J. Schneider, F. Drewnick, S. Borrmann, S. Weimer, K. Demerjian, D. Salcedo, L. Cottrell, R. Griffin, A. Takami, T. Miyoshi, S. Hatakeyama, A. Shimono, J. Y. Sun, Y. M. Zhang, K. Dzepina, J. R. Kimmel, D. Sueper, J. T. Jayne, S. C. Herndon, A. M. Trimborn, L. R. Williams, E. C. Wood, A. M. Middlebrook, C. E. Kolb, U. Baltensperger, and D. R. Worsnop, “Evolution of Organic Aerosols in the Atmosphere,” Science, vol. 326, no. 5959, pp. 1525–1529, 2009.

[91] Markku Kulmala, Hanna Vehkamäki, Tuukka Petäjä, Marko Dal Maso, Ari Lauri, Veli-Matti Kerminen, Wolfram Birmili, and Peter H. McMurry, “Formation and growth rates of ultrafine atmospheric particles: a review of observations,” Journal of Aerosol Science, vol. 35, no. 2, pp. 143–176, 2004.

[92] Mathew R. Heal, Prashant Kumar, and Roy M. Harrison, “Particles, air quality, policy and health,” Chemical Society Reviews, vol. 41, pp. 6606–6630, 2012.

[93] Health Council of the Netherlands, *Risks of ultrafine particles in the outside air*. The Hague, The Netherlands: Health Council of the Netherlands, 2021, publication no. 2021/38.

[94] P. Georgiades, M. Kohl, M. A. Nicolaou, T. Christoudias, A. Pozzer, C. Dovrolis, and J. Lelieveld, “Global high-resolution ultrafine particle number concentrations through data fusion with machine learning,” Scientific Data, vol. 12, p. 1790, 2025, doi: 10.1038/s41597-025-06055-9.

[95] Q.-Q. Li, Y.-T. Guo, J.-Y. Yang, and C.-S. Liang, “Review on main sources and impacts of urban ultrafine particles: Traffic emissions, nucleation, and climate modulation,” Atmospheric Environment: X, vol. 19, p. 100221, 2023, doi: 10.1016/j.aeaoa.2023.100221.

[96] D. Bousiotis, J. Brean, F. Pope, M. Dall’Osto, X. Querol, A. Alastuey, N. Perez, T. Petäjä, A. Massling, J. K. Nøjgaard, C. Nørdstrom, G. Kouvarakis, S. Vratolis, K. Eleftheriadis, J. V. Niemi, H. Portin, A. Wiedensohler, K. Weinhold, M. Merkel, T. Tuch, and R. M. Harrison, “The effect of meteorological conditions and atmospheric composition in the occurrence and development of new particle formation (NPF) events in Europe,” Atmos. Chem. Phys., vol. 21, pp. 16387–16411, 2021, doi: 10.5194/acp-21-16387-2021.

[97] Health Council of the Netherlands, *Risks of ultrafine particles in the outside air*. The Hague, The Netherlands: Health Council of the Netherlands, 2021, publication no. 2021/38.

[98] K. Li, D. Lyv, J. Jiang, X. Qiao, H. Ma, and X. Wang, “Temporal patterns and socioeconomic controls of $PM_{2.5}$ across global cities,” *Sustainable Cities and Society*, vol. 127, p. 106456, 2025.

[99] J. Liu, J. Li, and W. Li, “Temporal patterns in fine particulate matter time series in Beijing: A calendar view,” *Scientific Reports*, vol. 6, p. 32221, 2016, doi: 10.1038/srep32221.

[100] Z. Song and B. Chen, “Urban-rural patterns and driving factors of particulate matter pollution decrease in eastern China,” *Atmospheric Chemistry and Physics*, vol. 25, pp. 15487–15506, 2025, doi: 10.5194/acp-25-15487-2025.

[101] S. Mikkonen, Z. Németh, V. Varga, T. Weidinger, V. Leinonen, T. Yli-Juuti, and I. Salma, “Decennial time trends and diurnal patterns of particle number concentrations in a central European city between 2008 and 2018,” *Atmospheric Chemistry and Physics*, vol. 20, pp. 12247–12263, 2020, doi: 10.5194/acp-20-12247-2020.

[102] M. I. Manning, R. V. Martin, C. Hasenkopf, J. Flasher, and C. Li, “Diurnal patterns in global fine particulate matter concentration,” *Environmental Science & Technology Letters*, vol. 5, no. 11, pp. 687–691, 2018, doi: 10.1021/acs.estlett.8b00573.

[103] R. Dobson, K. Siddiqi, T. Ferdous, R. Huque, M. Lesosky, J. Balmes, and S. Semple, “Diurnal variability of fine-particulate pollution concentrations: data from 14 low- and middle-income countries,” *The International Journal of Tuberculosis and Lung Disease*, vol. 25, no. 3, pp. 206–214, 2021, doi: 10.5588/ijtld.20.0704.

[104] X. Wang, X. Chen, Z. Zhou, M. Teng, Y. Xiang, C. Peng, C. Huang, and C. Peng, “Dynamic patterns of particulate matter concentration and size distribution in urban street canyons: insights into diurnal and short-term seasonal variations,” *Environmental Monitoring and Assessment*, vol. 196, p. 953, 2024, doi: 10.1007/s10661-024-13104-0.

[105] Vaishali, G. Verma, and R. M. Das, “Influence of temperature and relative humidity on $PM_{2.5}$ concentration over Delhi,” *MAPAN – Journal of the Metrology Society of India*, 2023, doi: 10.1007/s12647-023-00656-8.

[106] J. Cyrys, M. Pitz, J. Heinrich, H.-E. Wichmann, and A. Peters, “Spatial and temporal variation of particle number concentration in Augsburg, Germany,” *Science of the Total Environment*, vol. 401, no. 1–3, pp. 168–175, Aug. 2008, doi: 10.1016/j.scitotenv.2008.03.043.

[107] D. Mecca, C. Boanini, V. Vaccaro, D. Gallione, N. Mastromatteo, and M. Clerico, “Spatial variation, temporal evolution, and source direction apportionment of PM1, PM2.5, and PM10: 3-year assessment in Turin (Po Valley),” *Environmental Monitoring and Assessment*, vol. 196, p. 1251, 2024, doi: 10.1007/s10661-024-13446-9.

[108] S. Mikkonen, Z. Németh, V. Varga, T. Weidinger, V. Leinonen, T. Yli-Juuti, and I. Salma, “Decennial time trends and diurnal patterns of particle number concentrations in a central European city between 2008 and 2018,” *Atmospheric Chemistry and Physics*, vol. 20, pp. 12247–12263, 2020, doi: 10.5194/acp-20-12247-2020.

[109] J. Rissler, E. Z. Nordin, A. C. Eriksson, P. T. Nilsson, M. Frosch, M. K. Sporre, A. Wierzbicka, B. Svenningsson, J. Löndahl, M. E. Messing, S. Sjögren, J. G. Hemmingsen, S. Loft, J. H. Pagels, and E. Swietlicki, “Effective density and mixing state of aerosol particles in a near-traffic urban environment,” *Environmental Science & Technology*, vol. 48, no. 11, pp. 6300–6308, 2014, doi: 10.1021/es5000353.